Kinetics of the Release and Precipitation of Phosphorus in Anaerobic Digesters Sequencing Biological Phosphorus Removal Systems

by

Dipankar Sen

Thesis submitted to the Faculty of the

Virginia Polytechnic Institute and State University

in partial fulfillment of the requirements for the degree of

Master of Science

in

Environmental Engineering (Department of Civil Engineering)

APPROVED:

William R. Knocke, Co-Chairman

Clifford W. Randall, Co-Chairman

James D. Rimstidt

June, 1986

Blacksburg, Virginia

Kinetics of the Release and Precipitation of Phosphorus in Anaerobic Digesters Sequencing Biological Phosphorus Removal Systems

by

Dipankar Sen

Committee Co-Chairmen: Dr. W. R. Knocke and Dr. C. W. Randall

Environmental Engineering

(ABSTRACT)

The extent of release and precipitation of phosphorus stored in the poly-phosphate granules of micro-organisms present in anaerobic digesters sequencing a biological phosphorus removal (BPR) activated sludge system was examined. The research was conducted at the York River Wastewaster Treatment plant which was converted from a conventional system to a A/O process for biological phosphorus removal. The primary and secondary anaerobic digesters each had a solids retention time of approximately 120 days.

The results indicated that at least 60 percent of the phosphorus in the poly-phosphate granules would be solubilized during endogenous decay and digestion under anaerobic conditions. This is accompanied by the release of potassium, magnesium and limited amounts of calcium.

The release of magnesium and phosphorus in the high ammonium containing environment of the primary digester results in the precipitation of about 1000 mg/L of struvite ($MgNH_4PO_4H_2O$), a relatively adhesive and kinetically fast precipitate. Struvite can form on flocs of biomass inside the primary digester, on walls, inside pipes, and in areas affected by lower temperatures and higher pH. The phosphorus level in the secondary digester effluent is controlled by the kinetics of formation of competitive precipitates like struvite, calcium-phosphorus compounds and vivianite ($Fe_3(PO_4)_2$). The formation of vivianite is limited by the competitive precipitation of siderite ($FeCO_3$). The extent to which the compounds are precipitated depends on the solids retention times, ionic strengths, size and amorphous nature of the precipitates and the substitution of foreign ions in the crystal lattice. The effective solubility products of these precipitates, as applicable to anaerobic digesters, were determined.

Acknowledgements

I would like to express my gratitude to Dr. William R. Knocke for advising me during the difficult stretches of my research and patiently keeping it on the right track. I deeply appreciate the encouragement and guidance provided by Dr. Clifford W. Randall, especially during the 'trips' to the plant and the 'non-office hours' meetings. The research would not have progressed this far without the help and advice provided by Dr. James D. Rimstidt with the geochemical aspects of my research.

As much as any other person, I would like to thank Ms. Marilyn Grender for doing the extra-ordinary amount of the analyses involving metals. And the long hours in the laboratory will be always remembered because of the sense of humor and the good natured fight for laboratory space and cleanliness kept up by Julie Petruska, while the involvement of the crowd in 325 with the fish in the aquarium just above my research space always provided food for thought.

Lastly, I would like to thank Dr. C. W. Randall for giving me the opportunity for working on a most unorthodox and interesting project, and to Air Products for the grant which supported my research.

Table of Contents

List of Illustrations

List of Tables

Glossary

Chemical compounds

Amorphous Calcium Phosphate		$Ca_9(PO_4)_6$
Aragonite	(Calcium carbonate)	$CaCO_3$
Bobierrite	(Magnesium Phosphate)	$Mg_3(PO_4)_2.8H_2O$
Brushite	[Calcium phosphate Dihydrate] (DCPD)	$CaHPO_4.2H_2O$
β-tricalcium phosphate		$(Ca\text{-}Mg)_9(PO_4)_6$
or		$\beta\text{-}Ca_3(PO_4)_2$
Calcite	(Calcium carbonate)	$CaCO_3$
Chlorapatite		$Ca_5(PO_4)_3Cl$
Dittmarite	(Magnesium Ammonium Phosphate)	$MgNH_4PO_4.H_2O$
Dolomite		$CaMg(CO_3)_2$
Farringtonite	(Magnesium Phosphate)	$Mg_3(PO_4)_2.3H_2O$
Ferric Hydroxide		$Fe(OH)_3$
Ferrous Ammonium Phosphate		$FeNH_4PO_4$
Ferrous Hydroxide		$Fe(OH)_2$
Fluorapatite		$Ca_5(PO_4)_3F$
Hydroxyapatite		$Ca_5(PO_4)_3OH$
Lansfordite	(Magnesium Carbonate)	$MgCO_3.8H_2O$
Magnesite	(Magnesium Carbonate)	$MgCO_3$

Monetite		$CaHPO_4$
Nesquehenite	(Magnesium Carbonate)	$MgCO_3.3H_2O$
Newberyite		$MgHPO_4.3H_2O$
Octo Calcium Phosphate		$Ca_8H_2(PO_4)_6.5H_2O$
Sarcopside		$(Fe\text{-}Mg)_3(PO_4)_2$
Siderite	(Ferrous Carbonate)	$FeCO_3$
Strengite	(Ferric Phosphate)	$FePO_4$
Struvite	(Magnesium Ammonium Phosphate)	$MgNH_4PO_4.6H_2O$
TCP	(Tricalcium phosphate)	$Ca_3(PO_4)_2$
Vivianite	(Ferrous Phosphate)	$Fe_3(PO_4)_2.8H_2O$

York River Sampling Points

PCE	Primary Clarifier Effluent
PCU	Primary Clarifier Underflow
ATE	Aeration Tank Effluent
ATI	Aeration Tank Influent
BF[1]	Belt Filtrate
CBR	Combined Recycle (GTS + FTS + BF + Septic Tank Flow)
CNx	Cell Number x (x = 1 to 7)
FTS	Dissolved Air Flotation (DAF) Thickener Subnatant
GTS	Gravity Thickener Supernatant
NPW	Non Potable Water
PD	Primary Digester (Mixed Liquor)
RAS	Return Activated Sludge
RI	Raw Influent
SDS	Secondary Digester Supernatant
SDU	Secondary Digester Underflow (Sludge)
SE	Secondary Clarifier Effluent
TPS	Gravity Thickened Primary Sludge
TWS	DAF Thickened Waste Sludge
WAS	Waste Activated Sludge

[1]Except for Tables A1 to A8, Appendix A where it was written as BFAN and the sample off the bottom of the belt was referred to as BF, this sample was collected after the filtrate mixed with non potable waster.

Introduction

Since the phenomenon of enhanced biological phosphorus removal in activated sludge systems was first observed (Srinath *et al.*, 1959), researchers have made attempts to determine the mechanisms and biochemical pathways governing the release and uptake of phosphorus from sludge containing phosphorus in excess of biological requirements. While conventional treatment systems produce biomass with two to three percent phosphorus (McCarty, 1970), systems operating for biological phosphorus removal (BPR) are capable of producing biomass with a phosphorus content of upto 14 percent (VIP report, CH_2M Hill, 1986) .

Regardless of the specific treatment scheme, a biological phosphorus removal process (BPR) differs from the conventional activated sludge process because it operates with an anaerobic selector zone followed by a zone of aeration (Figures 1 and 2). The bacterial species (possibly, the *Acinetobacter species*) in BPR systems invoke a poly-β-hydroxybutyrate (PHB) accumulation and breakdown cycle in the anaerobic and aerobic zones respectively. This is coupled with the breakdown and accumulation of phosphorus as polyphosphate in metachromatic granules which occupy up to sixty percent of the cell volume (Buchan, 1983 and Cloete, 1984). According to Fuhs and Chen (1975), the breakdown of poly-phosphate serves as the energy source for the storage of substrate as PHB. In the aerobic zones, the PHB serves as the source of energy for the formation of high energy poly-phosphate granules. The anaerobic zone therefore serves as a selector zone by allowing the *Acinetobacter species* of micro-organisms to partition the readily available substrate

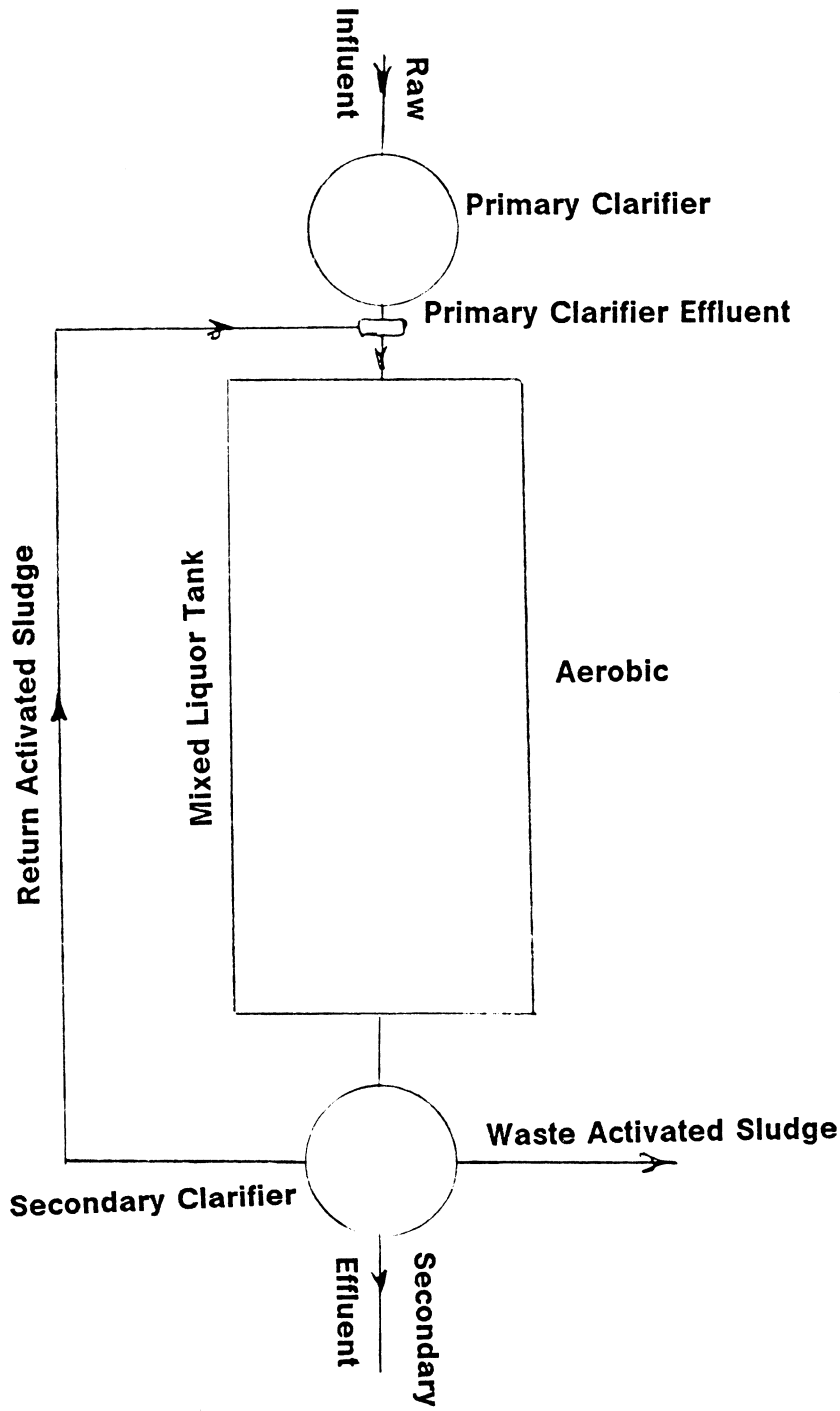

Figure 1. A schematic of a mixed liquor tank for COD removal only (Conventional).

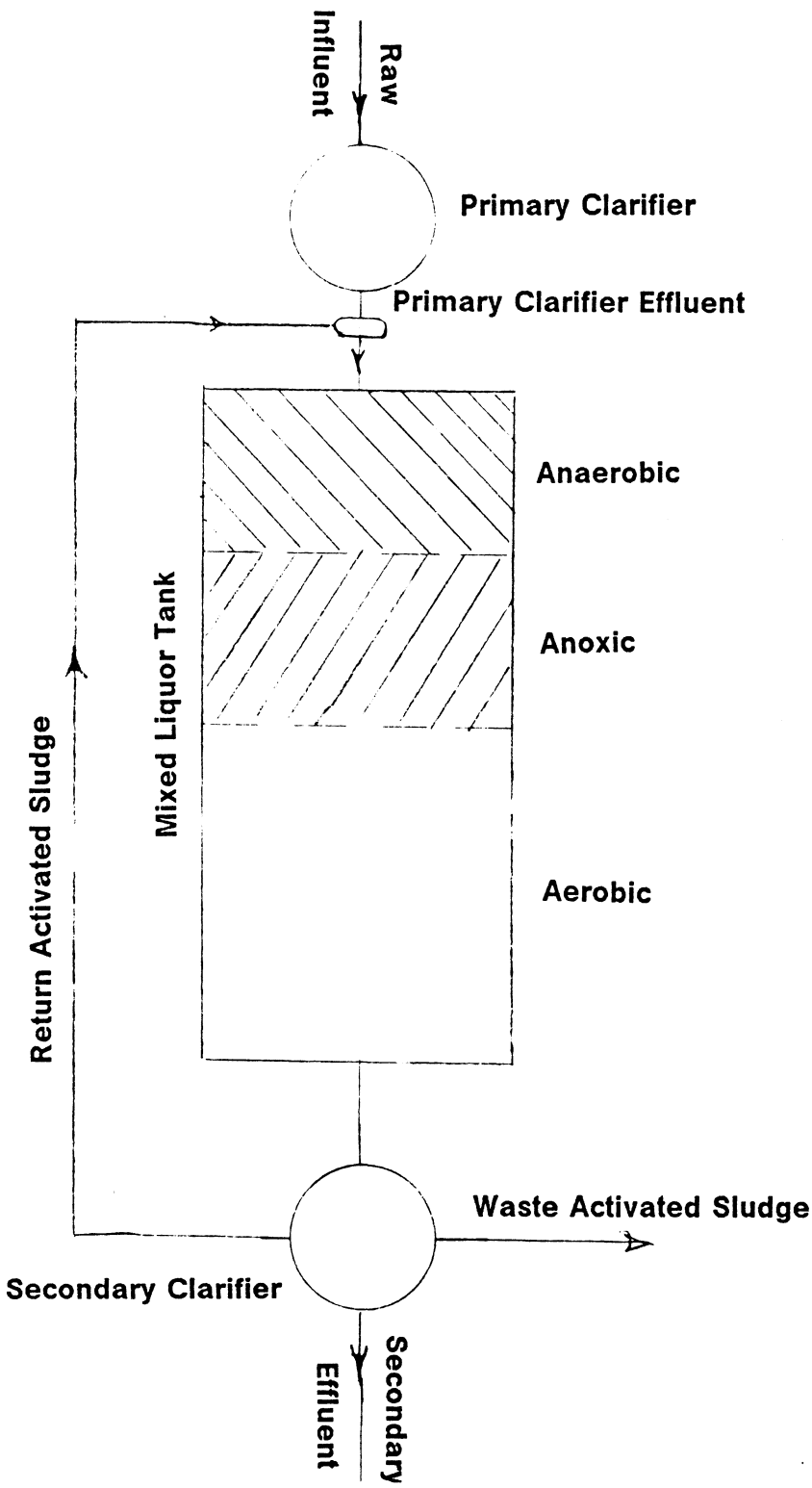

Figure 2. A Schematic of a mixed liquor tank designed for phosphorus and nitrogen removal in addition to COD.

for itself and synthesize PHB in an environment where other heterotrophs are hampered by the lack of an external electron acceptor mediated energy source.

Recent biochemical models for biological phosphorus removal have looked into the phenomenon of phosphorus release under anaerobic conditions as a result of the breakdown of poly-phosphate bonds in volutin granules. Wentzel *et al.* (1986) theorized that the dissociation of these bonds releases energy for maintenance, and possibly, for the storage of acetates released by the fermentation of dead micro-organisms, to synthesize PHB. The release of phosphorus is accompanied by the transfer of cations like potassium, magnesium and calcium to maintain the proton-motive force across the cell membrane. It is very probable that such a situation would arise when the sludge from a biological phosphorus removal system is sent into an anaerobic digester for solids reduction purposes. The extent to which the poly-phosphate granules are released has not been looked into and cannot be measured directly if precipitates are formed with soluble calcium, magnesium, ferrous and ferric cations in anaerobic digesters. It is important, however, for reasons mentioned below that both the nature of the precipitates and the extent of release be determined.

Under the influence of the high ammonium levels prevailing in anaerobic digesters, the release of magnesium and phosphorus makes the environment conducive to the formation of a precipitate like struvite ($MgNH_4PO_4.6H_2O$). This precipitate is of particular concern because it can coat the walls and clog the pipes of digesters(Snoeyink and Jenkins, 1980). The release may also result in high levels of soluble phosphorus in the dewatered secondary digester effluent recycled to the headworks. To meet the effluent standards, it would necessitate removal of additional amounts of phosphorus in the BPR system. This invokes the synthesis of additional amounts of PHB from fresh substrate in the anaerobic zone. The result is that very little substrate is left for utilization by the denitrifiers, hampering the denitrification process essential for the removal of nitrates from the effluent discharged by the system.

The objectives of this research were to

a) examine the extent of release of phosphorus from sludge containing phosphorus in excess of biological requirements under anaerobic conditions and in the absence of fresh substrate, and

b) investigate the nature and extent of chemical precipitates, particularly struvite ($MgNH_4PO_4.6H_2O$), formed during anaerobic digestion of BPR sludge.

Literature Review

Extensive research is currently underway to determine the parameters which lead to and control the uptake of phosphorus by biomass in excess of its biochemical composition: $C_{60}H_{87}O_{23}N_{12}P$ (McCarty, 1970). Recent models have accounted for the transfer of cations with the movement of phosphorus across the cell membrane with a reasonable degree of accuracy. These developments are significant because chemical interaction between ionic species in anaerobic digesters depend on the levels of release, which in turn depend on the extent of movement across the cell membrane.

Biochemical model for excess phosphorus removal

Acinetobacter species can grow on simple media, containing as low as a single source of organic carbon, serving both as a carbon and an energy source for anabolic processes (Juni, 1978). The ability of *Acinetobacter species* to use oxygen as an electron acceptor has been documented in this reference. More recently it has been shown that some strains of *Acinetobacter species* can also utilize nitrate as an external electron accepter in the absence of oxygen (Henriksen, 1976; Lotter, 1985; van Groenestijn and Dinema, 1985).

Lotter *et al.* (1986) have stated that none of the acinetobacter strains appear to possess the glycolytic (Emden-Meyerhoff) pathway. They did show that a number of acinetobacter strains

isolated both from anaerobic-anoxic-aerobic and from completely aerobic systems possessed the Entner-Duodoroff pathway to utilize glucose as a substrate under aerobic conditions. This pathway is inoperative when oxygen and/or nitrate is absent. In their studies, they observed that completely mixed single stage aerobic reactors had up to 40 percent *Acinetobacter species* , which increased to 60 percent with the introduction of an anaerobic selector zone. Acinetobacter strains isolated both from systems that exhibited excess phosphorus removal and from systems that did not, had the propensity to accumulate poly-phosphate (poly-P) and poly-β-hydroxybutyrate (PHB) under aerobic conditions when using acetate and/or glucose as the substrate. Imposing conditions conducive to excess phosphorus removal (by anaerobic-aerobic sequencing) did not stimulate the growth of new acinetobacter strains. Rather, they stimulated the poly-P and PHB accumulating propensities inherent in the strains already present. The period of four to eight weeks required for the onset of biological phosphorus removal (Lotter *et al.* , 1986, and Irvine, 1985) was felt by Lotter to be a period required to invoke the latent propensity for poly-P accumulation via the development of the appropriate enzyme systems, resulting in a progressive increase in poly-P and PHB accumulation.

Carbon Metabolism

Wentzel *et al.* (1986) have illustrated that the metabolism of carbon by *Acinetobacter species* in activated sludge incorporates three main metabolic pathways —

1) the tricarboxylic cycle;
2) the glyoxylate cycle; and
3) PHB synthesis and degradation cycle.

Much of the material in this section is summarized from the work done by Wentzel *et al.* (1986). For a more detailed understanding of the specifics regarding the uptake and removal of phosphorus, the reader is encouraged to refer to this publication.

Figure 3 shows the TCA and glyoxylate cycles starting from the input of one molecule of acetyl coenzyme A. Under aerobic conditions, the TCA cycle either supplies the intermediates for anabolism or generates ATP in combination with oxidative phosphorylation. Under anaerobic conditions, in the absence of external electron acceptors, unless some alternative electron sink is found, the NADH/NAD ratio increases and the ATP/ADP ratio decreases. The TCA cycle, and the glyoxylate cycle regulated by the four carbon (C4) intermediates of the TCA cycle, are inhibited by high NADH/NAD, NADPH/NADP and ATP/ADP ratios, each ratio affecting a separate enzyme.

Figure 4 (from Wentzel *et al.*, 1986) illustrates the synthesis and degradation of PHB, as observed in numerous bacterial species other than *Acinetobacter* , in which it is yet to be studied. The diagram shows that the synthesis of acetate serves as a sink for protons, electrons and organic carbon. The synthesis is stimulated by high NADH/NAD (or NADPH/NADP) ratios and high concentrations of acetyl-CoA. An inhibitory effect can be exerted on the synthesis pathway by a high concentration of CoASH enzyme ketothiolase. Therefore, the pathway will be functional when a high concentration of organic carbon is available to the organism but no external electron sink (i.e. an anaerobic state) is present. The degradation pathway is inhibited by a high concentration of pyruvate and/or high NADH/NAD ratios, since they inhibit the enzyme NAD $-$ β $-$ hydroxybutyrate dehydrogenase . PHB degradation is therefore favored under low extracellular organic substrate concentrations and in the presence of a terminal electron acceptor (i.e. an aerobic state).

Phosphorus metabolism

Buchan (1981) mentioned that *Acinetobacter species* can accumulate phosphorus as poly-phosphate (poly-P), the large negative charge on the poly-phosphate being stabilized by Mg^{2+}, K^{+} and Ca^{2+} ions. In order to achieve biological phosphorus removal, Wentzel *et al.*(1986) mentioned that poly-phosphate metabolism in *Acinetobacter species* can occur via two pathways:

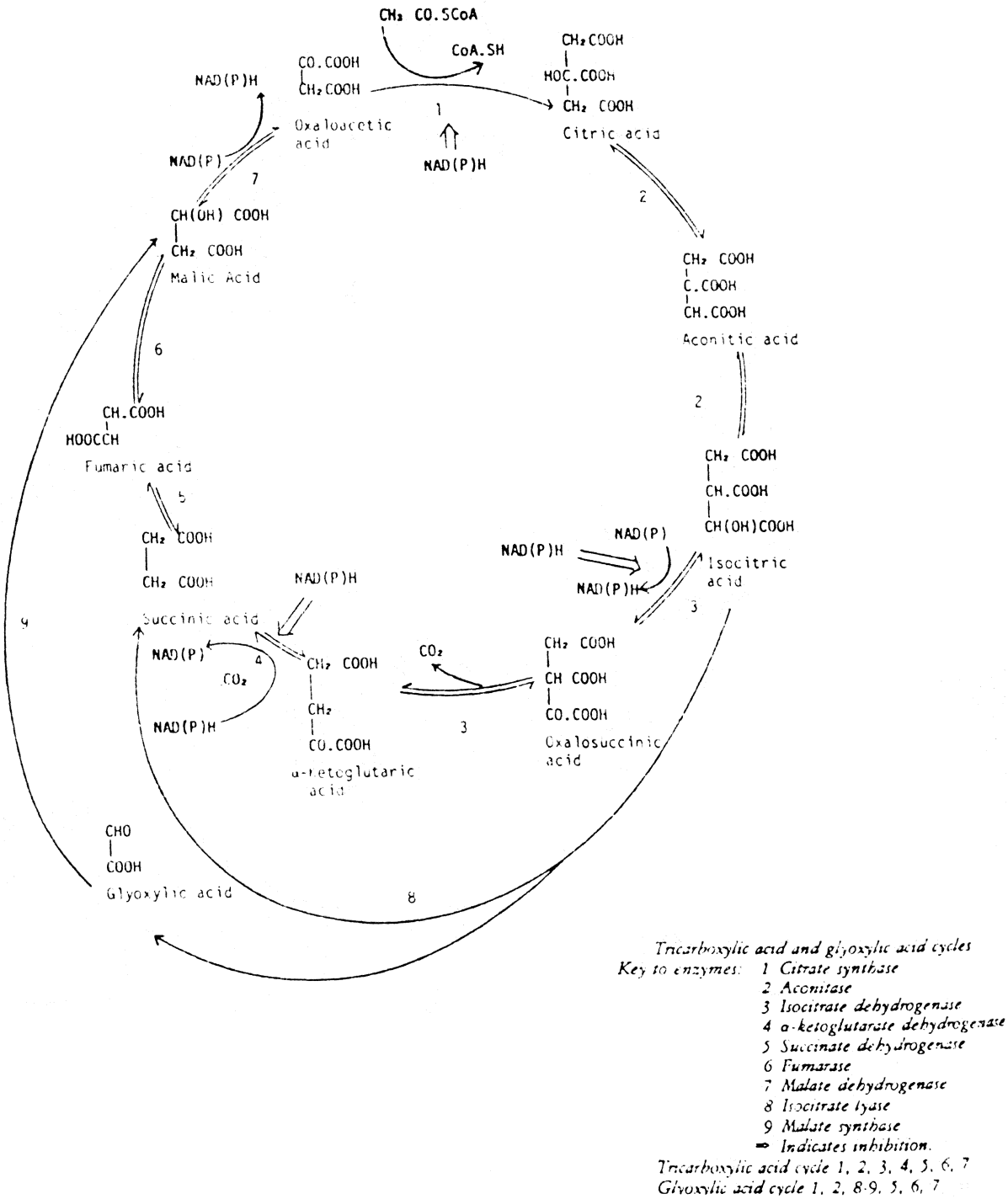

Tricarboxylic acid and glyoxylic acid cycles

Key to enzymes:
1 *Citrate synthase*
2 *Aconitase*
3 *Isocitrate dehydrogenase*
4 *α-ketoglutarate dehydrogenase*
5 *Succinate dehydrogenase*
6 *Fumarase*
7 *Malate dehydrogenase*
8 *Isocitrate lyase*
9 *Malate synthase*
⇒ *Indicates inhibition.*

Tricarboxylic acid cycle 1, 2, 3, 4, 5, 6, 7
Glyoxylic acid cycle 1, 2, 8·9, 5, 6, 7

Figure 3. Tricarboxylic acid and glyoxylate cycles

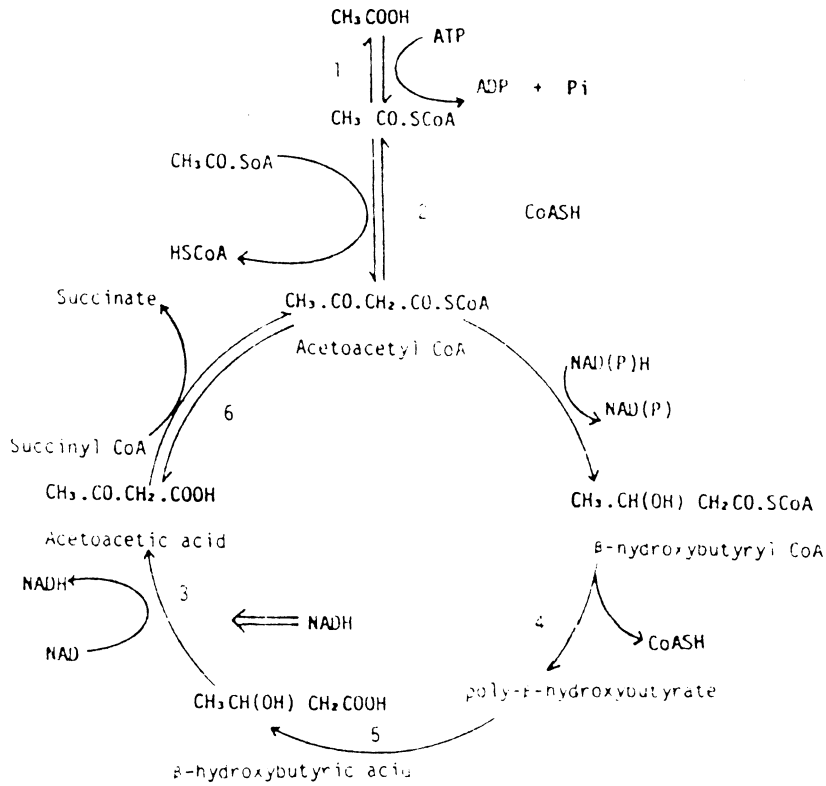

Synthesis and degradation of poly-β-hydroxybutyrate

Key to enzymes: *1 thiokinase*
2 β-ketothiolase
3 β-hydroxybutyrate dehydrogenase
4 β-hydroxybutyryl CoA polymerase
5 poly β hydroxybutyrate depolymerase
6 Acetoacetate succinyl CoA : CoA transferase
⇒ *indicates inhibition.*

Figure 4. Synthesis and degradation of PHB

1) **a Synthesis Pathway** — poly-P synthesis has been observed through

a) phosphorylation of the poly-P by 1,3 diphosphoglycerate

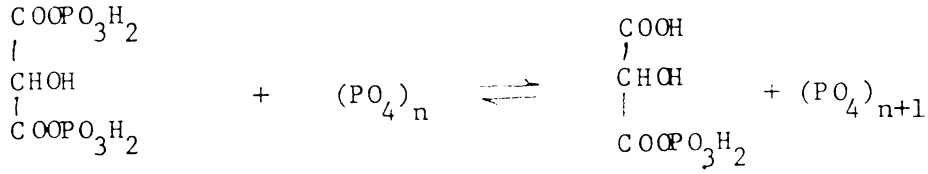

b) phosphorylation of poly-P by ATP (catalysed by enzyme polyphosphate phosphotransferase)

$$ATP + (PO_4)_n \rightleftharpoons ADP + (PO_4)_{n+1} \qquad [2.2]$$

Though neither of these pathways have been studied in *Acinetobacter species* , they have been identified in a variety of organisms. The synthesis of poly-P is inhibited by low ATP/ADP ratios, a condition likely under anaerobic conditions irrespective of the external substrate concentrations.

2) a Degradation Pathway — Three reaction pathways have been cited by Wentzel *et al.*(1986). The first of these is the reverse of the reaction as stated in equation 2.2, catalysed by the enzyme ATP: polyphosphate phosphotransferase. The pathway is inhibited by high ATP/ADP ratios, which exist at high ATP levels prevailing under aerobic conditions in the presence of internally stored PHB or external substrate (because PHB or external substrate is used to generate ATP from ADP). The hydrolysis of poly-P and the phosphorylation of AMP (Adenosine Mono Phosphate) to ADP are two other reaction pathways referenced in the literature.

Comeau *et al.*(1985) have mentioned that continued uptake of acetate as acetic acid under anaerobic conditions dissipated the proton motive force (pmf) essential for the translocation of molecules across the cytoplasmic membrane. This pmf ($\Delta\mu_H$) has a pH and a charge ($\Delta\psi$) component, which, according to Padan *et al.*(1976), are related as

$$\Delta\mu_H = \Delta\psi + \frac{2.3RT}{F}\Delta pH \qquad [2.3]$$

In order to restore the pmf, Comeau *et al.* (1985) and Wentzel *et al.* (1986) proposed a concomitant release of

a) phosphate via hydroxy mediated antiport protein carrier, a transport system commonly used in micro-organisms,

b) cation release via a proton mediated antiport protein, and

c) acetic acid uptake by passive diffusion. (Figure 5)

The pmf in equation 2.3 is kept at a certain level by maintaining the pH and charge difference between the inside and outside of the cell.

Under anaerobic conditions, the translocations across the cell wall occur as shown in Figure 5. The charge balances and net changes in alkalinity and acidity, as determined by Wentzel *et al.* (1986), show that while there is no net change intracellularly, extracellularly there is an increase in one mole of acidity and alkalinity per mole of phosphate taken up.

The cells can also use propionate and higher short chain fatty acids in place of acetate. Wentzel *et al.* (1986) suggested the following equation for the use of propionate by the *Acinetobacter species* ;

$$\text{Propionate} + \text{HSCoA} \rightleftharpoons \text{acetyl-CoA} + CO_2 \qquad [2.4]$$

Under aerobic conditions, the translocations across the cell wall are in accordance with Figure 6. The charge balances, net changes in alkalinity and acidity show no net change intracellularly, but extracellularly, a decrease of two moles of acidity and one mole of alkalinity occurs for every mole of phosphate taken up. For a pH greater than or equal to 6.8 after the anaerobic zone of a BPR system, they stated that the pH would increase in the aerobic zones in cultures dominated by *Acinetobacter species.*

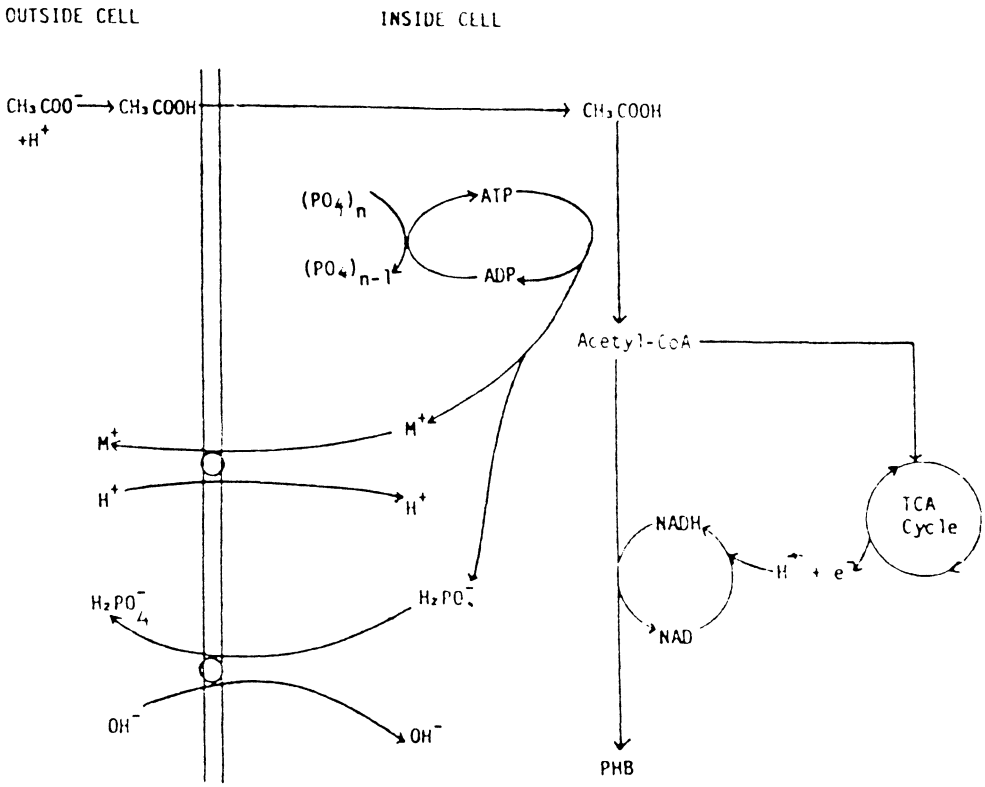

Figure 5. Translocation of acetate, phosphate and cations across the cytoplasmic membrane under anaerobic conditions

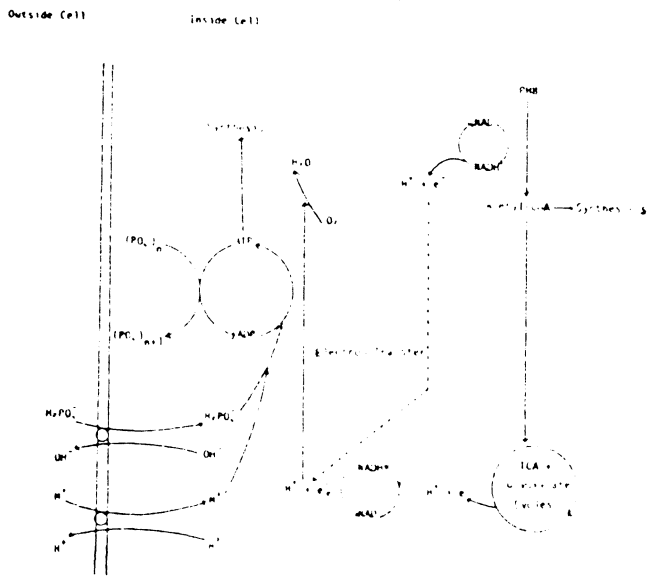

Figure 6. Translocation of phosphate and cations across the cytoplasmic membrane under aerobic conditions

Comeau *et al.* (1985) examined the charge balances in various studies with biological phosphorus removal systems (Table 1). Ideally, the biochemical model should show a complete balance of cationic and anionic species transferred across the cell membrane.

The behaviour of the *Acinetobacter species* during endogenous respiration (a process in which the cellular constituents are utilized for maintenance energy) under anaerobic conditions, as discussed by Wentzel *et. al* (1986), has special significance to this research. When the *Acinetobacter species* are placed in an environment where no external electron accepters are available, they are unable to utilize the organic material released by the death of cells for energy generation. (The cells may store the acetate generated during the fermentation of the protoplasm as PHB but will be unable to utilize it.) Phosphorus will be released because of

1) the cleavage of poly-P to form ATP. The ATP inturn forms ADP, releasing a phosphate molecule in the process, and provides for the maintenance energy and the energy required to store acetate as PHB;
2) uncleaved poly-P released through cell death and lysis.

Cations like potassium, magnesium and calcium, associated with the poly-P granule are released in soluble form because of the first mode of release of phosphorus.

Phosphate chemistry and precipitates

The interest in phosphate minerals spans several fields outside that of environmental engineering. Much of the literature pertaining to the precipitation of hydroxyapatite ($Ca_{10}(PO_4)_6OH_2$) and struvite ($MgNH_4PO_4.6H_2O$) has been published in the areas of geochemistry and medicine.

The list of thermodynamic constants for phosphate minerals is far from complete. Nriagu and Moore (1984), Stumm and Morgan (1981), Lindsay and Vlek (1977) and the CRC Handbook of

Table 1. Molar ratios of release and uptake of phosphorus and charge balance across the membrane

	1	2	3	4	4	5
Mg^{2+}/P	0.26	0.32	0.24	0.28	0.27	0.29
K^{+}/P	0.27	0.23	0.34	0.20	0.23	0.23
Ca^{2+}/P	0.00	-	0.06	0.09	0.12	0.07
Na^{+}/P	-	-	0.00	0.00	0.00	-
Sum of charges/P	0.79	0.87	0.94	0.94	1.01	0.95
P transport[1]	release	release	release	release	uptake	release

P transport[1] = Direction of transport across cell membrane

(1) Miyimato-Mills *et al.*, 1983
(2) Arvin and Kristensen, 1983
(3) ,(4) Comeau *et al.*, 1985
(5) Brannan, 1985

Chemistry and Physics, 65th ed. (1983-84) provided a list of free energies, enthalpies and solubility products of the more common precipitates.

Hydroxyapatite and other calcium-phosphorus phosphates

Nriagu and Moore (1984) detailed the precipitation of several calcium precipitates in soils, bones, calcified tissues and wastewaters. Posner *et al.* (1984) mentioned that though the unit cell (crystallographic) content of hydroxyapatite is written as $Ca_{10}(PO_4)_6(OH)_2$, there can be an isomorphous substitution of F^- or Cl^- for OH^-. Tomson and Vignena (1984) determined that besides hydroxyapatite, octocalcium phosphate, ($Ca_8H_2(PO_4)_6.5H_2O$) and tricalcium phosphate, $(Ca\text{-}Mg)_9(PO_4)_6$ properly predict the pH trend observed in phosphate removal from wastewaters. However, they added that the precipitated particles from these systems were so small that they did not produce good X-ray diffraction patterns or lend themselves readily to stoichiometric analysis.

LeGeros and LeGeros (1984) found that some of the vexing problems concerning biological apatites, as distinct from pure calcium hydroxyapatite, were

1) their non-stoichiometry (i.e. their calcium to phosphorus ratio ranges from 1.54 to 1.73 as compared to 1.67 for pure Ca-OH- apatite)

2) the structural or surface involvement of some "impurities" such as Na^+ , Mg^{2+}, F^-, HPO_4^{2-} , CO_3^{2-} and $P_2O_7^{4-}$ and

3) the co-existence and pre-existence of certain precursors such as Calcium phosphate dihydrate or Brushite, ($CaHPO_4.2H_2O$), Octocalcium phosphate, Tricalcium phosphate and Amorphous calcium phosphate.

They have also discussed the stability of different calcium-phosphate minerals like brushite, magnesium containing amorphous calcium phosphate, fluorapatites and β -tricalcium phosphate (β- stands for low temperature, as against α-Tricalcium phosphate which is high temperature whitlockite).

Gulbrandsen *et al.* (1983) conducted experiments to demonstrate the inhibitory effect of magnesium upon the crystallization of apatite from sea water. Crystallization occurred 9.3 years after the precipitation of the amorphous phase in samples using calcite as seed. Quartz, apatite and fluorite seeds required even longer periods of time. Data presented in Table 2 show the rate of precipitation of phosphorus using the different seed crystals, each of size 50μm. The initial phosphate concentration was raised to 32 mg/L of PO_4-P. No details were mentioned regarding the calcium and magnesium levels in their sea-water samples. The first evidence of crystallization of the amorphous phase caused a drop in the phosphorus levels to less than 1 mg/L (Table 2).

LeGeros and LeGeros (1984) cited references which stated that the presence of magnesium does not allow the formation of a pure β -tricalcium phosphate but a magnesium containing β-tricalcium phosphate. Gulbrandsen *et al.* (1984) observed that the molar ratio of calcium plus cationic substituents (magnesium, strontium and sodium) to phosphorus plus anionic substituents (carbon and sulfur) of their precipitates from sea-water was 1.50 only. However the X-ray diffraction patterns of the precipitates did not correspond to either tricalcium phosphate or hydroxyapatite. By assuming that H_3O^+ can substitute for some of the calcium ions, and F^- and OH^- can together be present, they balanced out the charges after considering a calcium to phosphorus ratio (inclusive of substituents) of 1.67. They assumed that H_3O^+ and OH^- were from water in the apatite structure. Though structural water of this type has not been identified in any marine apatite, they cautioned that freshly precipitated apatites (referred to by them as 'young' apatites) need to be carefully studied within this context.

McDowell *et al.*(1977) showed that an accurate determination of the solubility product for hydroxyapatite in high ionic strength systems could be carried out only after considering the effect of the ion pairs $CaHPO_4^0$ and $CaH_2PO_4^+$, and accounting for the effect of their association constants on the solubility product. The solubility product of hydroxyapatite (K_{sp}) is then given by the equation:

Table 2. Phosphate concentrations of solutions following precipitation, as mg/L of PO_4-P

Year	Time	seed			
		apatite	calcite	quartz	fluorite
		mg/L of PO_4-P			
1971	16 days	20	19	19	19
1972	6 months	17	17	17	16
1973	20 months	14	14	14	13
1974	32 months	8.2	7.9	9.5	9.2
1975	41 months	8.5	8.5	9.2	9.5
1978	74 months	6.5[1]	6.2	6.9	6.9
1981	111 months	0.20	0.27	7.2	7.2

[1]Following the determination of 6.5 mg/L of PO_4-P, the phosphate was decreased to 2.4 mg/L PO_4-P after heating the solution and precipitate at 90°C for about 6 hours.

$$\log K_{sp} = \frac{-8219.41}{T} - 1.6657 - 0.098215\,T \qquad [2.5]$$

where T = absolute temperature (°K)

The solubility of hydroxyapatite is therefore a maximum at 16.3°C .

Jenkins *et al.*(1970) mentioned that the kinetics of nucleation, the crystal growth rate and the composition of the chemical medium have a strong influence on calcium phosphate precipitation. The amorphous nature, substitution of foreign ions, and short reaction times in wastewater systems are responsible for their increased solubility. The authors also related increased carbonate concentrations to slower growth of calcium phosphate crystals, resulting in higher residual soluble phosphate residuals. (Figure 7). Finally, they showed that the induction period leading to the formation of calcium phosphate precipitates, can be reduced by seeding the systems with crystals of calcium phosphate (Figure 8).

LeGeros and LeGeros (1984) cited references which stated that the substitution of Cl^- for OH^- in apatite result in an expansion of the a-axis and a contraction of the c-axis. The atomic arrangement of chlorapatite and its larger unit cell volume as compared to hydroxy and fluorapatites, suggest that chloride ions contribute to the instability of the apatite structure. Their preliminary studies indicated that chlorapatites have a lower thermal (and perhaps chemical) stability than either hydroxy and fluorapatites.

Pyrophosphates, $P_2O_7^{4-}$ has been presumed to act as a crystal surface poison, suppressing the growth of the apatite crystals (LeGeros and LeGeros, 1984).

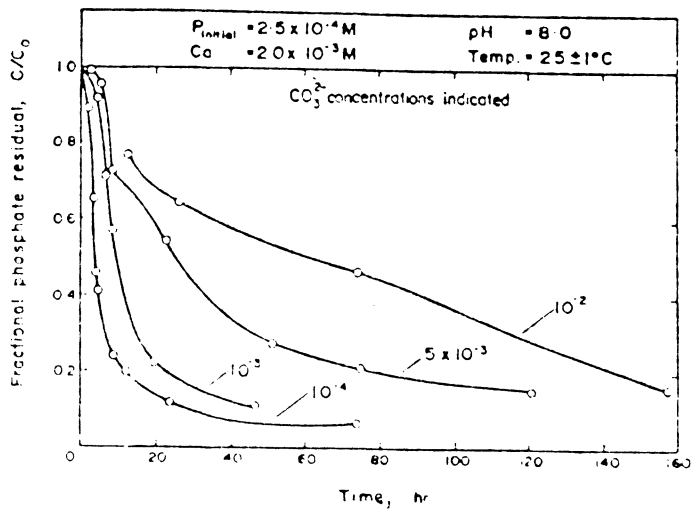

Figure 7. Effect of carbonate levels on phosphate precipitation at constant pH

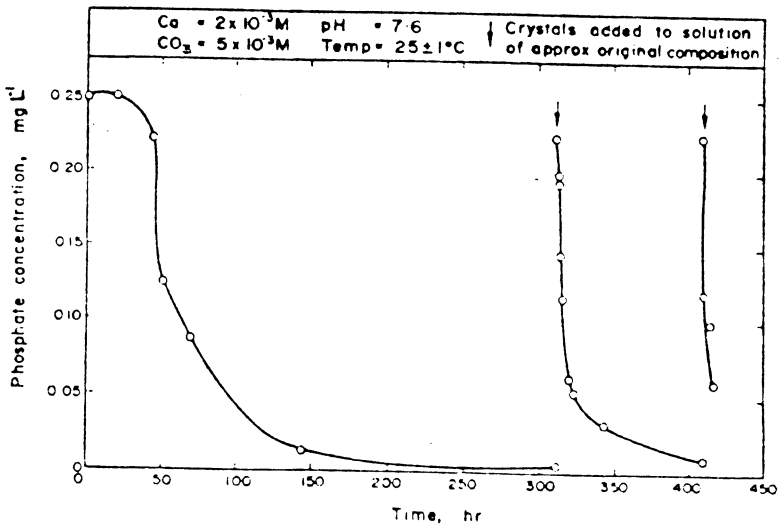

Figure 8. Effect of crystal seeding on the rate of calcium phosphate precipitation

Struvite and other magnesium precipitates

Struvite ($MgNH_4PO_4.6H_2O$) has been extensively studied in connection with its presence in urinary stones which are formed as a result of bacterial infection (Elliot, 1973 and Griffith *et al.*, 1976). LeGeros and LeGeros (1984) showed that struvite crystals grew very easily in gel systems containing Mg^{2+}, HPO_4^{2-}, PO_4^{3-} and NH_4^+. The simultaneous presence of $P_2O_7^{4-}$ caused a reduction in crystallite size, habit modification and twinning of the struvite crystals. They added that the presence of Ca^{2+} along with Mg^{2+} affected the potential for struvite formation in the following manner:

Mg/Ca	1:0 to 1:1	main product was struvite
Mg/Ca	approaching 1:1.5	main product was brushite
Mg/Ca	approaching 1:4.0	main product was whitlockite

However, their research was conducted in an environment appropriate for the growth of renal stones.

Snoeyink and Jenkins (1980) have cited examples related to the formation of struvite in pipes leading out of anaerobic digesters at the City of Los Angeles Hyperion plant and at the East Bay Municipal Utility District Plant at Oakland, California. The problem at the first plant, where a 14 inch diameter pipe was reduced to a diameter of 4 inches due to the precipitation of struvite, was solved by using a 3:1 dilution of the digested sludge with secondary effluent from the plant. This did not hamper disposal since the sludge was released into the ocean. At the second plant, a crystal formation inhibitor (a polyacrylamid — *Cyanamer P-70* , American Cyanamid Corporation) was added at doses of 10 to 20 mg/L to reduce scale formation. They added that the first treatment scheme — dilution, is better because thermodynamic stability against crystal formation is surer than kinetic stability.

Newberyite ($MgHPO_4.3H_2O$) has been cited by LeGeros and LeGeros (1984) as being a rare component of renal stones. It is sometimes formed along with struvite but its formation is affected by pH and inhibited by Sr^{2+}, Cu^{2+}, Mn^{2+} and $P_2O_7^{4-}$.

Gulbrandsen *et al.* (1983) observed that bobierrite ($Mg_3(PO_4)_2.8H_2O$) was precipitated in the first two to four years from sea water whose phosphorus level was raised to 32 mg/L PO_4-P. However, with the onset of crystallization of hydroxyapatite in about 9.3 years, bobierrite went back into solution. This was because the phosphorus levels were controlled by hydroxyapatite, and not bobierrite over the 10 year span of their study.

In the research conducted on the digester at the York River Wastewater Treatment Plant, special attention was paid to bobierrite, it being one of the more insoluble of the magnesium-phosphorus precipitates, as indicated in this study with sea-water. However, the sea-water environment did not contain sufficient levels of ammonium necessary for the precipitation of struvite, which would have reduced the levels of magnesium.

Methods and Materials

The research conducted for the purpose of this study can be divided into three phases. The first phase involved the measurement of loadings across sections of the York River Wastewater Treatment Plant to develop the infrastructure for interpreting the changes as the plant shifted its mode of operation from a conventional system for COD removal to a biological system for phosphorus, nitrogen and COD removal. The second phase involved a study of the kinetics of precipitation in the primary anaerobic digester by simulating its chemical environment in the laboratory. The third phase utilized data gathered in the first two phases in computer models developed to predict thermodynamic instability, and attempted to correlate the changes observed at the plant to the results obtained in laboratory simulations. The three phases did not necessarily sequence one another but were used to complement the information from each in arriving at the overall conclusions.

Description of the plant

The York River Wastewater Treatment Plant receives 6 to 8 million gallons of Raw Influent (influent wastewater) per day. The plant was designed to handle a maximum flow of 15 MGD using the step aeration activated sludge process. The Raw Influent (RI) passes through grit chambers, a preaeration basin and then undergoes primary clarification. The primary clarifier effluent (PCE) flows into an activated sludge mixed liquor tank.

The mixed liquor tank was designed with six parallel units, each with a volume of 0.674 MG and three were in operation before the modification. Only two units were modified such that the upstream first quarter was anaerobic, the second quarter anoxic and the downstream half aerobic. Each unit was originally divided into four sections for the step aeration operation and the pre-existing partitions were utilized. The anaerobic section was divided into three equal chambers and the anoxic into two equal chambers with the second twice as large as the first. The modifications to the plant were completed in August, 1986. (Figure 9).

The aeration tank effluent (ATE) is settled in secondary clarifiers. The secondary effluent (SE) is chlorinated and released as non-potable water (NPW). Secondary sludge is wasted from the bottom of secondary clarifiers as waste activated sludge (WAS), while the return activated sludge (RAS) is recycled back to the head of the anaerobic section.

The primary sludge is pumped from the bottom of the primary clarifiers to a pair of gravity thickeners. The waste activated sludge (WAS) is thickened by a pair of dissolved air flotation (DAF) thickeners. The average flows of gravity thickened primary sludge (thickened primary sludge, TPS) and dissolved air flotation thickened waste sludge (DAF thickened waste sludge, TWS) feeding into the primary digester were 0.013 MGD and 0.0064 MGD respectively for July 1986. The primary digester is maintained at 35°C by pumping its mixed liquor through heat exchangers. The mixed liquor from the primary digester is sent into a secondary digester, which serves as a holding tank for digested sludge. The underflow from the secondary digester (SDU) is dewatered in a belt filter press. The belt fitrate (BF), a major fraction of which is the washings off the press using non potable water (NPW), is combined with the supernatant from the gravity thickeners (GTS) and subnatant from the DAF thickeners (FTS) and recycled to the headworks as the combined recycle (CBR).

Typical monthly average flow values for a number of streams are given in Table 3.

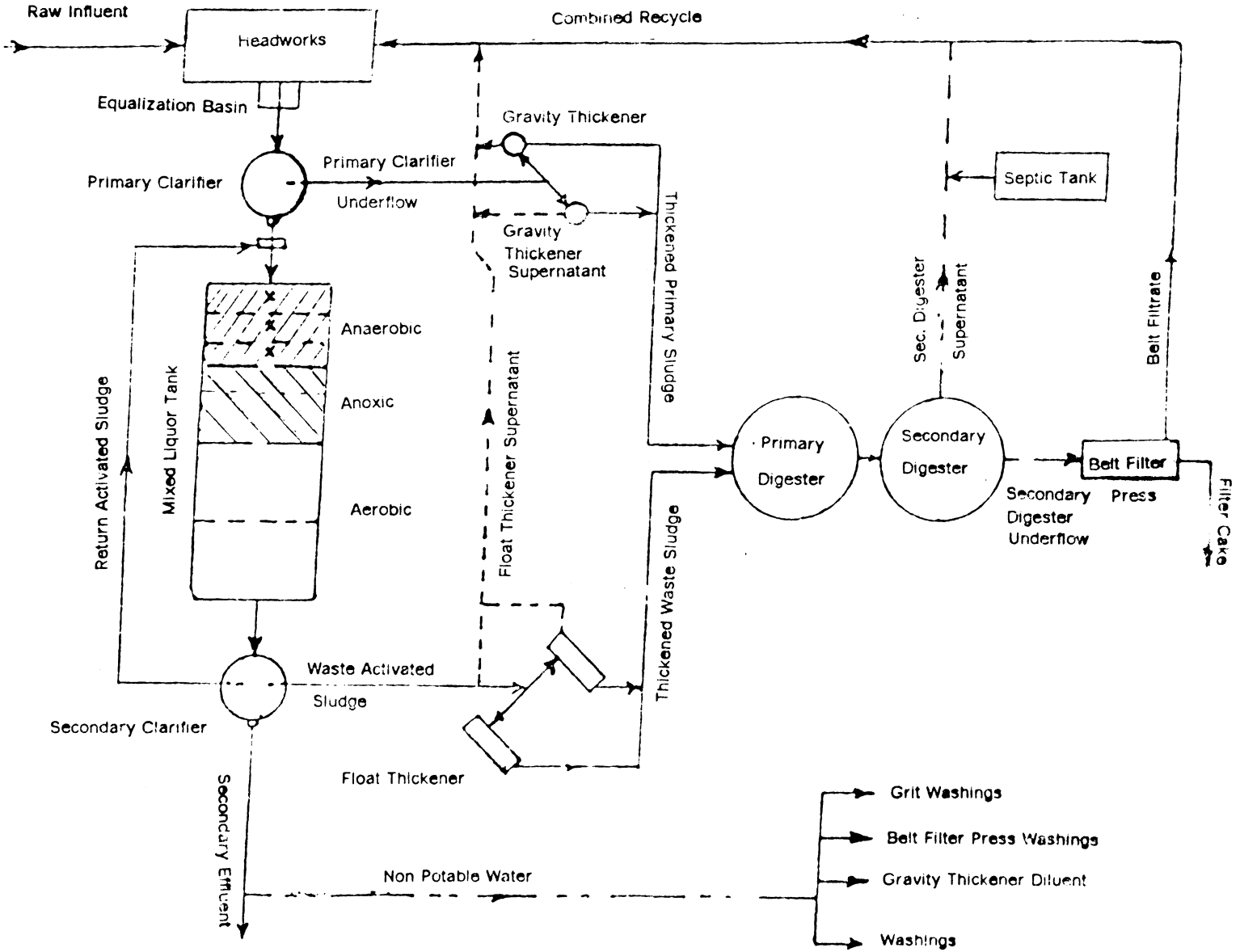

Figure 9. Schematic of the York River Wastewater Treatment Plant.

Table 3. Average Monthly flows for July '86

	Abbreviation	Flow (MGD)
Raw Influent	RI	6.24
Return Activated Sludge	RAS	5.24
Waste Activated Sludge	WAS	0.144
Primary Clarifier Underflow	PCU	0.256
Thickened Primary Sludge	TPS	0.013
Gravity Thickener Diluent		0.245
Gravity Thickener Supernatant	GTS	0.487
Thickened Waste Sludge	TWS	0.0064
Float Thickener Subnatant	FTS	0.138
Primary Digester Feed TPS + TWS		0.016
Secondary Digester Underflow	SDU	0.032
Belt Filtrate Feed Sludge	BF	0.032
Belt Filtrate	BF	0.032
Filter press wash (NPW) NPW = Non Potable Water		0.026
Combined Recycle GTS + FTS + BF	CBR	0.068

Phase I

Phase I involved the collection and analysis of samples at various locations in the plant to provide the data presented in Tables A1 to A8, Appendix A. After sampling all major waste streams for the first four months of the study, enough the information was deemed available to allow for a reduction in the number of samples collected and analyses performed.

Analytical procedures

Filtration

Samples were filtered through 0.45μm filter papers (Metricel Membrane Filter, Gelman Metricel Inc.). The samples with higher solids content were first centrifuged and filtered through 1.2μm , 5.5 cm GF/C glass microfibre filter paper (Whatman Ltd., Maidstone, England). A few samples were filtered through an AMICON (Danvers, MA 01923), Diaflo 10 YM 30, 62 mm. ultrafiltration membrane with an approximate pore size of 2.1nm to check if the 0.45μm filter was an effective separator of soluble and particulate fractions.

Since it took a few hours to filter the mixed liqour samples from the primary and secondary digesters through the 0.45μm filter, the loss of carbon dioxide due to the partial vacuum inside the Buchner funnel caused an increase in the pH of the filtrate. The effect was countered by acidifying the samples after filtration to keep all the ions of the 0.45μm filtrate in solution.

Chemical Oxygen Demand (COD)

The chemical oxygen demand of filtered and unfiltered samples was determined by the dichromate closed reflux, titrimetric method outlined in Section 508B, Oxygen Demand (Chemical), Standard Methods for the Examination of Water and Wastewater (Standard Methods, 1985). Corrections were made for the COD exerted by Nitrite (NO_2^-), which amounted to 1.1 mg O_2 per mg NO_2-N.

Total Kjeldahl Nitrogen (TKN)

TKN was measured in accordance with the semi-micro-kjeldahl method outlined in Section 420B, Standard Methods (1985).

Ammonium Nitrogen and Organic Nitrogen

Ammonium nitrogen (NH_4^+-N) and Organic Nitrogen were also measured as outlined in the semi-micro-kjeldahl method mentioned above.

On some of the filtered samples, ammonium nitrogen was measured by the phenate method discussed later.

Orthophosphate Phosphorus (PO_4-P), Nitrite Nitrogen (NO_2-N), Nitrate Nitrogen (NO_3-N), Sulfate-S (SO_4-S), and Chloride (Cl)

When more than one of these ions were to be analysed for, the Dionex 2010i Ion Chromatograph (Dionex Corporation, Palo Alto, CA) was used. The equipment has an anion separator (Dionex p/N 30985), an anion fiber suppressor and a conductivity detector. The eluent was 0.0028N sodium bicarbonate ($NaHCO_3$) / 0.0022N sodium carbonate (Na_2CO_3) pumped at a rate of 2.5 mL/min., and the regenerant for the fiber suppressor was 0.025N H_2SO_4 fed by gravity at a rate of 3.0 mL/min. The 50µL loop on the injector valve was flushed and filled with 3 mL aliquots of 0.45µm filtered sample. The output was set at 30 µs (micro Siemens) full scale and the signal was recorded with a Spectra-Physics 4270 integrator.

The combined standard for calibrating the ion-chromatograph was prepared by adding measured quantities of stock solutions, each containing 1000 mg/L of one of the five ions mentioned above. The standard solution had 20 mg/L of PO_4-P and SO_4-S, and 10 mg/L of NO_3-N , NO_2-N and Cl. The filtered samples were not acidified but refrigerated for storage because acidification caused an evolution of carbon dioxide from the eluent, and/or overlapped one or more of the ions' peaks with the peak for the acid.

Alkalinity

Alkalinity measurements on the filtered samples were conducted in accordance with the procedures outlined in section 403, Alkalinity, Standard Methods (1985). Samples having high

levels of alkalinity were diluted so that 'reasonable' amounts of 0.02N sulfuric acid would be used in titrations. The titrations were terminated when the pH decreased to 4.3.

Calcium, Magnesium, Sodium, Potassium and Iron

The concentrations of these cations in solution were measured by analyzing the 0.45μm filtered samples using a Model 703, Perkin-Elmer (Norwalk, CN) Atomic Absorption Spectrophotometer. The samples were preserved by acidifying them with concentrated nitric acid to a pH lower than 2.0.

In order to analyze for the total recoverable metal fractions, a method suggested by the USEPA (EPA-600/4-79-020, Revised March 1983) was followed. The samples were digested by adding 5.0 mL of concentrated hydrochloric acid to 100 mL of the sample or an appropriate dilution of it, and boiled to decrease to a volume to between 10 and 15 mL. After digestion, the sample was cooled, diluted to 100 mL and filtered through a coarse filter to remove the particulate matter. The filtered samples were analyzed using the Atomic Absorption Spectrophotometer described above.

Total Phosphorus

The total phosphorus content of samples was measured by first using the persulfate digestion method, Section 424C, Standard Methods (1985) as a preliminary digestion step; this was followed by the Ascorbic Acid Method, Section 424F, Standard Methods (1985) to colorimetrically measure for ortho-phosphates in the digested sample. The colorimetric measurements were done using a Beckman Instruments, Inc. (Irvine, CA) DU-6 Spectrophotometer with a one centimeter light path at a wavelength of 880 nm. The standard curve was developed for each new set of samples. The concentration of phosphorus in the dilutions of the samples were kept in the range from 0.15 to 1.0 mg/L of PO_4^{3-}-P, the range in which the standard curve is accurate.

pH

pH was measured with a FISHER ACCUMET pH meter (Model 610). Repeated calibrations and checks using standard buffer solutions were conducted to obtain pH readings accurate to the second decimal place.

Solids Determinations

The mixed liquor total solids were measured in accordance with Section 209A, Total Solids Dried at 103-105°C, Standard Methods (1985). Total volatile solids were determined by igniting the sample dried sample (103°C for atleast 2 hours) at 550°C for 30 minutes and measuring the difference in sample weight.

Total Dissolved Solids were measured by drying a known volume of a filtered sample (0.45μm) at 103 to 105°C for at least two hours.

In samples where the suspended solids content was less than 1000 mg/L, the total suspended solids were measured by filtering through a Whatman (Whatman Limited, Maidstone, England) 934-AH glass fiber filter paper. For others, the total suspended solids were measured by subtracting the total dissolved solids from total solids.

Phase II

As mentioned earlier, phase II involved setting up samples at 35°C by adding known quantities of ions to a distilled water *i.e.* 'clean' environment in order to simulate the chemical environment and kinetics of precipitate formation in the primary anaerobic digester at the York River Wastewater Treatment Plant.

The 'clean' sample was formulated by adding stock solutions containing one compound each in the sequence described below. A set of simultaneous equations containing 'n' variables was solved by using the mathematical subroutine LEQT1F available on the mainframe computer at VPI&SU in the following manner:

If A, B, C, --- and N are the masses of N ions in a liter of the liquid phase of the chemical matrix of the composite sample,

a_1, a_2, --- and a_n are the concentrations of ion A in stock solutions 1 to n,

v_1, v_2, --- and v_n are the volumes of stock solutions 1 to n to be used in building the matrix, then,

$$a_1v_1 + a_2v_2 + \text{---} + a_nv_n = A \quad [3.1]$$

$$b_1v_1 + b_2v_2 + \text{---} + b_nv_n = B \quad [3.2]$$

$$c_1v_1 + c_2v_2 + \text{---} + c_nv_n = C \quad [3.3]$$

$$n_1v_1 + n_2v_2 + \text{---} + n_nv_n = N \quad [3.4]$$

If the amount of composite sample, V_c is different from one liter, the volume of each stock to be used, V_{Tn} is given by equation 3.5.

$$V_{Tn} = v_n \times \frac{V_c}{1.0} \quad [3.5]$$

To prepare the composite sample, the ions were added using of the following stock solutions:

Magnesium as magnesium chloride,

Potassium as potassium chloride or potassium dihydrogen phosphate,

Calcium as calcium chloride,

Phosphorus as sodium dihydrogen phosphate or potassium dihydrogen phosphate,

Ammonium-N as ammonium chloride and

Carbonate alkalinity as sodium bicarbonate.

In some experiments, acetates were added as sodium acetate.

This list of stock solutions was arrived at after rejecting compounds like ammonium bicarbonate and carbonate whose high pH and strengths made them unstable with respect to their ammonium and carbonate contents. The stock solutions were added in a particular sequence to prevent the formation of chemical precipitates while the composite sample was being prepared, i.e. before all the stock solutions could be added.

To prepare 1500 mL of a composite sample, magnesium and calcium chloride were added to a 500 mL volumetric flask, and the rest of the stock solutions to a 1000 mL volumetric flask. After

the addition of the stock solutions, the flasks were filled to the mark with distilled water, and the pH of the 1000 mL flask solution adjusted to 7.30 with 1N hydrochloric acid in a 2000 mL beaker. 500 mL of the magnesium and calcium chloride were poured in with stirring and the pH adjusted back to 7.30 with 1N sodium hydroxide or hydrochloric acid. The composite sample was then poured into a set of 150 mL bottles sealed with no air space and incubated at 35°C for different lengths of time. The total volume of acid and/or base was noted for future calculations.

Stock solutions containing phosphorus, nitrogen and carbonate were stored at 0 to 4 °C. The strength of the stock solutions had to be within a range so that equations 3.1 to 3.4 solved for positive volumes. The commonly used concentrations were:

1,500 mg/L of magnesium as magnesium chloride,

3,000 mg/L of potassium as potassium chloride,

3,000 mg/L of calcium as calcium chloride,

5,000 mg/L of sodium as sodium dihydrogen phosphate,

10,000 mg/L of ammonium nitrogen as ammonium chloride and

12,500 mg/L of sodium as sodium bicarbonate.

Chloride and sodium ions did not enter the set of equations to be solved. However, if a sufficient number of compounds were available for use as stock solutions to come up with the additional equations, the system could be solved for specific values of these ions.

Framework of the Kinetics Study

Three levels of soluble phosphorus were used to simulate the conditions in the digester prior to, intermediate and at near steady state after the modification of the plant *i.e.* 100, 300 and 600 mg/L. The molar ratios for proportionately increasing magnesium and potassium levels with phosphorus above 100 mg/L in the digester were 0.26 and 0.24 mole respectively per mole of phosphorus released. These values were obtained from release ratios observed in the BPR unit of

the plant (Table 10, Chapter IV). Table 4 gives the levels of phosphorus and the corresponding levels of magnesium and potassium used in the kinetics study. Table 5 is a set by set layout of the experiment.

The length of the incubation period for the composite samples in the 150 mL bottles is shown in Table 6. Samples D, F and H of each set in the experiment were duplicated as E, F and J, respectively, except for the fact that balls of cotton fibers were added to the latter to serve as additional surfaces for precipitate formation.

Analysis of precipitates

pH

The pH was measured immediately after taking the cap off the bottles following their incubation. Exposure to the normal atmosphere for extended periods of time resulted in a significant loss of carbon dioxide from the composite sample and a corresponding increase in the pH.

Filtration

The samples were filtered using a glass syringe holding a 25 mm diameter, 0.45μm Metricel Membrane Filters, Gelman Sciences Inc., in a syringe filter holder. Filtration was conducted immediately after pH measurement to avoid an increase in pH due to the evolution of carbon dioxide.

Alkalinity

Alkalinity measurements were conducted on 2 mL of the filtered sample by diluting it and titrating against 0.02N sulfuric acid. Only 2 mL samples were used because the alkalinities ranged between 1800 and 3000 mg/L as calcium carbonate. Alkalinities were measured immediately after filtration to avoid increases in pH which could lead to precipitate formation.

Preservation

Table 4. Levels of phosphorus, magnesium and potassium in kinetics study

Phosphorus	Magnesium	Potassium
mg/L		
100	15	69
300	55	125
600	115	210

Table 5. Set by set layout of kinetics study

Set	Ca	Mg	K	NH_4-N	P	Alk[1]	Expected precipitate
	mg/L						
6-4	100	0	69	800	100	2500	Ca-P
6-5	100	0	125	800	300	2500	Ca-P
6-6	100	0	210	800	600	2500	Ca-P
6-7	0	15	69	800	100	2500	Mg-NH_4-P, Mg-P
6-8	0	55	125	800	300	2500	Mg-NH_4-P, Mg-P
6-9	0	115	210	800	600	2500	Mg-NH_4-P
6-10	100	15	69	800	100	2500	Ca-P, Mg-NH_4-P, Mg-P
6-11	100	55	125	800	300	2500	Ca-P, Mg-NH_4-P, Mg-P
6-12	100	115	210	800	600	2500	Ca-P, Mg-NH_4-P, Mg-P
6-13	0	55	125	0	300	2500	Mg-P
6-14	0	115	210	0	600	2500	Mg-P
6-15	100	115	210	0	600	2500	Ca-Mg-P, Ca-P, Mg-P/$C0_3$
6-16	100	115	210	0	0	2500	Ca-Mg-CO_3, Ca/Mg- CO_3

Alk[1] = alkalinity as mg/L of $CaCO_3$

Table 6. Time Frame for each combination of a set

Sample	Solid Surface	Days	Hours
A		0	0.5
B		0	1
C		0	6
D		1	0
E	Cotton	1	0
F		5	0
G	Cotton	5	0
H		30	0
J	Cotton	30	0
K		> 90	0

After alkalinity measurements, the samples were acidified with approximately 2.5 mL of concentrated nitric acid per 50 mL of filtered sample. The amount of acid required to maintain the pH below 2.0 was relatively high because of high carbonate alkalinities.

Metals

The acidified samples were analysed for soluble metals — calcium, magnesium, potassium and sodium — using an Atomic Absorption Spectrophotometer.

Precipitation

The levels of ions precipitated were calculated from the difference in the concentration between the incubated sample and the initial sample at time zero.

Separation of the precipitates

Samples were processed by centrifugation to separate the liquid phase of the 'clean' sample from the solid phase of the precipitate. The incubated samples were first stirred and the crystals and precipitates scraped off the sides of the bottle. The samples were centrifuged at 15000 rpm for 15 minutes in plastic tubes in a Beckman Model J-21C Centrifuge. The supernatant was poured off and the residue at the bottom of the centrifuge tubes mixed with 190 proof ethanol to remove most of the solution. The mixture was recentrifuged under similar conditions, the clearer portion of the alcohol decanted off and the alcohol-precipitate mix poured into a clean glass petri-dish.

Storage of precipitate

The alcohol was allowed to evaporate off the mix in the petri-dish and the precipitate stored in a constant humidity environment at room temperature to prevent dehydration of the precipitate/crystals. Subjecting the crystals of struvite to a temperature of 65°C resulted in partial loss of the water of crystallization.

X-Ray diffraction analysis

The precipitate was crushed to a fine powder in an agate mortar and pestle grinder. The grain size of the powder was examined under a Bausch and Lomb binocular microscope (0.7X - 3.0X) operated in conjunction with a Bausch and Lomb External Lamp. The powder had to be

sufficiently fine to expose most of the crystal planes. A few drops of acetone were added to smear the powder on a glass slide and leave a uniform coat after the acetone evaporated.

The crystalline powder was mounted on an Open Beam Analytical X-Ray equipment, Philips Electronic Instruments, Mount Vernon, N.Y.. The instrument uses a Copper K α X-Ray Beam with a wavelength of 1.54178 A°. The instrument is integrated with a DIGITAL PAP11 printer (Digital Equipment Corp., Maynard, MA). The normal scan speed was 2°θ per minute with the strip chart moving an inch in the same time. For very fine precipitates, the scan speed was slowed to 0.5°θ per minute.

The pattern generated was compared with those of the crystalline species listed in the Powder Diffraction File published by the Joint Committee on Powder Diffraction Standards, Swarthmore, Pennsylvania. The standard patterns for struvite and hydroxyapatite are shown in Appendix B.

Solubility studies on precipitates

For those precipitates which were amorphous or whose particle sizes were too fine, the X-ray diffraction pattern could not be correlated to any particular compound. The solubility of the precipitate and the stoichiometry of the release of ions at different pH levels were studied in an attempt to identify the precipitate. The pH was adjusted with 0.02N sulfuric acid and the molar ratios of the cations and anions released quantified. The cations were measured on the Atomic Absorption Spectrophotometer, phosphorus by the ascorbic acid method and chlorides on the ion-chromatograph.

Phase III

Thermodynamic model

A computer model was written in FORTRAN 77 on the IBM 3090 Mainframe computer at VPI&SU to predict the thermodynamic equilibrium with respect to a number of compounds. The present version of the model handles calculations of supersaturation with respect to 72 compounds, most of which are precipitates of calcium, magnesium and iron with phosphorus and carbonates. Ionic strength effects are also incorporated into the structure of the model.

An auxiliary program (STRUVAUX) was used to calculate the solubility product at 25°C, Ksp_{25}, for each of the compounds. The Ksp_{25} was calculated at zero ionic strength with respect to a maximum of twelve speciations. Four of the speciations were for phosphorus, i.e. PO_4^{3-}, HPO_4^{2-} , $H_2PO_4^-$ and H_3PO_4 , three for carbonate and two for compounds containing chloride and sulfide ions. In other words, the solubility product of a compound like struvite was calculated using equations like

$$MgNH_4PO_4.6H_2O\ (s) = Mg^{2+} + NH_4^+ + PO_4^{3-} + 6H_2O \qquad [3.6]$$

or

$$MgNH_4PO_4.6H_2O\ (s) + H^+ = Mg^{2+} + NH_4^+ + HPO_4^{2-} + 6H_2O \qquad [3.7]$$

to describe two. The program had an override feature which allowed it to use a reported value of Ksp_{25} with respect to a reaction if data on the standard free energy (ΔG^0) was not available for use in the calculation of the solubility product.

The value of Ksp_{25} was calculated thermodynamically by using the relationship

$$\Delta G^0 = -RT \ln Ksp_{25}$$

where $\Delta G^0 = (\Sigma v_i G_i^0)_{products} - (\Sigma v_i G_i^0)_{reactants}$

v_i = stoichiometric coefficient

G_i^0 = free energy of the species in kilojoules per mole at 25°C and 1 atm. pressure [3.8]

R = universal gas constant

T = 298°K(25°C)

The output file contains the values of the solubility products and serves as the data file for the main program (STRUV).

The main program had the following features.

1) It speciated anionic species based on the pH value of the system entered by the user.

2) The ionic strength was calculated from the concentrations of ions read in and the acid dissociation constants were modified using activity coefficients calculated in step 3. The ionic strength was calculated iteratively with the modification of the hydrolysis constants (which affect the concentration of the speciations) until successive calculations differed by less than 0.01.

The ionic strength was calculated as

$$I = \frac{1}{2}\Sigma C_i Z_i^2$$

where Z_i = charge on an species i [3.9]

and C_i = concentration of the species i

3) Calculated the activity coefficients as

$$\log f = -A Z^2 \sqrt{I} \qquad [3.10]$$

for ionic strengths less than 0.1, or

$$\log f = -A Z^2 \frac{\sqrt{I}}{1 + \sqrt{I}} \qquad [3.11]$$

for ionic strengths in excess of 0.1

In equations 3.10 and 3.11, the value of A was given by the relationship

$$A = 1.82 \times 10^{6}(DEC * T)^{3/2} \qquad [3.12]$$

where DEC is the Dielectric Constant for water

A multiple regression fit was used to calculate the dielectric constant for water by extrapolating the values listed in Table 3.5 (from the CRC Handbook of Chemistry and Physics, 65th ed. page 56) for the atmospheric pressure and interpolating for the temperature in the digester or the sample.

4) The program used the van't Hoff equation to adjust the values of the solubility products and the acid dissociation constants for the temperature of the sample —

$$\text{where} \qquad \ln\frac{Ksp_{25}}{Ksp_{T2}} = \frac{\Delta H^{\circ}}{R}\left(\frac{1}{T_{T2}} - \frac{1}{T_{25}}\right) \qquad [3.13]$$

In the above equation

$$\Delta H^{\circ} = (\Sigma v_i H^{\circ}_i)_{products} - (\Sigma v_i H^{\circ}_i)_{reactants} \qquad [3.14]$$

where

v_i = the stoichiometric coefficient

H°_i = the enthalpy of formation of the species i in kilojoules/mole under standard conditions of 25°C and 1 atmosphere pressure,

R = the universal gas constant, and

T = the temperature in degrees Kelvin.

5) The degree of supersaturation was calculated on a log scale by subtracting the log of the solubility product, Ksp_T from the log of the reaction quotient, Qsp_T.

Table 7. Static Dielectric constant of Water Substance

	T	273.15	298.15	323.15
P				
10		88.28	78.85	70.27
20		88.75	79.24	70.63
30		89.20	79.63	70.98

P = Pressure in MegaPascals (MPa)
1 atmosphere = 1 MPa × 9.8692
T = Temperature in °K

Analysis of the primary digester sample for crystals

About 100 mL of the primary digester mixed liquor was centrifuged to separate out the solid phase from the supernatant. Small quantities of the centrifuged sludge mass was dried at room temperature and examined under a compound microscope at magnifications of 100 and 400X. The crystals, which on occasions were visible to the naked eye, were separated from the sludge with pair of tweezers under a Bausch and Lomb (0.7X - 3X) binocular microscope. Because of the tendency of the dried sludge mass to stick to some of the crystals, care was taken to remove as much of the unwanted residue as possible from the crystals to be crushed. The X-ray diffraction pattern was studied to identify the crystals and compare them to those precipitated in phase II.

Studies on the Return Activated Sludge

Return activated sludge samples collected on March 24th, 1986 were sealed in bottles and incubated under anaerobic conditions for different lengths of time to examine the extent of release of phosphorus from the volutin granules (poly-phosphate granules). The levels of soluble phosphorus, calcium, magnesium, sodium, potassium, and in some cases, iron, were measured by methods described earlier. The levels of acetates and propionates were measured using a Dionex HP1CE-AS1 ion exclusion column on the Dionex 2010i Ion Chromatograph.

The experiment was also designed to examine the characteristics of *Acinetobacter species* at York River by aerating the return activated sludge after it had been incubated anaerobically. In a few samples, additional phosphorus was added as potassium dihydrogen phosphate, KH_2PO_4 to examine if the bacteria could take up additional amounts of phosphorus in the absence of fresh substrate. The results of this experiment are tabulated in Chapter IV and discussed in the following chapter.

Results

The results have been arranged in a manner to support the objectives of this research in the order of the phases outlined earlier. The first part of this chapter presents data which elucidate the changes across the plant with the onset of biological phosphorus removal. The second portion covers the data collected as part of the kinetics study and applies it in the thermodynamic model. The remainder presents conclusive evidence which allows one to correlate the findings of the kinetics study to changes observed in the digester. In addition, the chapter will cover the results of experiments dealing with some of the characteristics of the biological sludge which had an impact on the interpretation of some of the observations.

Trend in data with the onset of biological phosphorus removal

Data collected by sampling at various locations throughout the plant before and during the onset of biological phosphorus removal are presented in Appendix A. Though it took only four weeks for phosphorus removal to be established to levels that the secondary effluent phosphorus content dropped from above 5 mg/L to about 2 mg/L, the primary and secondary anaerobic digesters, each with an operational hydraulic retention time of about 120 days and operating

essentially as flow through systems, took over four months to reach 'near' equilibrium levels. The condition of a flow through system was violated only very rarely when some of the supernatant from the secondary digester was sent directly to the headworks.

The trend in the raw influent and secondary effluent phosphorus levels over the course of this study is presented in Table 8. The data show that phosphorus removal was established between August 4th and September 4th. The sampling dates have been linearized as the number of days from the modification of the plant on August 4th , negative numbers representing days prior to the BPR modification.

Tables C1 to C4 (Appendix C) present the trend in concentrations of various cationic species and phosphorus across the digesters and over the course of the study.

A charge balance conducted on September 4th and based on the release of ions above the levels in the secondary effluent is presented in Tables 9 and 10. The release was mediated through the storage of fresh substrate as PHB, besides the possible breakdown of poly-P granules for maintenance energy (Chapter II).

From the data presented in Table C3, Appendix C, the trend in increase in phosphorus in the primary digester was plotted in Figure 10. The figure showed a significant increase in the soluble phosphorus levels from about 50 mg/L before the modification to 300 mg/L after the modification. On the basis of the observations made by Wentzel *et al.* (1986), a major portion of this increase could be attributed to the breakdown of poly-P granules for maintenance energy. The increase in average soluble phosphorus levels from 6 mg/L in the secondary effluent to 50 mg/L in the primary digester before the BPR modification was due to lysis (and digestion) of biomass. After the modification, lysis of cells may have released a fraction of the undissociated poly-phosphate granules, if any remained undissociated.

Table 8. Trend in raw influent and secondary effluent phosphorus levels with the establishment of biological phosphorus removal

Date	Days[1]	RI Tot P	SE Sol P	% Removal
		mg/L		
June 29th	-36	8.20	6.74	17.8
July 17th	-21	9.08	6.44	29.1
July 31st	- 4	9.05	6.57	27.4
Aug 5th	1	9.87	7.06	28.5
Aug 19th	15	7.62	4.23	44.4
Aug 31st	27	7.70	2.07	73.1
Sept 16th	43	10.35	2.12	79.5
Oct 14th	71	9.20	1.11	87.9
Oct 28th	85	9.46	2.04	78.4

Day[1] = Days since BPR modification
RI Tot P = Total Phosphorus in raw influent (influent wastewater)
SE Sol P = Soluble Phosphorus in secondary effluent (the total phosphorus in the secondary effluent is representative of the clarifier's efficiency in removing suspended biomass in addition to the soluble phosphorus and cannot therefore be used to calculate removal efficiencies).

Table 9. Moles of cations released with phosphorus over secondary effluent levels at York River(9/4/86)

		Release (mM) of 0.45μ filterable species					
Zone		P	Ca	Mg	Na	K	Fe x 10^{-3}
SE	aero	0.00	0.000	0.000	0.00	0.000	0.0
CN2	anaer	1.51	0.015	0.377	-0.49	0.314	4.5
CN4	anaer	1.20	-0.020	0.335	-0.39	0.283	1.8
CN6	aero	0.56	-0.070	0.149	-0.86	0.118	2.0
ATE	aero	0.31	-0.028	0.129	-0.35	0.123	2.7
RAS	anaer	1.90	0.113	0.463	1.00	0.448	9.9

aero = aerobic
anaer = anaerobic
SE = Secondary Effluent
CN2, CN4, CN6 = Mixed liquor cell nos 2, 4 and 6.
ATE = Aeration Tank Effluent
RAS = Return Activated Sludge

Table 10. Molar ratios of release of cations with phosphorus over secondary effluent levels at York River on 9/4/86.

		Release (mM/mM) of 0.45μ filterable species				
Zone		Ca/P	Mg/P	Na/P	K/P	Fe x 10^{3}/P
SE	aero					
CN2	anaer	0.010	0.250	-0.32	0.208	3.0
CN4	anaer	-0.017	0.279	-0.33	0.283	1.5
CN6	aero	-0.125	0.266	-1.54	0.211	3.6
ATE	aero	-0.09	Erw	-1.13	Erw	8.7
RAS	anaer	0.059	0.243	0.53	0.236	5.2
Mean			0.260		0.235	
St. Dev.			0.016		0.035	

aero = aerobic
anaer = anaerobic
Erw = Error with respect to reference
SE = Secondary Effluent
CN2, CN4, CN6 = Mixed liquor cell nos 2, 4 and 6.
ATE = Aeration Tank Effluent
RAS = Return Activated Sludge
St. Dev. = Standard Deviation

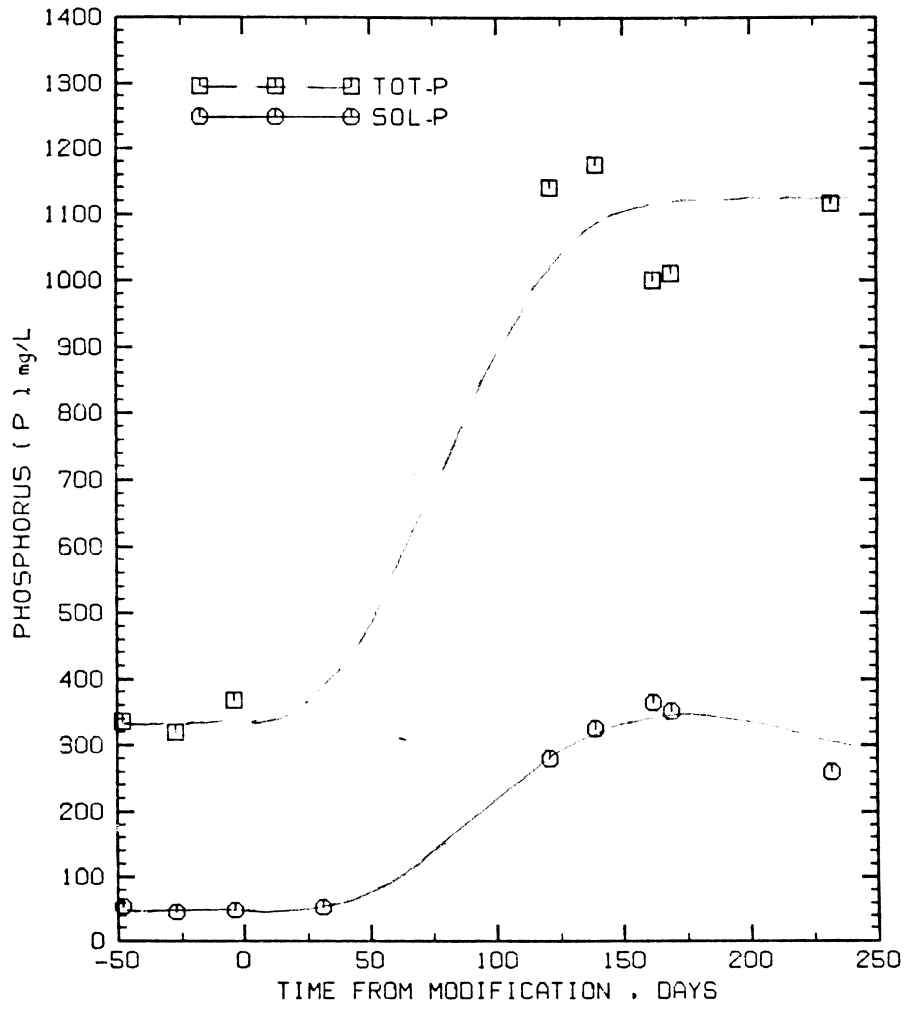

Figure 10. Graph of Soluble and Total Phosphorus levels in the Primary Digester with Time from the Modification

In order to determine the nature of the precipitates which could have formed in the primary digester as a result of the increase in phosphorus and the release of cations associated with poly-P and ATP, the trend in the concentrations of soluble metal species in the primary digester was studied with respect to time (Figure 11). As would be expected from the data presented in Table 9, the level of soluble potassium showed an increase paralleling the increase of soluble phosphorus in the digester. Since the literature reviewed yielded no potassium precipitates having solubilities low enough to precipitate out of solution at pH levels less than 7.5 for the potassium levels expected in the digester, the trend in increase in potassium should be an accurate measure of its release from the cells. Sodium did not show any correlation, as would be expected from the trend in Table 10 and various literature sources. The increase in soluble potassium was statistically significant as seen from the analysis performed in Table 11.

The level of soluble calcium should either have remained constant, if the apparent lack of correlation (Table 10) between calcium and phosphorus uptake and release held true, or have increased because of the reported association of poly-P with calcium (Buchan, 1983). The drop in soluble calcium levels, was statistically significant (Table 11), and can be explained on the basis of the formation of a Ca-P precipitate at higher levels of soluble phosphorus in the digester after the BPR modification.

The curve for soluble magnesium did not show the increase expected on the basis of the ratio its release with phosphorus (Table 10 and Table 11). However, the total magnesium increased significantly because of its association with the volutin in the sludge (Table 12). At the same time, Figure 11 could not provide any evidence of a concomitant release and precipitation of magnesium, which was a definite possibility.

The plot of total recoverable metals in the digester against the time since the modification (Figure 12) presented some interesting insights. The levels of total potassium and magnesium, each showed increase; however unlike magnesium, most of the potassium remained soluble. As would be expected from its lack of association with poly-P, the total sodium levels remained more or less

Table 11. **Analysis of the difference in mean soluble metal concentrations in the TPS, TWS and PD before and after BPR modification.**

Analysis of means performed by the two sample t-parameter test.

Null Hypothesis: $H_o\ \mu_1 = \mu_2$, $H_1\ \mu_1 \neq \mu_2$.

Calcium

		Samples[2]	Mean	St. Dev.	t_{calc}	$t_{0.95}$	
TPS	BM[1]	3	182	36			
	AM[1]	4	233	87	0.94	2.57	accept $\mu_1 = \mu_2$
TWS	BM[1]	1	87				
	AM[1]	3	137	40	1.09	4.30	accept $\mu_1 = \mu_2$
PD	BM[1]	3	104	9			
	AM[1]	5	29	3.	17.	2.45	reject $\mu_1 = \mu_2$

Magnesium

TPS	BM[1]	3	20.3	2.5			
	AM[1]	4	31.0	16.2	1.11	2.57	accept $\mu_1 = \mu_2$
TWS	BM[1]	3	23.0	3.2			
	AM[1]	3	124	45.0	3.86	2.78	reject $\mu_1 = \mu_2$
PD	BM[1]	1	7.6				
	AM[1]	5	9.4	1.8	0.92	2.77	accept $\mu_1 = \mu_2$

Iron

TPS	BM[1]	1	0.22				
	AM[1]	4	0.47	0.23	0.98	3.18	accept $\mu_1 = \mu_2$
TWS	BM[1]	1	0.21				
	AM[1]	4	4.4	3.46	1.09	3.18	accept $\mu_1 = \mu_2$
PD	BM[1]	1	0.24				
	AM[1]	5	0.58	0.22	1.92	2.78	accept $\mu_1 = \mu_2$

Potassium

TPS	BM[1]	3	41.	21			
	AM[1]	4	31.1	10.3	-0.84	-2.57	accept $\mu_1 = \mu_2$
TWS	BM[1]	3	73.3	16.2			
	AM[1]	4	267.3	104.2	3.12	2.57	reject $\mu_1 = \mu_2$
PD	BM[1]	3	54.	4.36			
	AM[1]	5	229.	15.6	18.5	2.45	reject $\mu_1 = \mu_2$

BM[1] = Samples collected before BPR modification TPS = Thickened Primary Sludge
AM[1] = Samples collected after BPR modification TWS = Thickened Waste Sludge
Samples[2] = Number of samples PD = Pimary Digester mixed liquor

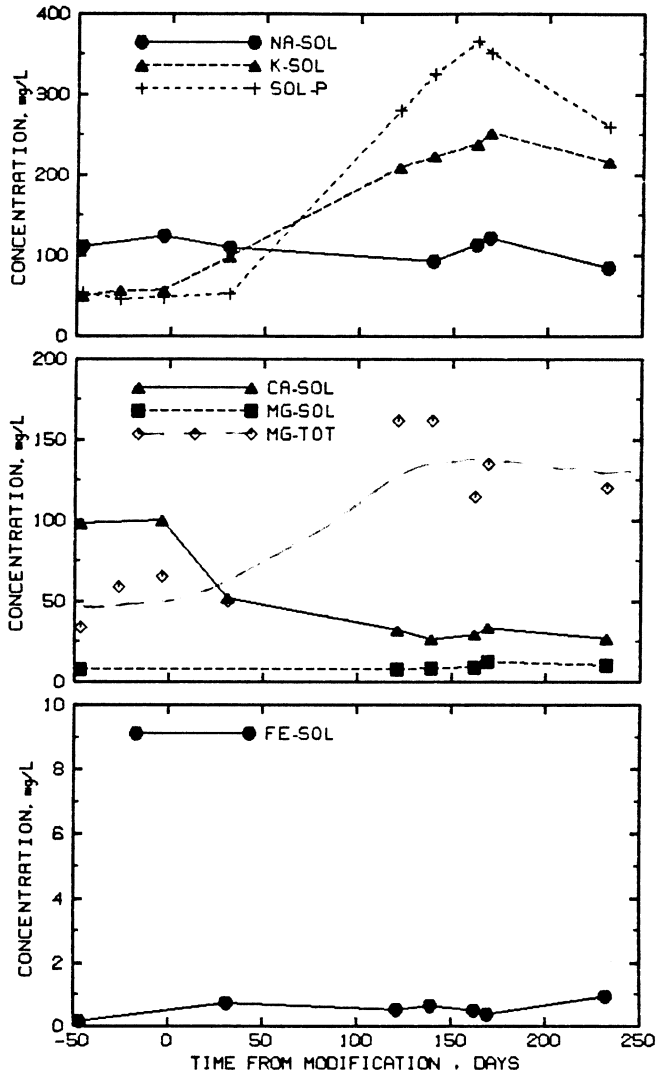

Figure 11. Trend in Soluble Metals in the Primary Digester with Time from the Modification

Table 12. Analysis of the difference in mean total metal concentrations in the TPS, TWS and PD before and after BPR modification.

Analysis of means performed by the two sample t-parameter test on a percent of total solids content basis.

Hypothesis: $H_o\ \mu_1 = \mu_2$, $H_1\ \mu_1 \neq \mu_2$.

Calcium

		Samples[2]	Mean	St. Dev.	t_{calc}	$t_{0.95}$	
TPS	BM[1]	3	2.17	0.47			
	AM[1]	2	2.66	0.28	1.28	3.18	accept $\mu_1 = \mu_2$
TWS	BM[1]	2	2.40	0.21			
	AM[1]	3	2.86	0.49	1.20	3.18	accept $\mu_1 = \mu_2$
PD	BM[1]	2	3.28	0.29			
	AM[1]	5	3.45	1.60	1.05	2.57	accept $\mu_1 = \mu_2$

Magnesium

TPS	BM[1]	3	0.112	0.045			
	AM[1]	3	0.247	0.068	2.88	2.78	reject $\mu_1 = \mu_2$**
TWS	BM[1]	2	0.281	0.002			
	AM[1]	3	1.05	0.311	3.31	3.18	reject $\mu_1 = \mu_2$
PD	BM[1]	2	0.267	0.046			
	AM[1]	5	5.0	1.21	2.74	2.57	reject $\mu_1 = \mu_2$

Iron

TPS	BM[1]	2	1.26	0.23			
	AM[1]	3	2.21	0.41	2.90	3.18	accept $\mu_1 = \mu_2$
TWS	BM[1]	2	1.56	0.22			
	AM[1]	3	1.98	0.28	1.79	3.18	accept $\mu_1 = \mu_2$
PD	BM[1]	2	0.24	0.17			
	AM[1]	5	0.25	0.26	0.34	2.57	accept $\mu_1 = \mu_2$

BM[1] = Samples collected before BPR modification
AM[1] = Samples collected after BPR modification
** need more data to prove this case
TPS = thickened primary sludge
TWS = thickened waste sludge
PD = primary digester mixed liquor

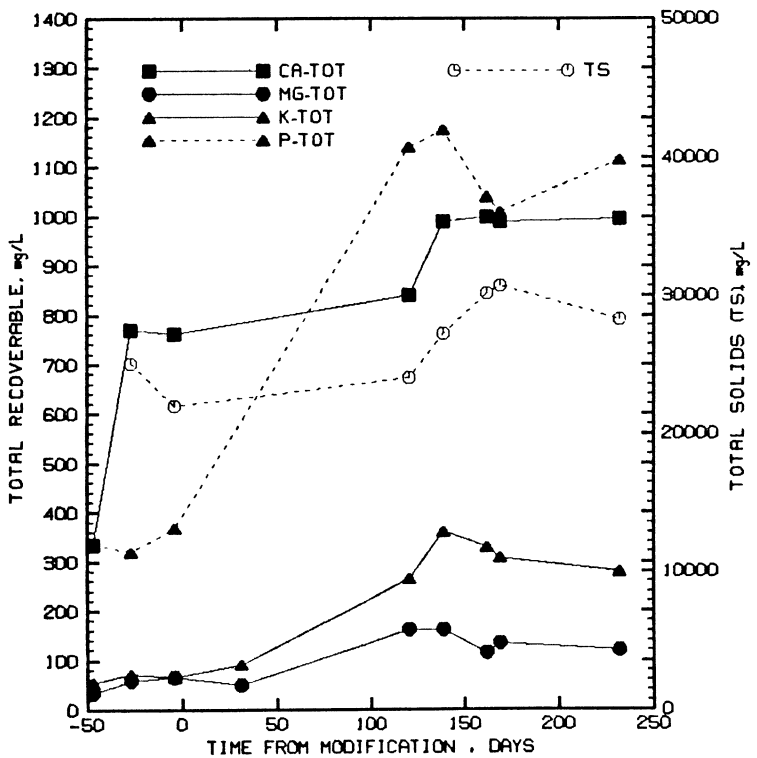

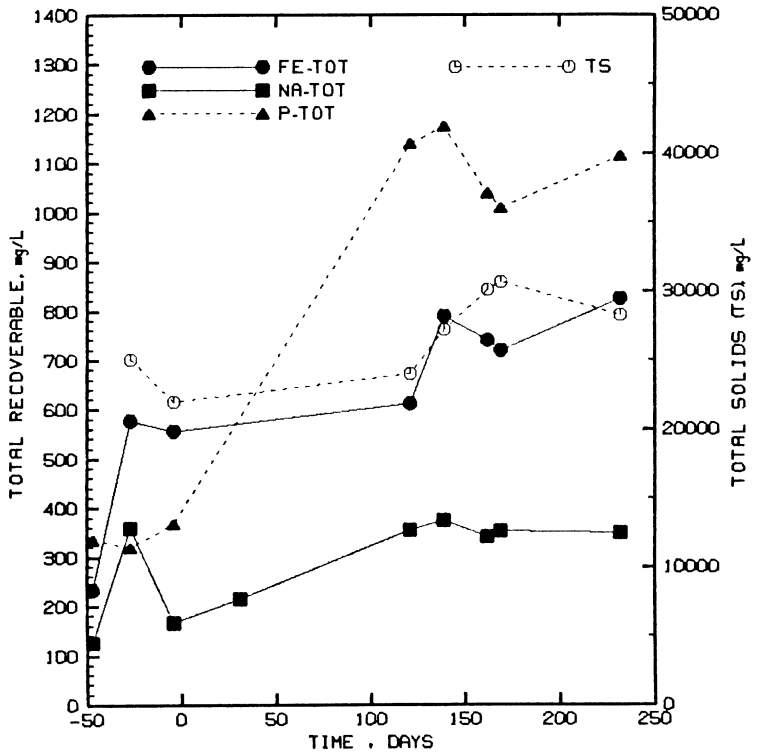

Figure 12. Trend in Total Metals in the Primary Digester with Time from the Modification

constant throughout this study. Due to the fluctuation in the total solids content of the samples analyzed, it was necessary to examine total concentrations of individual ions in terms of their percentages in the total solids present.

As seen from Figures 13 and 14, and the t-parameter tests in Tables 11 and 12, the soluble and total calcium levels (expressed as the percent of total solids) in the thickened waste sludge (TWS) stream remained fairly constant during the study. The calcium level in the thickened primary sludge (TPS) may have increased slightly in winter. Infiltration from snow-melt runoff resulted in higher levels of soluble calcium in the influent wastewater. Due to the addition of chlorinated plant effluent (non potable water) in the belt filter press for cleansing purposes, the high levels of soluble calcium in winter may have increased interaction between phosphorus and calcium in the belt filtrate flowing into the headworks. This has been discussed in the following chapter. If half the phosphorus in the secondary digester effluent were to removed by this precipitation reaction, its contribution to the amount of calcium removed in the primary clarifier from a mass balance standpoint would be less than 20 percent of the phosphorus content in the primary sludge.

The apparent increase in the percent calcium content of the primary digester mixed liquor over that in the feed streams was because of the decrease in solids in the digester (Figure 14). This decreased the denominator, while keeping the calcium level in the numerator essentially constant, thereby increasing the calcium content expressed on a percent of total solids basis.

Data presented in Figures 13 and 15 answered some of the questions concerning magnesium. In the thickened primary sludge, the magnesium level remained fairly constant. Because of the strong association between magnesium and poly-P granules, the onset of biological phosphorus removal caused a significant increase in soluble and total magnesium levels in the thickened waste sludge stream. The total magnesium content of the primary digester mixed liquor therefore increased over four months after the onset of biological phosphorus removal, a period during which the digester moved towards a state of equilibrium. A mass balance on the soluble magnesium levels in the sludge streams feeding into the digester would predict an equilibrium soluble magnesium level

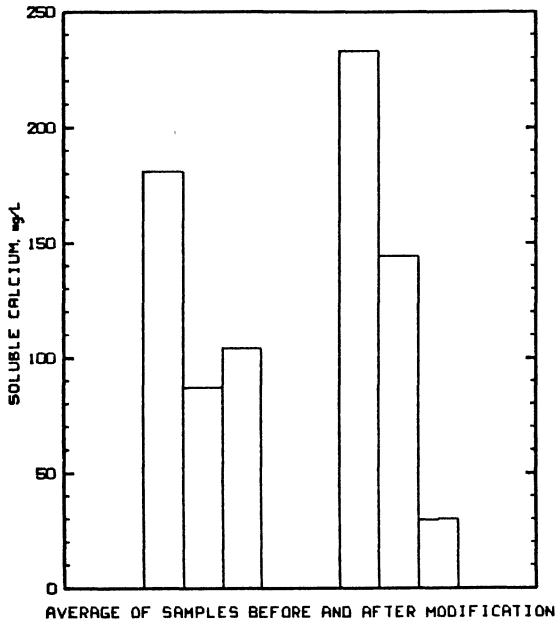

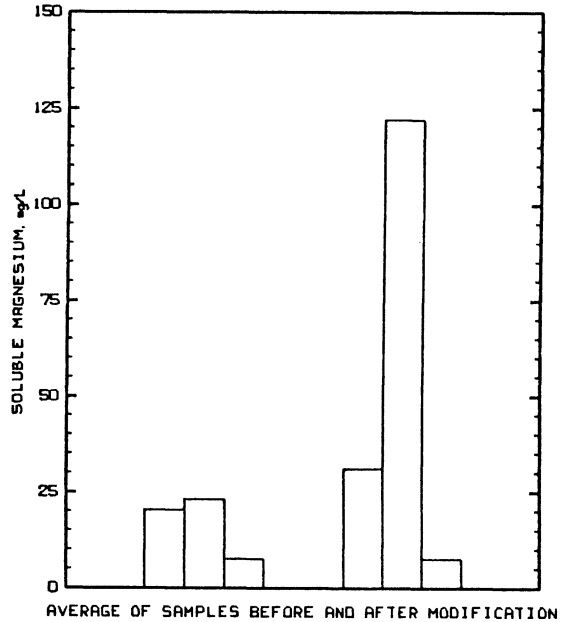

CHART 1 = Calcium CHART 2 = Magnesium
charts drawn after averaging the samples at equilibrium before and after the modification
TPS = Thickened Primary Sludge feeding into the digester
TWS = Thickened Waste Sludge feeding into the digester
PD = Primary Digester mixed liquor
* Primary Digester mixed liquor averaged on samples collected four months since the BPR modification

Figure 13. Barcharts of Soluble Calcium and Magnesium in the TPS, TWS and PD before and after BPR modification)

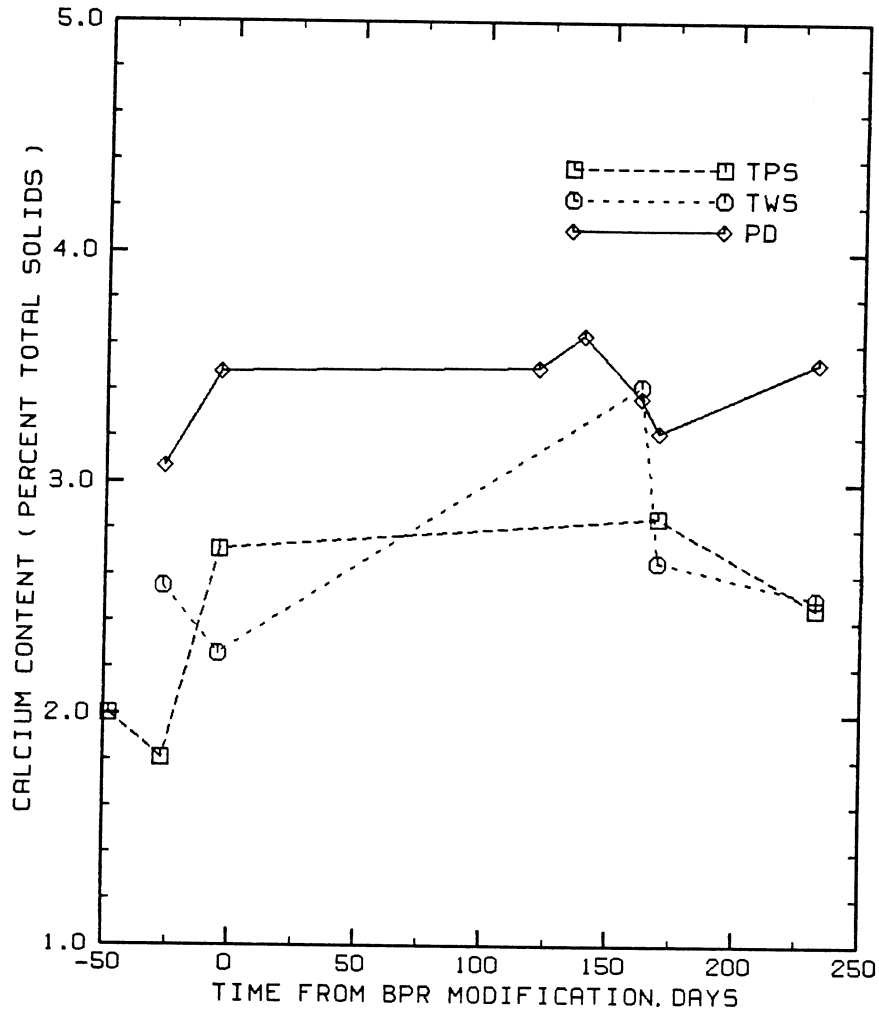

Figure 14. Plot of Percent Calcium in the Total Solids of the Primary Digester versus Time from the BPR Modification

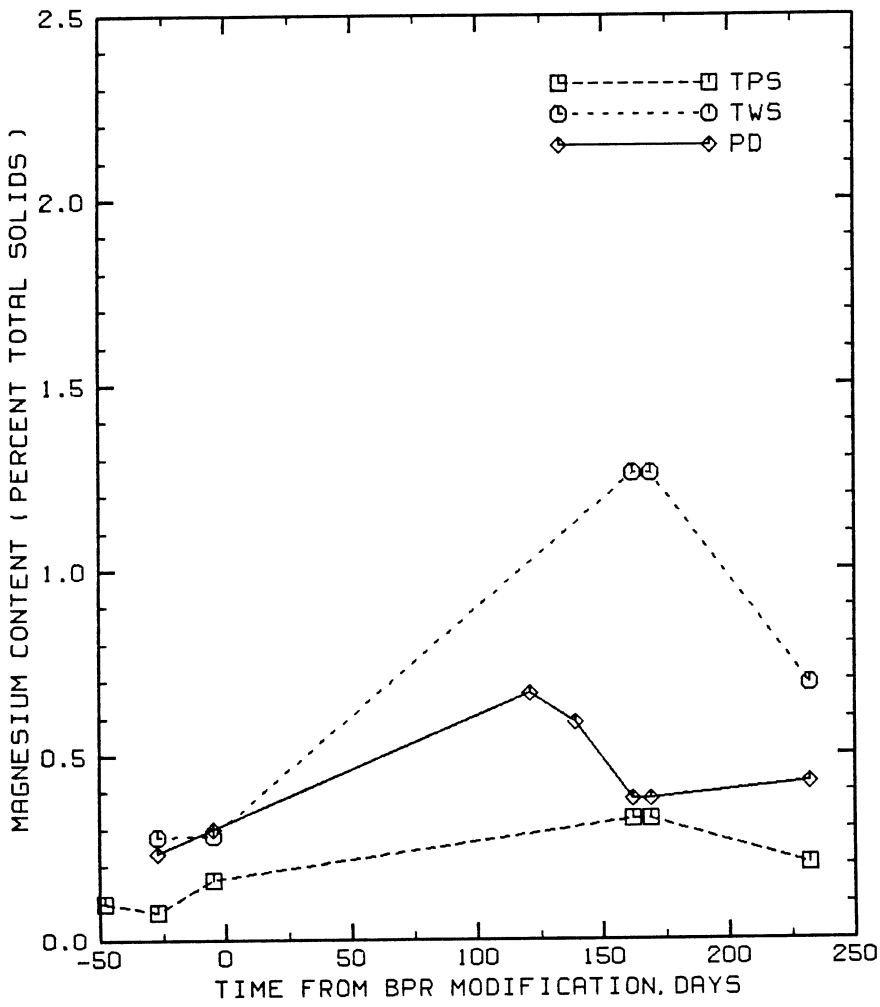

Figure 15. Plot of Percent Magnesium in the Total Solids of the Primary Digester versus time from the BPR modification

of at least 50 mg/L in the primary digester after the modification. However, the measured level was significantly lower. What may be observed in addition is that there was a similar decrease of a lower magnitude even before the modification. Obviously, a fraction of the soluble magnesium was precipitating from the solution, the nature of which was focused on in phases II and III.

Iron was not incorporated in a proportionate manner during phosphorus uptake by the biomass at the York River Plant. As long as the concentration of soluble iron in the activated sludge basin (mixed liquor tank) is not significant and very little is available for movement across the membrane, iron probably does not involve itself in the biological phosphorus removal process. This was confirmed by the relatively constant levels of iron in the thickened waste sludge stream, both before and after the modification (Figure 16). The level of soluble iron in the digester remained below 1 mg/L throughout the study. It is possible that some of the insoluble iron went from a ferric (Fe^{3+}) to a ferrous (Fe^{2+}) form in the primary digester (Singer, 1972) and precipitated some of the soluble phosphorus in the process. For this research, iron was analysed on the AA Spectrophotometer and the instrument did not distinguish between ferric and ferrous forms. An analysis of the digested sludge at York River (Nash, 1987) showed that 80% of the total iron was present in ferrous form. The fraction of ferric iron in solution should have been even lower, as observed from the analysis of saturation levels with respect to ferric compounds.

The Kinetics Study

The kinetics study was designed to isolate each possible precipitate by excluding one or more of the ions of the digester matrix at a time. Tables 4, 5 and 6 gave the framework and set by set layout of the kinetics study. The stoichiometric ratios of the precipitates or a combination of them in each set of this study are presented in Appendix D, Tables D4 to D16. The average molar ratios are listed in Table 13.

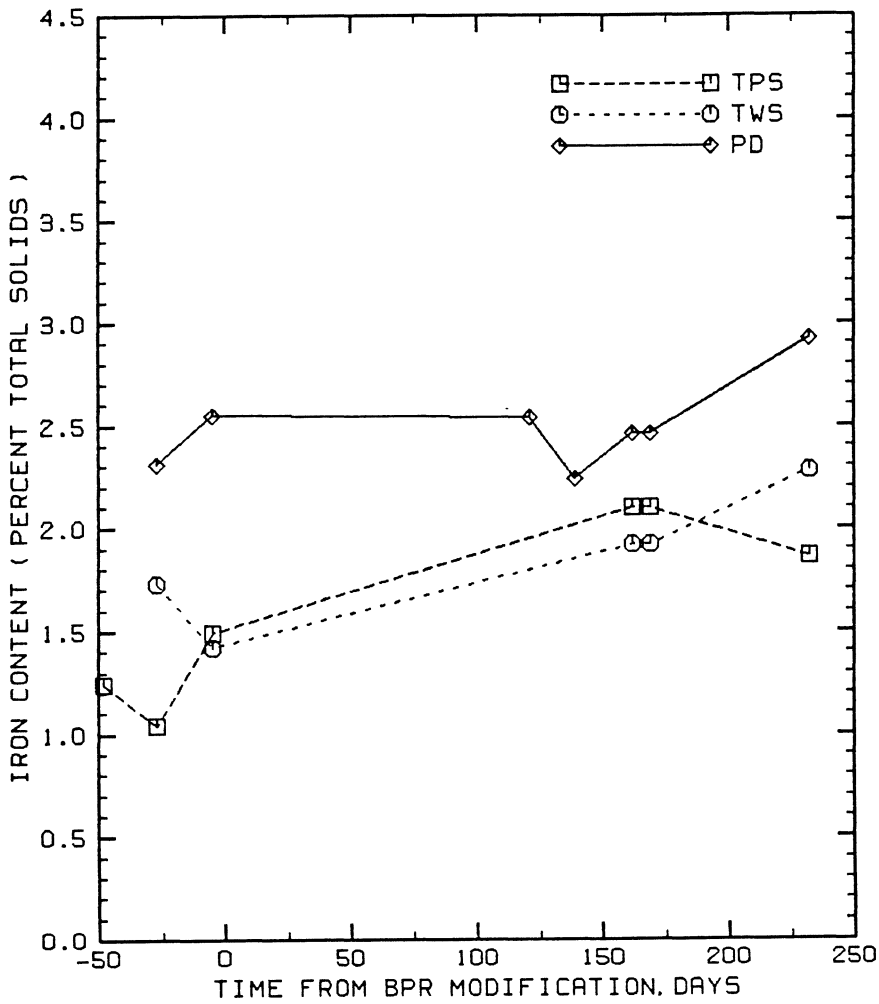

Figure 16. Plot of Percent Iron in the Total Solids of the Primary Digester versus time from the BPR modification

Table 13. Stoichiometric ratio of precipitates formed in the Kinetics Study (results in Tables D4 to D16, Appendix D)

Set	Average Ratio	St. Dev.	Comments	ppt.
6-4			Slight ppt.	fw[1]
6-5	$\Delta Ca/\Delta P = 1.50$	0.14		fw
6-6	$\Delta Ca/\Delta P = 1.50$	0.19		fw
6-7	$\Delta Mg/\Delta P = 0/0$		No ppt.	no struvite
6-8	$\Delta Mg/\Delta P = 1.07$	0.16		struvite[5]
6-9	$\Delta Mg/\Delta P = 1.11$	0.20		struvite
6-10			slight ppt.	fw[6] + struvite
6-11	$\Delta Ca/(\Delta P - \Delta Mg) = 1.62$	0.13		struvite + fw
6-12	$\Delta Ca/(\Delta P - \Delta Mg) = 1.71$[4]	0.20		struvite + fw
6-13	$\Delta Mg/\Delta P = 0/0$		No ppt.	
6-14	$\Delta Mg/\Delta P = 0/0$		No ppt.	
6-15			uc[2]	fw + uc
6-16	$(\Delta Ca + \Delta Mg)/\Delta CO_3 = 1.15$		umg[3]	aragonite[5]

[1]a fine white precipitate

[2]unidentified crystalline precipitate

[3]unidentified magnesium ppt., may be substituted in aragonite

[4]mean of last four samples only, discussed later.

[5]identified by X-ray diffraction

[5]has approximately 5 % substitution of Mg for Ca on molar basis

St. Dev = Standard Deviation

The Magnesium precipitates

The decrease in soluble magnesium concentration with time for sets 6-9, 6-12, 6-14, 6-15 and 6-16, (each having an initial concentration of approximately 600 mg/L phosphorus and 115 mg/L magnesium) is shown in Figure 17. While the decrease was zero for sets 6-13 and 6-14 and small in sets 6-15 and 6-16, it was significantly larger and more rapid in sets 6-9 and 6-12 (Appendix D). Of these sets, 6-9 and 6-12 were the only ones containing ammonium (at levels approximately equal to 750 mg/L NH_4-N). What may be inferred as a result is that a magnesium-ammonium-phosphate compound was rapidly precipitated in these sets.

In set 6-7, containing 100 mg/L of phosphorus and 15 mg/L of magnesium, there was no precipitation of magnesium. Set 6-10 had a similar composition except for the presence of 100 mg/L of calcium. The small drop in magnesium with the drop in calcium in Set 6-10 may therefore be attributed to the incorporation of magnesium in the calcium precipitate. The last column in Table D10, Appendix D, shows that a 5 percent substitution on a molar basis can be expected.

Data collected in set 6-14 showed that magnesium was not precipitated from the solution in the absence of ammonium and calcium. In spite of it being thermodynamically oversaturated with respect to some magnesium-phosphorus compounds, especially bobierrite (Figure 18), it was kinetically stable after 92 days of incubation. It may be added that the precipitation of bobierrite did not occur in the absence of seeds at a Q/Ksp ratio of $10^{4.5}$.

In set 6-15, which contained all the ions of the chemical matrix except for ammonium, small transparent crystals were observed after 94 days of incubation, in addition to a fine white precipitate formed almost instantaneously. The fine precipitate was one or more of the calcium-phosphorus precipitates discussed later. The precipitation of dolomite could be excluded because calcium was precipitated in association with phosphorus and the samples were undersaturated with respect to magnesium carbonate species. (To precipitate dolomite, it is essential that the system be supersaturated with respect to both calcium and magnesium carbonates over thousands of years.)

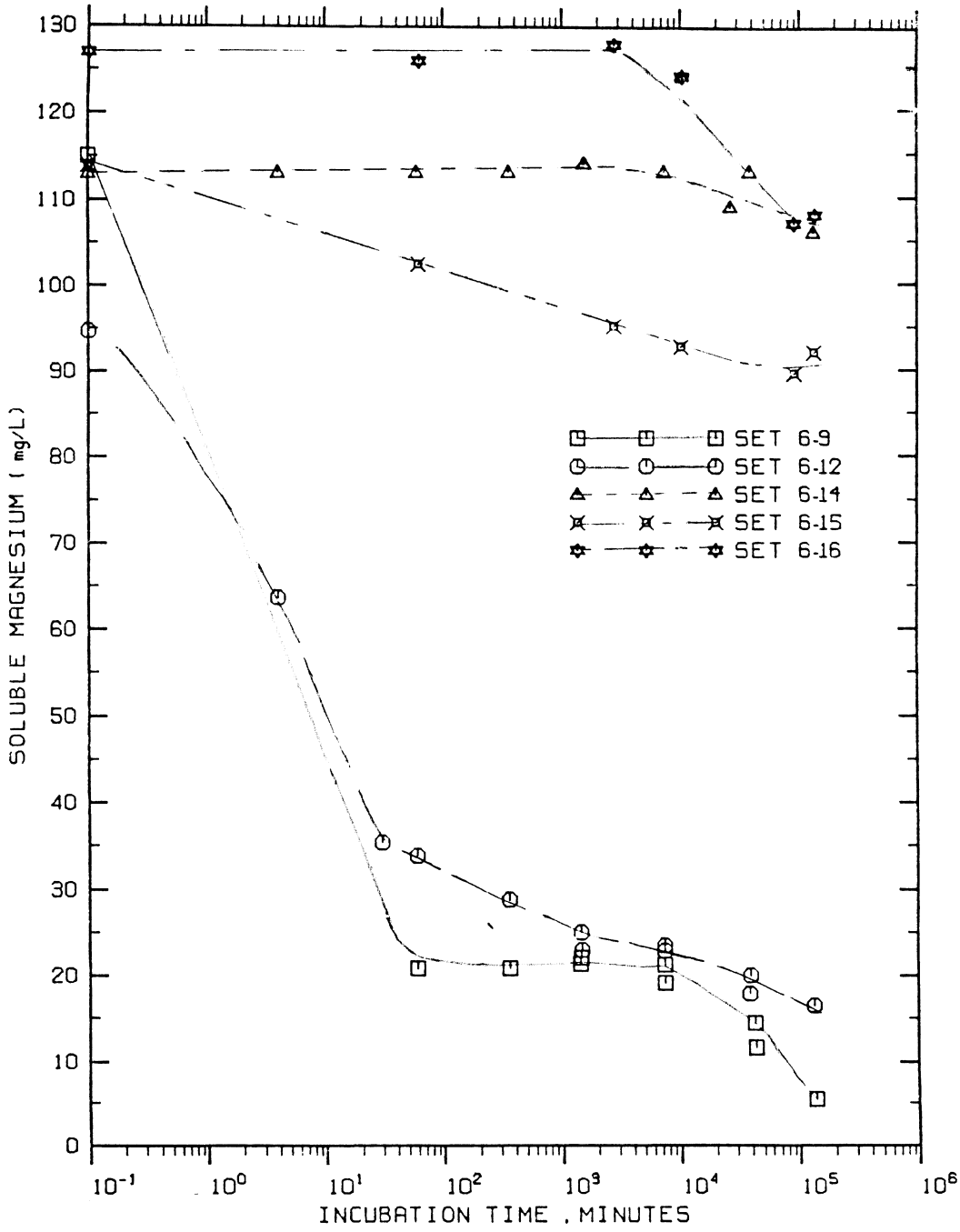

Figure 17. Magnesium levels as a function of Time in sets with an initial phosphorus level of 600 mg/L phosphorus.

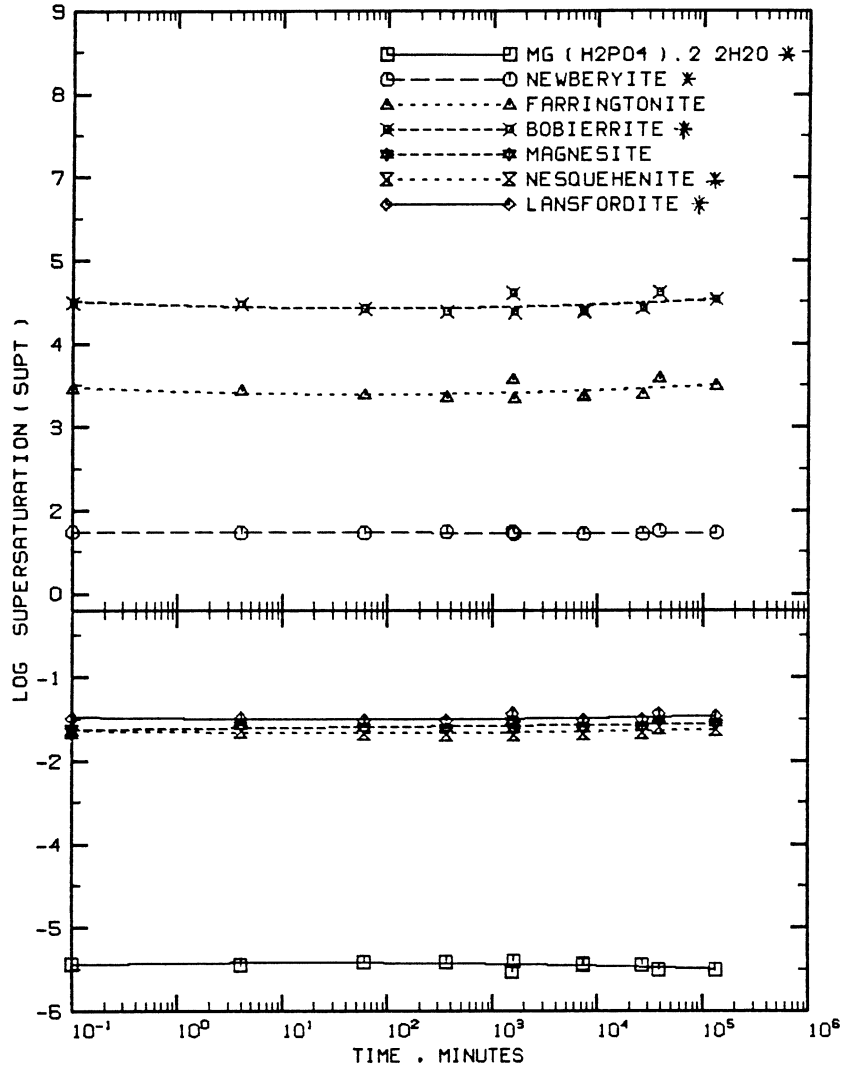

* saturation curve calculated at 25° C
Log SUPT = Log (Q/Ksp)
Newberyite = $MgHPO_4.3H_2O$
Farringtonite = $Mg_3(PO_4)_2.3H_2O$
Bobierrite = $Mg_3(PO_4)_2.8H_2O$
Magnesite = $MgCO_3$
Nesquehenite = $MgCO_3.3H_2O$
Lansfordite = $MgCO_3.5H_2O$

Figure 18. Levels of Supersaturation for potential Magnesium precipitates in Set 6-14 versus time

The X-ray diffraction pattern for the crystalline species did not match bobierrite or newberyite. Assuming a 5 percent substitution of magnesium for calcium in the calcium precipitate, and a calcium to phosphorus ratio of 1.67 to 1.7, the magnesium to phosphorus ratio in the unidentified crystal worked out as close to 1.0 (Table D15, Appendix D). [The moles of calcium involved in the stoichiometric ratio calculations were the moles of calcium plus the substituent magnesium.] The '90 degree parrallelopiped' shape of the crystal could match newberyite ($MgHPO_4.3H_2O$) or phosphoesslerite ($MgHPO_4.3H_2O$). While the X-Ray diffraction pattern did not match the former, it could not be verified with respect to the latter.

On examining the drop in magnesium for sets 6-15 and 6-16 (Figure 19 and Tables D12 and D15, Appendix D), it is evident that in the absence of ammonium, magnesium levels dropped only after 7 days (and to levels above 90 mg/L after 90 days), while in its presence, the drop was significant within the first few hours. It may therefore be concluded that in a digester containing less than 90 mg/L of soluble magnesium, the unidentified species formed in set 6-15 will not be competitively viable because struvite will precipitate out the magnesium to levels less than 20 mg/L in solution within the first seven days.

If the batch samples comprising the kinetics study were allowed to incubate for longer periods of time, the final level of magnesium could be controlled by bobierrite provided that the ammonium levels were low enough for the sample to be supersaturated with respect to bobierrite and not struvite. In this situation, the precipitation of bobierrite would drive some of the struvite precipitated earlier back into solution. The ammonium levels would rise until the solution was at steady state with respect to both compounds. As to how far a continuous flow mixed system like the primary digester would proceed towards a state of therodynamic equilibrium is controlled by the rate of inflow of soluble magnesium, the kinetics of solubilization and precipitation of magnesium, and the solids retention time (approximately 120 days).

In set 6-16, which contained no phosphorus and ammonium, small crystals of aragonite were detected (identified by X-ray diffraction, Appendix B) after 95 days' incubation. Figure 19 provided

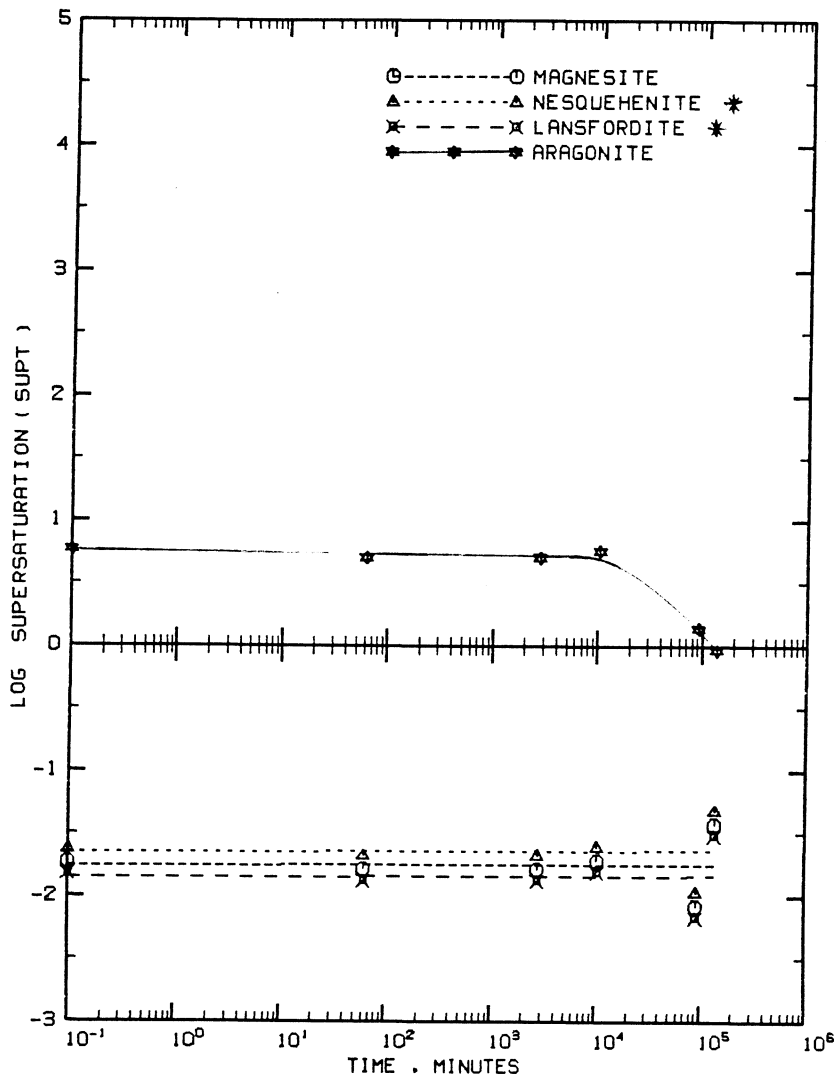

* saturation curve calculated at 25 ° C
Log SUPT = Log (Q/Ksp)
Magnesite = $MgCO_3$
Nesquehenite = $Mg.CO_3.3H_2O$
Lansfordite = $Mg.CO_3.8H_2O$
Aragonite = $CaCO_3$

Figure 19. Levels of Supersaturation for potential precipitates in Set 6-16 against time

further proof that the calcium precipitate was aragonite, since its level of supersaturation dropped to zero on a log scale between 65 and 90 days of incubation.

At the temperature of incubation, the stable calcium carbonate species is calcite. However, the presence of magnesium acted as a poison and resulted in the formation meta-stable phase — aragonite. The drop in magnesium in set 6-16 could not be accounted for, except for a fraction which may have precipitated as some high magnesium containing calcite.

As can be inferred from sets 6-14, 6-15 and 6-16, set 6-12 was supersaturated with respect to several compounds in the initial stages. However, only one crystalline species — struvite, was identified by X-ray diffraction. After five days, the other magnesium species which were supersaturated were bobierrite ($Mg_3(PO_4)_2.8H_2O$) and newberyite ($MgHPO_4.3H_2O$) [Figure 20]. The Q/Ksp ratio for struvite levelled off at $10^{0.35}$ with respect to the thermodynamically calculated solubility product for struvite. At 35°C, the effective Ksp value for struvite was therefore equal to $10^{-12.29}$ with respect to PO_4^{3-} getting involved in the precipitation reaction, as against $10^{-12.64}$ from thermodynamic equilibria considerations (Equation 3.6). This value is applicable to batch systems similar to this kinetics study run over a period of 30 to 90 days. Larger crystal sizes, seeding effects and longer periods of incubation may be expected to produce values of Q/Ksp closer to 1.0 (the equilibrium level expected from thermodynamics).

What may therefore be concluded is that a level of magnesium higher than those used in these experiments and expected in the digester, would be required for the precipitation of 'non-ammonium containing' magnesium compounds. Further, the kinetics of formation of the magnesium-ammonium-phosphorus compound outpaced, and its precipitation undersaturated a majority of the magnesium precipates, effectively eliminating their chances of formation.

The 1:1 ratio of magnesium to phosphorus in this compound (Table 13) could be for

1) $MgNH_4PO_4$

2) Dittmarite, $MgNH_4PO_4.H_2O$, or

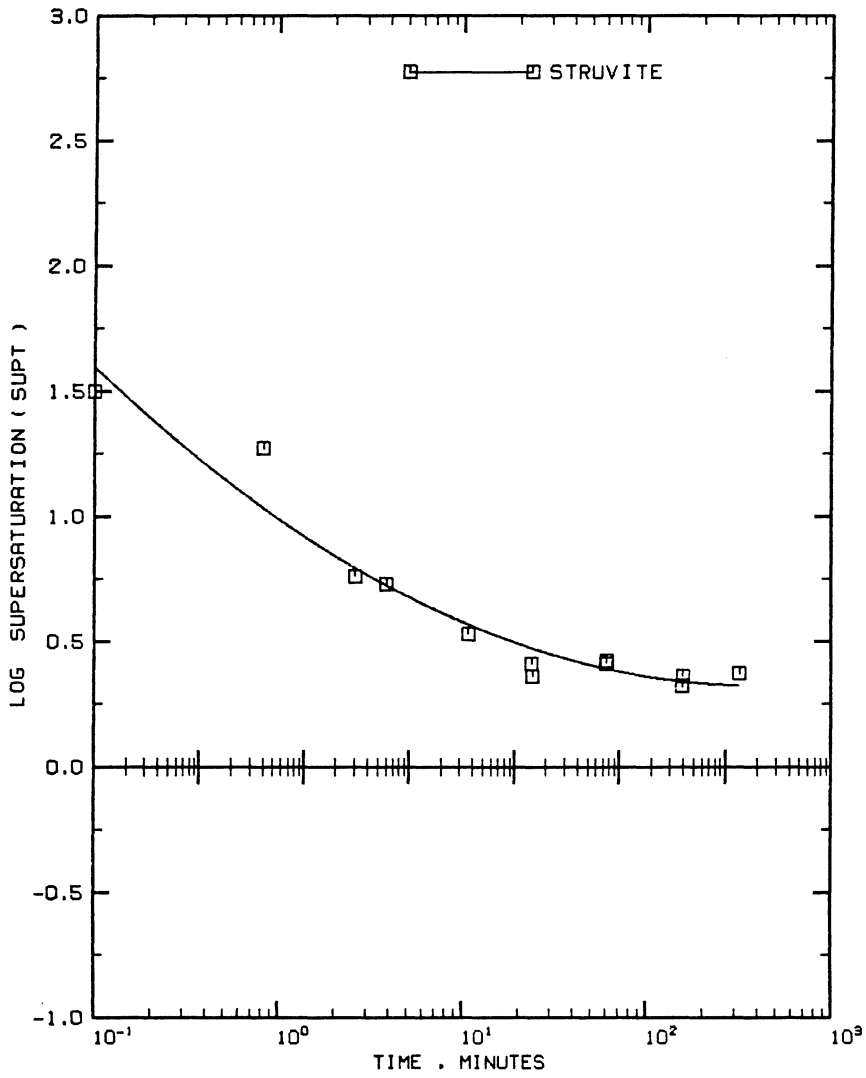

LOG SUPT = Log Q/Ksp
* saturation curve calculated at 25° C
Struvite = $MgNH_4PO_4.6H_2O$.

Figure 20. Levels of Supersaturation for potential Magnesium precipitate(s) in Set 6-12 against time

3) Struvite, $MgNH_4PO_4.6H_2O$.

Of this list, the crystalline precipitate was identified by X-ray diffraction analysis and microscopic examination as struvite.

The calcium precipitate

In all sets containing calcium and phosphorus, a fine white precipitate appeared at some stage during the incubation period. The precipitate appeared almost instantaneously in sets 6-6 and 6-12, (600 mg/L phosphorus, 100 mg/L calcium) and after five days in sets 6-4 and 6-10 (100 mg/L phosphorus, 100 mg/L calcium) [Table D4, D6, D10 and D12, Appendix D]. Little success was met with in outright identification of the precipitate(s). The problems faced were similar to those faced by previous researchers, and were because of the fineness (and possible amorphous nature) of the precipitate and the potential for substitution of cations and anions by foreign ions. The method of calculating the stoichiometric ratios of calcium to phosphorus in Tables D4 to D16, Appendix D, was very sensitive to small variations in measured levels of phosphorus in the initial sample, well within the accuracy of the ascorbic acid test. Calcium and magnesium also contributed to the sensitivity, but the accuracy of measurements on the atomic absorption spectrophotometer was greater than that achieved during serial dilutions performed for the ascorbic acid test for phosphorus. The initial concentration of ions in each sample set was therefore measured three times. Table 14 shows the sensitivity of the ratio to this limitation of the analytical procedure for set 6-12, designed to have a phosphorus level of 600 mg/L. Because of smaller amounts of precipitation in sets having lower levels of phosphorus, a variation of 5 mg/L in the initial sample could have even greater effects on the calculations of stoichiometric ratios. However, the error in phosphorus measurement decreases proportionately with the level of phosphorus in the set, the sensitivity remaining at about the same level.

Table 14. Sensitivity of stoichiometric ratios calculated for Set 6-12 to the phosphorus level in the initial sample

Initial P (mg/L)	540	545	550
Sample	$\Delta Ca/(\Delta P - \Delta Mg)$		
6-12-A1			
6-12-A2	0.95	0.79	0.67
6-12-B1	0.74	0.64	0.57
6-12-B2	0.77	0.66	0.58
6-12-C	1.39	1.23	1.11
6-12-D	1.72	1.51	1.34
6-12-E	1.30	1.18	1.07
6-12-F	1.21	1.11	1.02
6-12-G	1.68	1.48	1.33
6-12-H	2.24	1.93	1.69
6-12-J	1.81	1.60	1.43
6-12-K	2.08	1.81	1.61
$Mean_{C-K}$	1.68	1.48	1.33
St. Dev.	0.37	0.30	0.25
$Mean_{G-K}$	1.95	1.71	1.52
St. Dev.	0.25	0.20	0.16
$Mean_{C-F}$	1.41	1.26	1.14
St. Dev.	0.22	0.18	0.14

In set 6-12, which had a high level of magnesium in addition to calcium, the stoichiometric ratios indicated that calcium precipitates containing at least equal amounts of calcium and phosphorus (eg. Brushite, $CaHPO_4.2H_2O$, or $Ca(H_2PO_4)_2.H_2O$) could have precipitated in the first hour (Table D12, Appendix D). However, the initial samples in this set were undersaturated with respect to $Ca(H_2PO_4)_2.H_2O$ (Figure 21). The initial calcium precipitates lowered the concentration of calcium from 92 to approximately 60 mg/L within the first four minutes. It steadied at this level for atleast an hour before reprecipitating as one of the calcium precipitates listed below. If all the precipitated magnesium is treated as struvite, the ratio in the last column of Tables E11 and E12, Appendix D, is representative of the calcium to phosphorus ratio in the remaining precipitates. After the first five days, the ratio of calcium to phosphorus tended to increase such that it averaged 1.7:1. This raised the possibility of the precipitation of a transient precipitate in set 6-12, and is discussed later.

The probable calcium precipitates after 25 days were one or more of the following:

1) β-Tricalcium phosphate (β-$Ca_3(PO_4)_2$,/ β-$(Ca\text{-}Mg)_9(PO_4)_6$),
2) Octocalcium phosphate ($Ca_8H_2(PO_4)_6.5H_2O$), and
3) Hydroxyapatite ($Ca_{10}(PO_4)_6OH_2$)/ Chlorapatite ($Ca_{10}(PO_4)_6Cl_2$)

While β-tricalcium phosphate is stable in the presence of magnesium, octocalcium phosphate has the property of transforming itself rapidly to hydroxy-apatite in biological systems (LeGeros and LeGeros, 1984). Substitution of some of the calcium by magnesium has been reported in all three precipitates listed above, and could be about 5 percent on a molar basis (Set 6-10). Figures 21 to 23 show the supersaturation of sets 6-6 and 6-12 with respect to a number of calcium compounds. Of the three compounds listed above, they show that the samples were thermodynamically more unstable with respect to hydroxyapatite. None of the calcium precipitates appeared to have reached an equilibrium after 120 days.

In addition to the compounds listed above, the samples were also supersaturated with respect to molecularly simpler structured compounds like brushite ($CaHPO_4.2H_2O$) and monetite

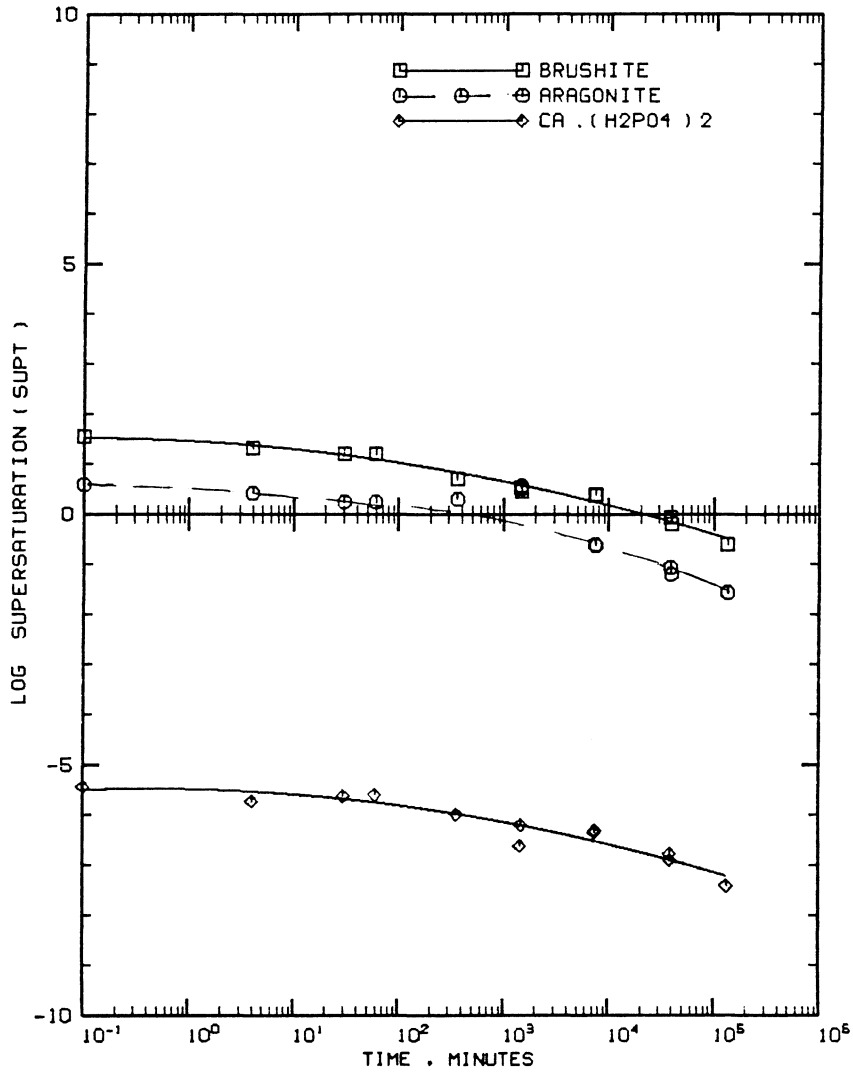

* saturation curve calculated at 25 ° C.
Log SUPT = Log (Q/Ksp)
Brushite = $CaHPO_4.2H_2O$
Aragonite = $CaCO_3$

Figure 21. Levels of Supersaturation for potential calcium precipitates with the Length of Incubation in Set 6-12.

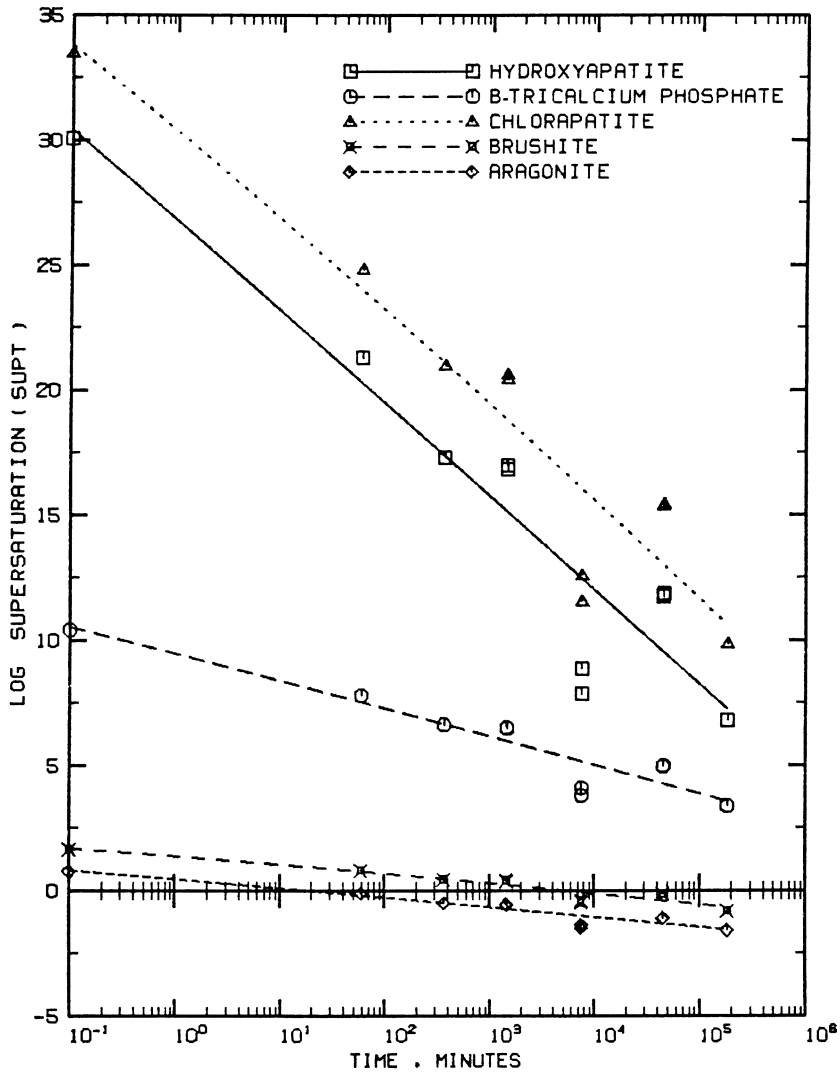

* saturation curve calculated at 25° C
Log SUPT = Log (Q/Ksp)
Hydroxyapatite = $Ca_5(PO_4)_3(OH)$
B-tricalcium phosphate = β-$Ca_3(PO_4)_2$
Chlorapatite = $Ca_5(PO_4)_3(Cl)$
Brushite = $CaHPO_4.2H_2O$
Aragonite = $CaCO_3$

Figure 22. Levels of Supersaturation for some Calcium compounds in Set 6-6 versus the Length of Incubation

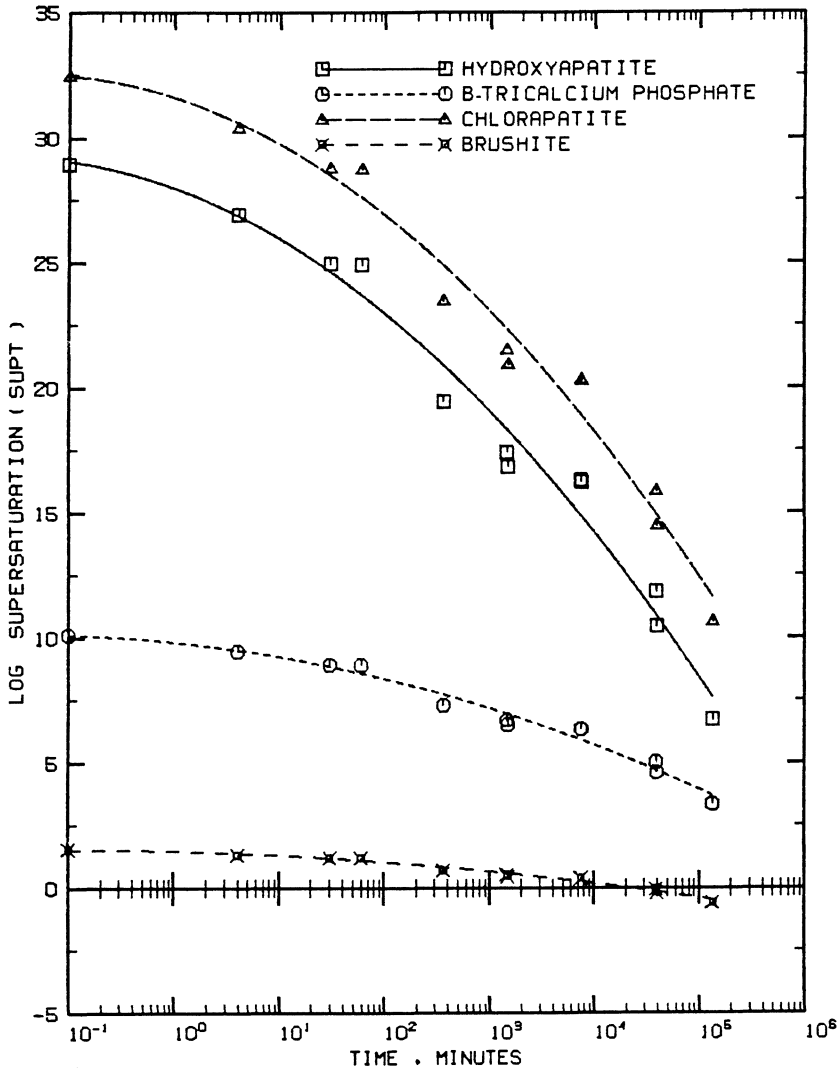

Brushite introduced for comparison of saturation levels with Figure 21
* saturation curve calculated at 25 ° C
Log SUPT = Log (Q/Ksp)
Hydroxyapatite = $Ca_5(PO_4)_3(OH)$
B-tricalcium phosphate = β-$Ca_3(PO_4)_2$
Chlorapatite = $Ca_5(PO_4)_3(Cl)$
Brushite = $CaHPO_4.2H_2O$

Figure 23. Levels of Supersaturation for four calcium compounds with the Length of Incubation in Set 6-12.

($CaHPO_4$), and a rapidly forming and usually transient amorphous calcium phosphate (whose stable chemical composition is close to $Ca_9(PO_4)_6$) in the initial stages. The presence of magnesium can delay the precipitation of hydroxyapatite (observed in Set 6-12 and discussed later), leading to the precipitation of one or more of the simpler and/or rapidly forming compounds. However, after five days, the calcium levels in the batch studies were controlled by hydroxy-apatite and/or β-tricalcium phosphate and not brushite, because the sample was undersaturated with respect to the latter. Sufficiently long periods of incubation lead to the dissolution of the initial precipitate and its reprecipitation as hydroxyapatite or β-tricalcium phosphate, evidence of which exists in the stoichiometric ratios calculated in for set 6-12 (Table D12, Appendix D). In samples 6-12-C to 6-12-F, the dissolution was responsible for calcium to phosphorus ratios sligthly above 1.0:1.0 while they averaged 1.7:1.0 after the dissolution was complete (samples 6-12-G to 6-12-K).

Though Figures 21 to 23 indicate that the systems were highly supersaturated with respect to chlorapatite, researchers have pointed out that chlorapatite is structurally less stable than hydroxyapatite (LeGeros and LeGeros, 1984). Because of the exclusion of chloride from the system of equations to be solved (eqns 3.1 to 3.4), and the use of chloride stock solutions, the simulated 'clean' samples had chloride levels of around 2000 mg/L, far in excess of the digester with about 125 mg/L (Table 7, Appendix A).

pH-Solubility Study on the calcium precipitate(s)

The release of calcium and phosphorus at different pH levels was examined by titrating a small quantity of the centrifuged precipitate of sample 6-6-J (31 days of incubation, Table D6, Appendix D) with 0.02N sulfuric acid. The results are shown in Table 15. The analysis of the molar ratios in Table 16 provides further evidence that the dominant precipitate in set 6-6 after 90 days was hydroxyapatite (β-tricalcium phosphate could not have formed in the absence of magnesium, Chapter VI). The results cannot be interpreted in terms of the ratios of calcium to phosphorus at

Table 15. Results from the pH-Solubility Study on the Precipitate of Sample 6-6-J of the Kinetics Study

pH	Ca	P	Cl	Ca	P	Comments
	mg/L			milli-moles		
7.72	0.88	6.3	66.6	0.022	0.203	
6.75	3.82	7.7	50.2	0.096	0.248	
6.01	19.3	15.9	39.9	0.483	0.511	
5.72	40.3	25.1	36.0	1.008	0.807	
5.50	52.3	35.5	42.6	1.308	1.141	unsat.[1]

[1]sample was apparently undersaturated at this pH

Table 16. Analysis of the pH-Solubility Study Data

Range	pH steps	ΔCa	ΔP	ΔCa/ΔP	
		milli-moles			
6.75 to 7.72	1	0.075	0.045	1.67	
6.01 to 6.75	1	0.387	0.263	1.47	
5.72 to 6.01	1	0.525	0.296	1.77	
5.50 to 5.72	1	0.300	0.334	0.90[1]	
$Mean_{i=1 \text{ to } 3}$					1.64
St. Dev					0.15
6.01 to 7.72	2	0.461	0.308	1.50	
5.72 to 6.75	2	0.912	0.559	1.63	
5.72 to 7.72	3	0.986	0.604	1.63	
$Mean_{i=6}$					1.61

[1]this ratio is significantly different from the rest of the ratios

St. Dev. = Standard Deviation

a particular pH because small quantities of 'foreign' compounds precipitated from the solution which adhered to the precipitated flocs after they were centrifuged out. Since these precipitates remained in solution till the flocs dried, they were more soluble and appeared in the initial sample dissolved in distilled water at a pH of 7.72. This was corrected for by calculating ratios on the basis of increases in concentrations above those at this pH. The data on chloride levels were less than satisfactory. What may be concluded is that the solution adhering to the flocs was responsible for a part of the chlorides. There could have been some chlorapatite, but the evidence was not in favor of its existence in significant quantities. The faint white color of the precipitate disappeared at a pH between 5.50 and 5.72, raising the possibility that the sample was undersaturated at a pH of 5.50. The calcium to phosphorus release ratio was significantly different for the lowest pH, probably due to an error in the measurement of calcium or phosphourus.

The Primary Digester Sludge

Figures 24 to 26 show the levels of supersaturation of magnesium, calcium and iron precipitates in the primary anaerobic digester, based on samples collected over the period of the study. For Figure 26, 80% of the soluble iron was assumed to be in a ferrous form (Nash, 1987). The simulations were performed at a pH of 7.3, which was the average pH of the digester and was 0.1 pH unit lower than the pH of the 1.2μm filtrate (the 1.2μm filtrate had an average pH of 7.4, and was filtered through a 0.45μm filter paper to obtain the sample for analyses).

From Figure 24, it can be seen that the 0.45μm filtrate of the primary digester mixed liquor was undersaturated with respect to struvite before the BPR modification. Subsequent to the modification, it steadied at an average Q/Ksp ratio of $10^{0.22}$. As to how pH changes and refrigeration could have affected the saturation levels is discussed in the following chapter.

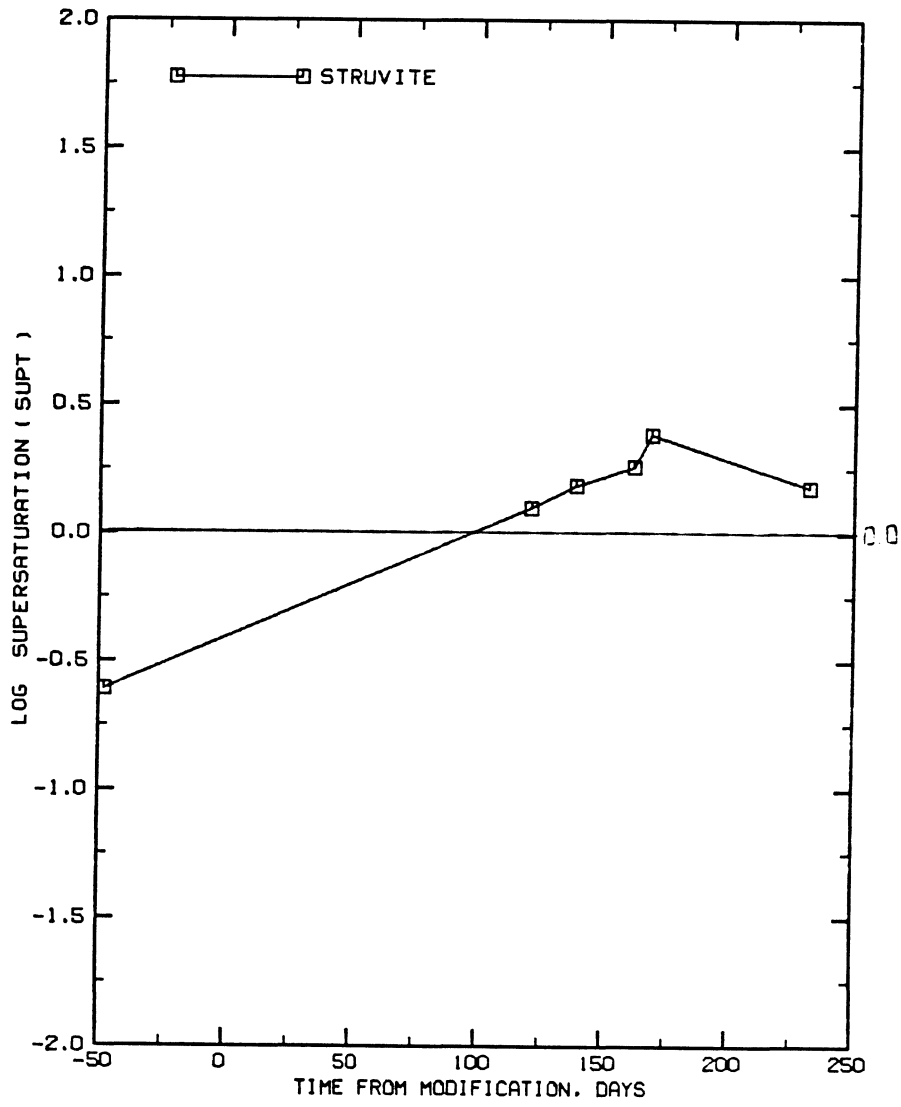

* saturation curve calculated at 25° C
Log SUPT = Log (Q/Ksp)
Struvite = $MgNH_4PO_4.6H_2O$.

Figure 24. Levels of Supersaturation for Struvite in the primary digester with time

A two parameter t-test performed on the levels of supersaturation for brushite before and after the modification showed a significant difference at a 90 % level of confidence. On the other hand, the Q/Ksp ratios for hydroxyapatite and β-tricalcium phosphate did not change significantly (Figure 25). If the feed rate of soluble calcium and the kinetics of solubilization of calcium are rapid, and the kinetics of precipitation slow as may be expected for a precipitate like hydroxyapatite, the levels of calcium in solution both before and after the modification in a continuous flow system will be much higher than that required for saturation.

As mentioned earlier, based on the fraction of ferrous iron, 80 % of the soluble iron was assumed to be ferrous. The transformations from ferric to ferrous forms should have taken place over a period of time in the primary digester. If the redox potentials of the gravity thickened primary sludge and float thickened waste sludge streams feeding into the digester were low enough, it is possible that some of the transformation took place before the primary digester. With most of the iron in the solid phase, it is obligatory that one or more of the following anionic species be available for the transformation — hydroxide, phosphate, carbonate (the carbonate alkanities in this digester were in the range of 2000 to 2200 mg/L) and/or sulfides. At a pH of 7.3, the hydroxide levels were too low for the precipitation of ferrous hydroxide (Figure 26). Since the steady state equilibrium level in the primary digester is determined by the rate of inflow, transformation and precipitation, and the solids retention time in the digester, Singer's value of $10^{-29.9}$ for the Ksp of vivianite has to be interpreted in this light. At the higher solids retention time in the digester, the value of Ksp will approach the value of 10^{-36} reported by Nriagu, 1984, and equal to that calculated from thermodynamic equilibrium conditions. Unless a competitive supersaturated ferrous compound has a markedly faster rate of precipitation as compared to vivianite, there will be some vivianite in the precipitate. With the levels of iron and the carbonate alkalinity remaining fairly constant, the Q/Ksp for siderite ($FeCO_3$) for the entire period averaged 0.70, with a standard deviation of 0.21 on a log scale. Since the reaction quotients for siderite closely approximated the solubility product throughout the study, and the solution was also saturated with respect to vivianite, (Figure 27), one may expect both precipitates to form if their rates are compatible (*i.e.* do not differ by several orders

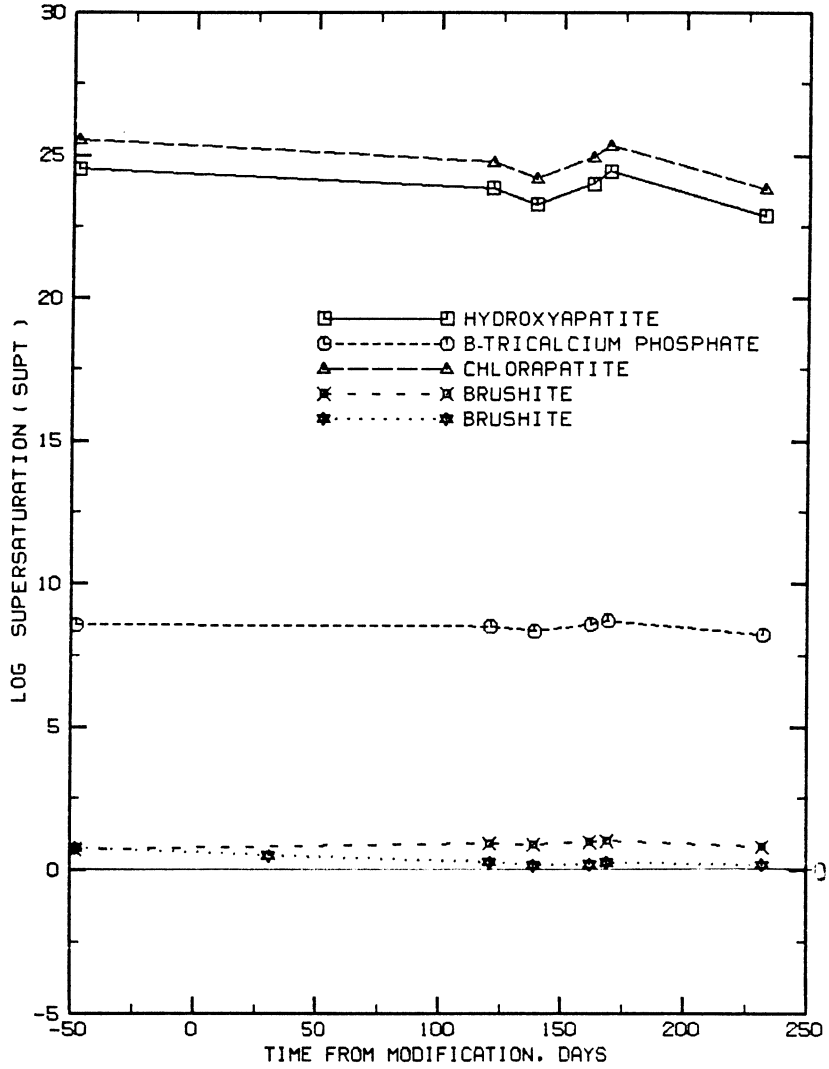

* saturation curve calculated at 25 ° C
Log SUPT = Log (Q/Ksp)
Hydroxyapatite = $Ca_5(PO_4)_3(OH)$
B-tricalcium phosphate = β-$Ca_3(PO_4)_2$
Chlorapatite = $Ca_5(PO_4)_3(Cl)$
Brushite = $CaHPO_4.2H_2O$

Figure 25. Levels of Supersaturation for potential Calcium precipitates in the primary digester over the period of the study.

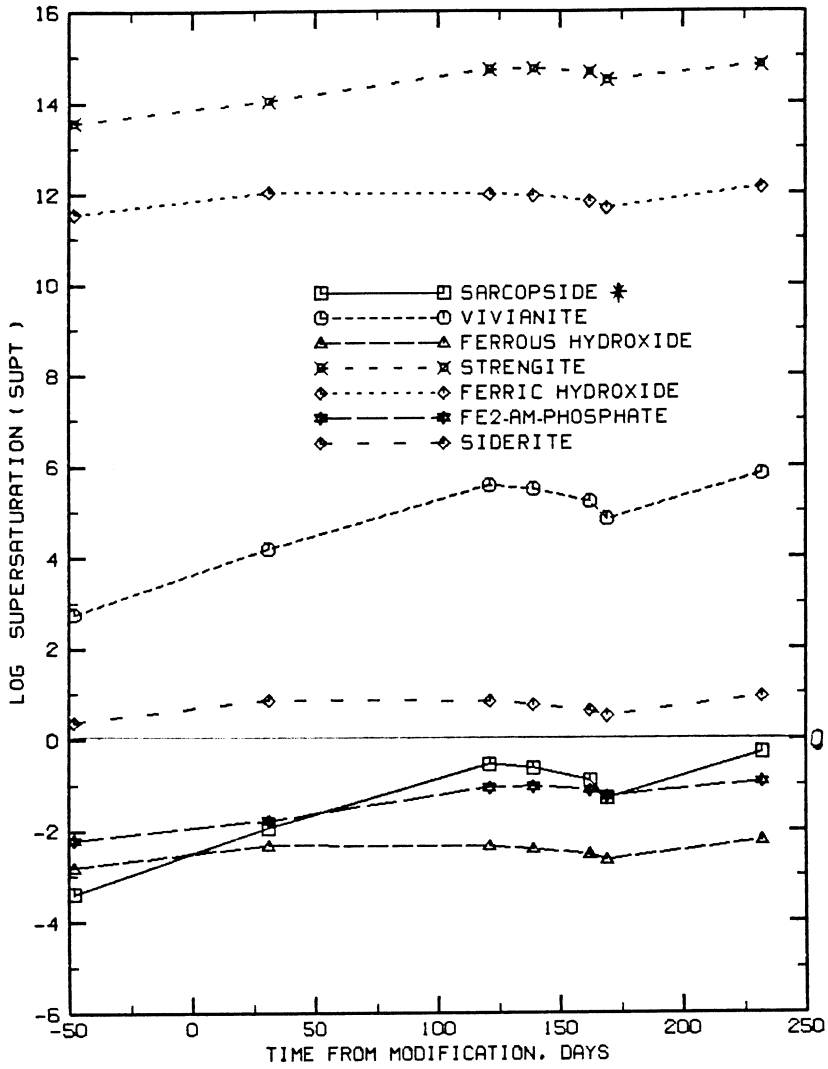

* saturation curve calculated at 25 ° C
Log SUPT = Log (Q/Ksp)
Sarcopside = $(Fe\text{-}Mg)_3(PO_4)_2$
Vivianite = $Fe_3(PO_4)_2.8H_2O$
Ferrous Ammonium Phosphate = $FeNH_4PO_4$
Ferrous Hydroxide = $Fe(OH)_2$
Strengite = $FePO_4.2H_2O$
Ferric Hydroxide = $Fe(OH)_3$
Siderite = $FeCO_3$

Figure 26. Levels of Supersaturation for potential Ferric and Ferrous pp. in the primary digester over the period of the study.

of magnitude). If the level of soluble iron dropped with the increase in phosphorus, the rate of precipitation of siderite should have decreased or stopped altogether if the Q/Ksp ratio fell below 1.0. However, based on the samples collected, the soluble iron increased, probably due to

1) an increase in the supply of iron to the digester resulting in higher rates of transformation to ferrous iron, which would be matched by rate of precipitation at a higher level of soluble iron; and

2) error in the analyses due to pH fluctuations and/or low levels of soluble iron.

Therefore, the amount of ferrous iron precipitated as vivianite may increase after the modification till the post precipitation levels of phosphorus dropped such that the amount of ferrous iron in solution was sufficient to precipitate out siderite. The trend in Figure 27 is indicative of a similar situation, with the relative amounts of siderite and vivianite being controlled by the ratio of their rates of formation at the steady state level.

The X-Ray diffraction pattern of the crystals isolated from the primary digester sludge is shown along with the standard pattern for a struvite crystal in Figure 28. The peaks were sufficiently prominent to confirm the presence of struvite.

The Return Activated Sludge

In order to estimate the extent of solubilization of the poly-phosphate granules and the release of phosphorus and cations, the Return Activated Sludge from the bottom of the secondary clarifiers was subjected to different lengths of anaerobic incubation at room temperature. The amount of phosphorus released in soluble form (in the 0.45μm filtrate) increased with the length of anaerobic incubation. Subsequent aeration resulted in the uptake of the ions released. Tables 17, 18 and 19 present the raw data, percent releases and uptakes. In sets C and D, additional phosphorus was added as potassium dihydrogen phosphate to examine if *Acinetobacter species* would have the

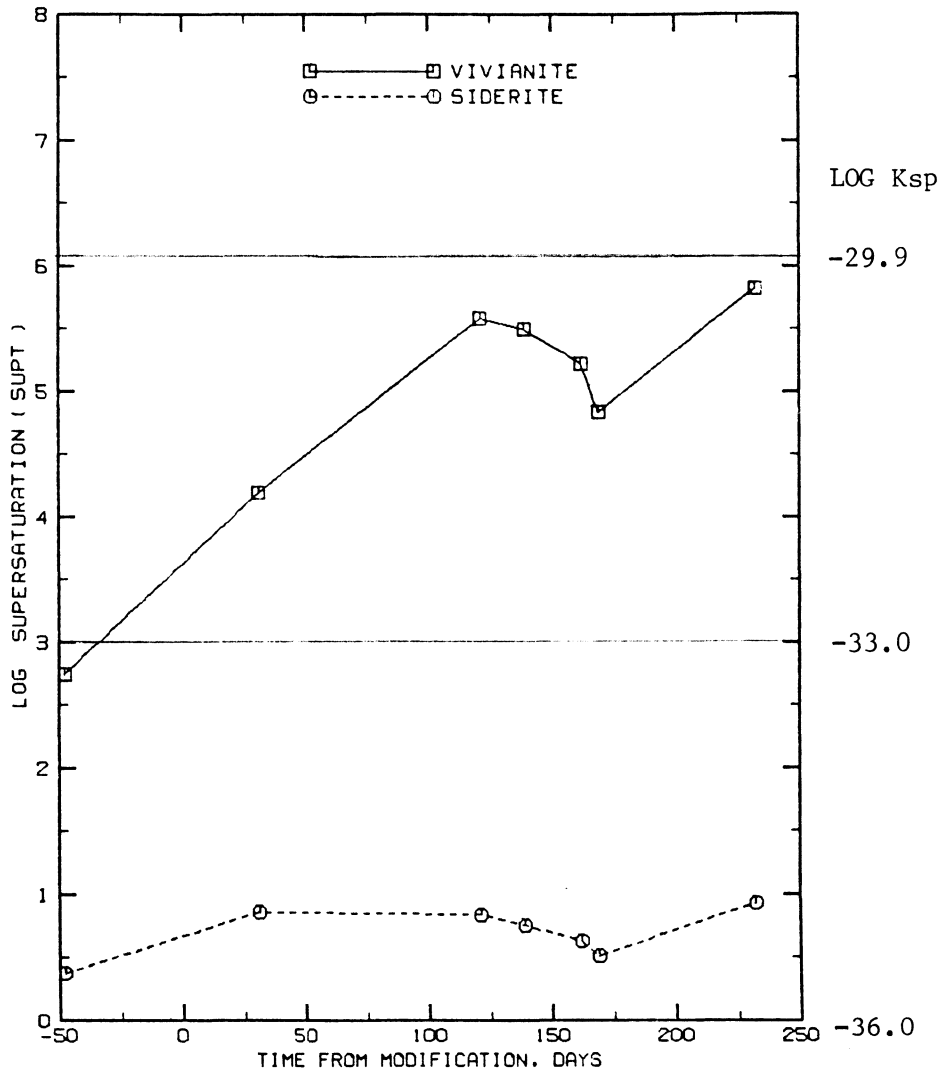

* saturation curve calculated at 25 ° C
Log SUPT = Log (Q/Ksp)
Vivianite = $Fe_3(PO_4)_2.8H_2O$
Siderite = $FeCO_3$

Figure 27. Reported Ksp values for vivianite and supersaturation levels for vivianite and siderite over the period of the study.

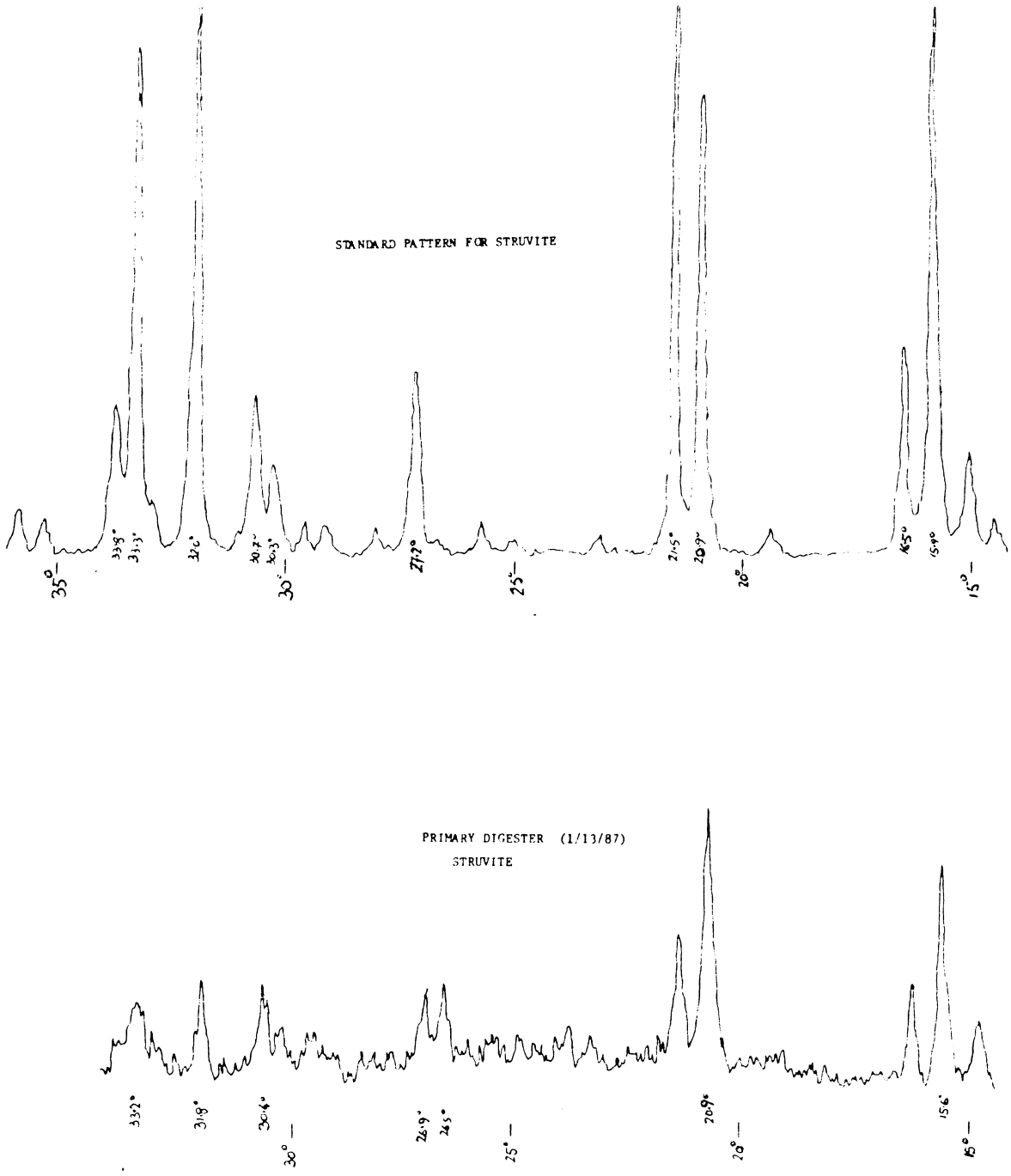

Figure 28. X-ray diffraction patterns of a standard struvite crystal and that of crystals picked out of the primary digester sludge.

ability to accumulate it as poly-phosphate granules. The evidence was not in favor, but may have been caused by the lack of stabilizing cations for the poly-P granule (Chapters II and V).

The pH of the samples dropped during anaerobic incubation in the absence of methanogenic organisms, possibly due to fermentation reactions. Subsequent aeration resulted in increases in pH. According to Wentzel *et al.* (1986), this is characteristic of a biomass population dominated by *Acinetobacter species* . It is probable that the increase in pH could have precipitated some of the calcium and phosphorus released during anaerobic incubation, which is otherwise kept in solution by the low pH before aeration. While the charge balance was fairly close to 1 in set A of the experiment in which the variation in pH and extent of release was the least, it was grossly unbalanced in set D (Table 20). This could have been the result of the formation of a calcium-phosphorus precipitate and is discussed in the following chapter.

The lower calcium and magnesium levels in set C of the experiment after 93 hours of incubation could not be explained, except for the possible formation of a calcium-magnesium-phosphorus precipitate. The analysis shown in Table 19 provides some information regarding the amount of poly-phosphate which may be dissociated under anaerobic conditions, either for maintenance energy or through lysis. Atleast sixty percent of the total calcium and magnesium can be released under these conditions. The release of calcium was at approximately half the rate for the other species, unless there was some interference due to the precipitation of calcium and phosphorus. Unlike a batch system in which this experiment was conducted, the primary digester is a continous flow unit and the rate of release of ions should be constant and dictated by the ultimate releases which may occur over the residence time of the sludge in the digester (approximately 120 days for the primary digester).

Table 17. Release and Uptake during anaerobic and aerobic exposures of the Return Activated Sludge of 3/24/87

Sludge refrigerated for 48 hours before experiment

Time (hrs:min)		pH	Ca	Mg	Na	K	Fe	P	Ac	Pr
Anaer	Aer		mg/L							
Set A										
0:00	0:00		60.1	23.8	88.2	35.9		75.	ND	11.3
0:00	1:10		47.8	5.8	84.2	12.8		1.83	ND	15.3
0:00	6:50		46.9	6.9	92.2	17.3		1.38	ND	7.0
Set B										
21:30	0:00		78.0	31.1	88.4	60.4		135.	80.4	43.1
21:30	1:05		13.5	9.0	87.0	35.8		33.	ND	1.6
21:30	6:40		17.3	8.04	84.0	28.2		7.3	ND	ND
Set C										
93:05	0:00		38.2	28.8	82.4	68.1	1.12	185.	285.	100.
93:05	1:02		9.9	19.5	90.0	52.7	0.35	100.	190.	49.
						+ 164.*		+ 130*		
93:05	8:30		3.24	3.57	96.0	186.	0.32	135.	ND	3.5
93:05	25:00**		6.93	1.05	148.	275.	0.21	162.	1.9	13.5
Set D										
297:55	0:00	5.77	114.	39.3	90.0	74.7		205.	385.	820.
297:55	1:05	6.72	66.1	33.7	89.0	65.4		160.	400.	145.
297:55	6:37	6.64	51.2	31.0	96.0	60.6		115.	3.	14.
						+ 235.*		+ 139*		
297:55	23:17	7.50	18.6	16.6	98.2	200.		200.	2.	< 1.

Total Recoverable	328.	65.1	365.0	101.	174.	340.		

* amount of phosphorus added as KH_2PO_4
** this sample suffered from anaerobic conditions due to a failure of the aeration apparatus
Anaer = length of anaerobic period
Aer = length of aerobic period
Ac = acetates Pr = Propionates
ND = Not Detected
Total Suspended Solids = 6325 mg/L Total phosphorus (P) content = 5.38 %

Table 18. Percent Release and Uptake of P during anaerobic and aerobic exposures of the Return Activated Sludge in the laboratory

Time (hrs:min)		P	% Release[1]	% Uptake[2]
Anaerobic	Aerobic	mg/L		
0:00	0:00	75.	22.1	0.
0:00	1:10	1.83		98.
0:00	6:50	1.38		98.
21:30	0:00	135.	39.7	0.
21:30	1:05	33.		76.
21:30	6:40	7.4		95.
93:05	0:00	185.	54.	0.
93:05	1:02	100.		45.
93:05	8:30	5. + 130.*		97.
93:05	25:00	30. + 130.*		84.**
297:55	0:00	205.	60.	0.
297:55	1:05	160.		22.
297:55	6:37	115		44.
297:55	23:17	60. + 140.*		71.

* amount of phosphorus added as KH_2PO_4
* the sample suffered from anaerobic conditions due malfunction of the apparatus

[1]Percent of the total phosphorus in the RAS released following anaerobic incubation

[1]Percent of the released phosphorus taken up in aeration

Table 19. Percent of total phosphorus, magnesium, potassium and calcium released with the length of anaerobic incubation

Duration	P	Mg	K	Ca	Comments
hrs, mins					
0, 00	22.1	36.6	35.6	18.3	
21, 30	39.7	47.8	59.9	23.8	
93, 05	54.	44.2	67.4	11.6[1]	ppt?[1]
297, 55	60.	60.4	74.0	34.7	

[1]a precipitate may have formed with phosphorus if the pH was not low enough

Table 20. Mass balance on sets A and D based on Comeau and Wentzel.

Set A

Aer time	Ca	Mg	Na	K	P	Ratio[1]
		milli-moles				
0,00-1,10	0.31	0.75	0.17	0.59	2.34	1.23
0,00-6,50	0.33	0.70	-0.17	0.48	2.36	1.07

Set D

pH Range	Ca	Mg	Na	K	P	Ratio[1]
		milli-moles				
5.77-6.64	1.57	0.35	-0.26	0.36	2.93	1.35
5.77-6.72	1.20	0.23	0.04	0.39	1.43	2.3
5.77-7.50	2.39	0.95	-0.35	1.14	4.68	1.60

[1](2.* [Ca + Mg] + Na + K) / P

Discussion

The objectives of the research, as outlined in Chapter I were to

a) examine the release of phosphorus from sludge containing granules of poly-phosphate, and

b) investigate the nature of chemical precipitates formed in the primary digester during the digestion of excess phosphorus containing sludges.

The results met the stated objectives to a fair extent. There were some limitations to the attempts to simulate the chemical environment of the primary digester in the laboratory. However, the scope of the experiments were broad enough to allow the data to be interpreted for wastewaters different from that at York River.

Release Ratios and charge balance

The release ratios at York River were fairly consistent with those observed in other biological phosphorus removal systems. As can be seen from Table 10, the charge balance was not as satisfactory. Variations in the concentration of ions in the influent wastewater at different times during the day affected the calculation of releases over the secondary effluent levels. This could be overcome by compositing the samples over extended periods of time. The data for York River was based on releases observed in six-hour composite samples over a 24 hour period only (September 3rd – 4th, 1986).

The pattern of releases in experiments with the return activated sludge (RAS) showed an association between calcium and phosphorus (Table 17). This is significant because Buchan (1983) observed from electron microscopy analysis that poly-phosphate was largely stabilized by Ca^{2+} ions. Comeau *et al.* (1985), mentioned that co-transport ratios of ions across the membrane may not be representative of ions stabilizing the poly-phosphate chains. Since K^{+} and Mg^{2+} are the most abundant monovalent and divalent cations present in bacterial cells, (Schuldiner and Padan, 1982; Sorensen and Rosen,1982), an ion such as Ca^{2+} could be outcompeted by them in stabilizing phosphate molecules before their expulsion from the cell but after the hydrolysis of poly-phosphate. Because of the relative paucity in the transport of calcium across the membrane, the hydrolysis of poly-P will result in the accumulation of free calcium within the cell. The calcium ions necessary for the stabilization of poly-P in the aerobic zone would then be extracted from the 'bank' within the micro-organism. In set D of the experiment on the return activated sludge, extended periods of anaerobic conditions released calcium from this 'bank', either by transport across the membrane or as a result of the lysis of cells.

Fermentation reactions during anaerobic conditions released acetates and propionates, the release increasing with the length of exposure to anaerobic conditions (Table 17). The absence of methanogenic bacteria prevented the production of alkalinity, with the result that the fermenters lowered the pH. The high levels of calcium and phosphorus released in the dissociation process remained in solution because of this drop in pH. However, aerating a system containing a large number of *Acinetobacter species* results in an increase in pH with uptake of phosphorus (Wentzel *et al.* , 1986). A precipitate like hydroxyapatite, if analysed in terms of the biochemical model would yield the following charge balance —

$$Ca_5(PO_4)_3OH + 6H^+ = 5\,Ca^{2+} + 3H_2PO_4^- + 2\,OH^- \qquad [5.1]$$

where $5Ca^{2+}$ = 10 units of positive charge and

$3H_2PO_4^-$ = 3 units of negative charge

This results in a charge balance of 10:3, as against a 1:1 ratio for biochemical uptake or release. This may have happened in set D of the experiment with the return activated sludge when the pH rose from 5.8 to 7.5 during aeration (Tables 17 and 20). On the other hand, set A did not show large releases or uptakes and the increase in pH should therefore have been smaller. As a result, the probability of forming a calcium-phosphorus precipitate in set A was slim, and the charge balance was much closer to one (Table 20).

Transient precipitates

The high values of magnesium in the initial stages of set 6-12 of the kinetics study (Table D12, Appendix D) may have delayed the formation of hydroxyapatite. This is evident from the plateau- observed in the drop in calcium in set 6-12 between 4 minutes and 1 hour (Figure 29). The initial precipitate which dropped the calcium from 92 to 61 mg/L had a Ca/P ratio of less than or equal to 1/1. After six hours, the Ca/P ratio kept increasing till it averaged 1.7 after 30 days. Set 6-6 did not show any evidence of the plateau. It may therefore be concluded that the presence of magnesium delayed the foramtion of hydroxy-apatite or β-tricalcium phosphate in Set 6-12. The gradual increase in Ca/P ratio between 6 hours and 30 days is indicative of the dissolution of the precipitate at lower calcium and phosphorus levels.

In this respect it may also be noted that

1) the structure of hydroxyapatite is more complex than a competitive precipitate like brushite, $CaHPO_4.2H_2O.$, and may therefore take a longer time to form,

2) the substitution of calcium by magnesium can delay the precipitation of hydroxyapatite (Gulbrandsen, 1983), and

3) pure β tricalcium phosphate is not found in biological systems and cannot be prepared be prepared from aqueous systems. It can only be prepared at high temperatures (900°C) by solid state reactions (LeGeros and LeGeros, 1984). This effectively removes it from the list of possible precipitates in set 6-6. It does not however exclude the formation of a transient amorphous calcium precipitate (ACP) in the initial stages.

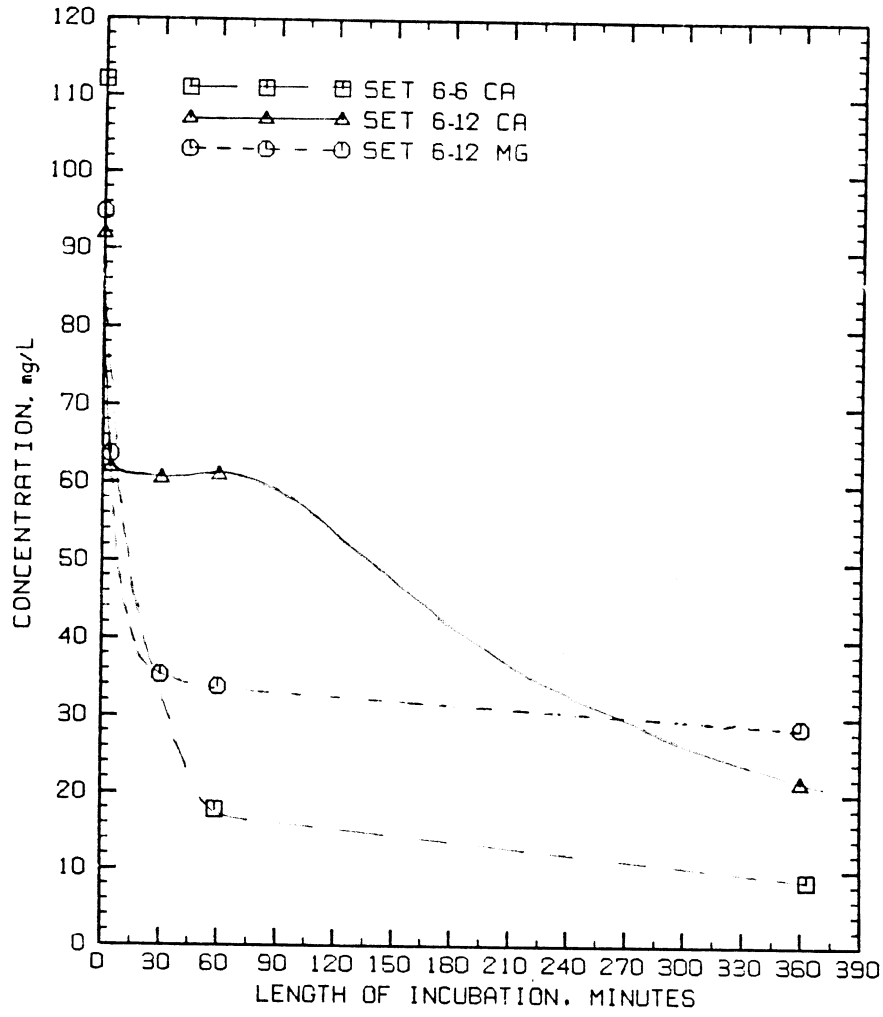

Figure 29. Calcium levels in sets 6-6 and 6-12 and magnesium levels in sets 6-9 and 6-12 in the first six hours of incubation

4) Without quoting specific rates, LeGeros and LeGeros (1984) mentioned that brushite could be hydrolysed to hydroxyapatite in the presence of Mg^{2+} over a period of time. The rate could be influenced by changes in pH, temperature and composition. The extent of transformation within the primary digester will be limited by the residence time of the solids in the primary digester.

5) β-tricalcium phosphate can exist with hydroxyapatite in gel systems at 37°C (LeGeros and LeGeros, 1984).

The magnesium levels in sets 6-9 and 6-12 did not show any evidence of a plateau while precipitating out as struvite. The result was that 78 % of the magnesium precipitated within the first hour as against 34 % for calcium (Table D12, Appendix D). Therefore, the formation of struvite will not be inhibited by the uptake of phosphorus by some other cation in the primary digester.

When the thickened waste sludge having high levels of soluble magnesium, calcium and phosphorus and a relatively lower pH of around 6.5 enters the primary digester, the formation of brushite cannot be discounted. Because of the striking structural similarities of octocalcium phosphate and hydroxyapatite, it has been theorized that the former is a precursor to the formation of hydroxyapatite. Seeding effects due to preformed hydroxyapatite in the primary digester (Figure 8 — Jenkins 1971), may induce its formation earlier than would otherwise occur. At the same time the level of calcium at equilibrium in the primary digester will not allow any of the precipitated brushite to resolubilize as in set 6-12. As a result, the digester may differ from the kinetics study in that brushite, if formed, may exist as a permanent precipitate within the residence time of the sludge. However, the kinetics of formation of hydroxyapatite at calcium levels less than 60 mg/L can compete with brushite, and at a level of 30 to 40 mg/L, it may not be a major precipitate (Set 6-12, samples C to K).

Effect of Temperature and pH on Thermodynamic Equilibrium

Temperature dependence of the level of supersaturation

Using the Van't Hoff equation (3.8) to adjust solubility products and acid dissociation constants for changes in temperature, it was observed that the levels of supersaturation of the samples increased for struvite but decreased for calcium precipitates like hydroxyapatite, β -tricalcium phosphate, brushite and aragonite with a drop in temperature. The effect was simulated for struvite and hydroxyapatite in the primary digester at 15, 25 and 35°C (Figure 30). The solubility products for struvite averaged $10^{-13.70}$, $10^{-13.15}$ and $10^{-12.64}$ while the reaction quotients at steady state after the modification averaged $10^{-12.6}$, $10^{-12.5}$ and $10^{-12.4}$ at the respective temperatures. Struvite may therefore be expected to precipitate in the secondary digester and the effluent lines where the mixed liquor cools down from 35°C to room temperatures. The temperature dependence also decreases the possibility of precipitating struvite in the lines of the heat exchanger. For the same reason, the walls of the digester, whose temperatures are lower than the mixed liquor's, may form a coat of struvite.

pH dependence of the level of supersaturation

pH dependence was examined by increasing the pH of the 0.45μm filtrate of the primary digester mixed liquor by 0.5 and 0.9 unit for simulation purposes (Figure 31). The solubility products for struvite and hydroxyapatite dropped sharply with these increases in pH. Since the pH of the secondary digester underflow may increase if a vacuum pump installed in line causes a loss of carbon dioxide from the mixed liquor, additional struvite may be precipitated at the point where the digested sludge is relieved of the 'closed' environment with which it had come to equilibrium.

It is important that a distinction be made between digesters forming struvite during the digestion of sludge from conventional systems and those digesting sludge from a BPR units. In the former, the amount of magnesium and phosphorus released is much lower and conditions like a pH increase and/or a temperature drop may be essential for the formation of struvite. In a BPR system with

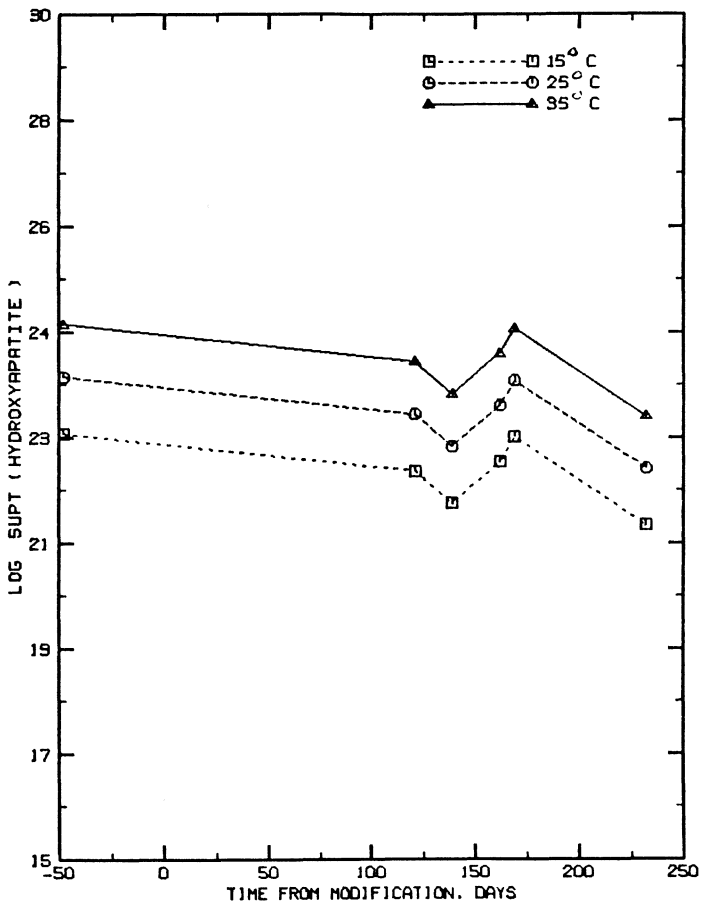

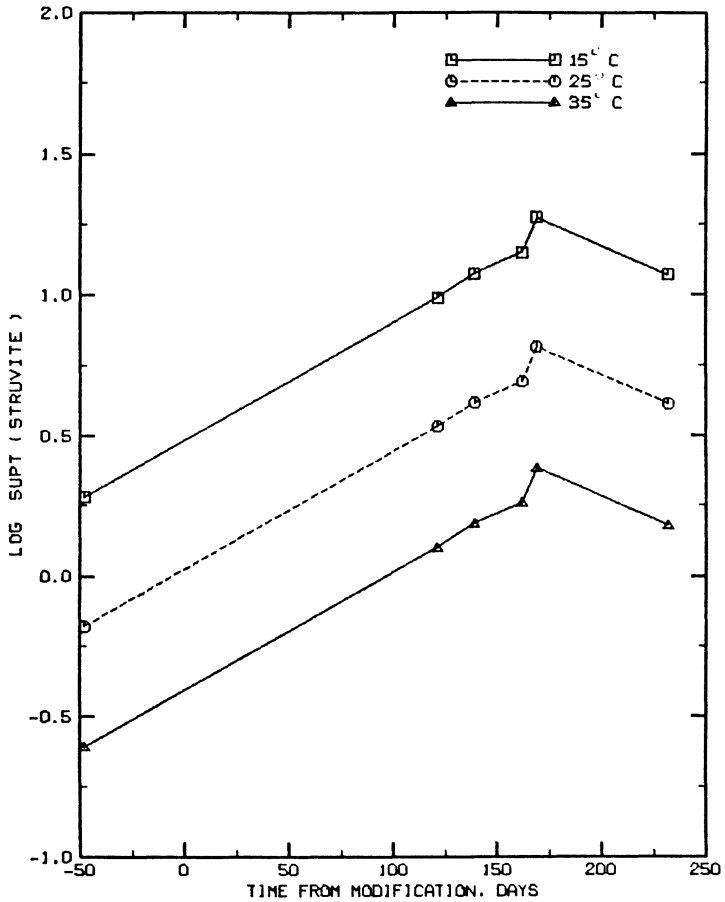

Log SUPT = Log (Q/Ksp)
Struvite = $MgNH_4PO_4.6H_2O$
Hydroxyapatite = $Ca_5(PO_4)_3OH$

Figure 30. Effect of temperature on the level of saturation of struvite and hydroxyapatite in the primary digester.

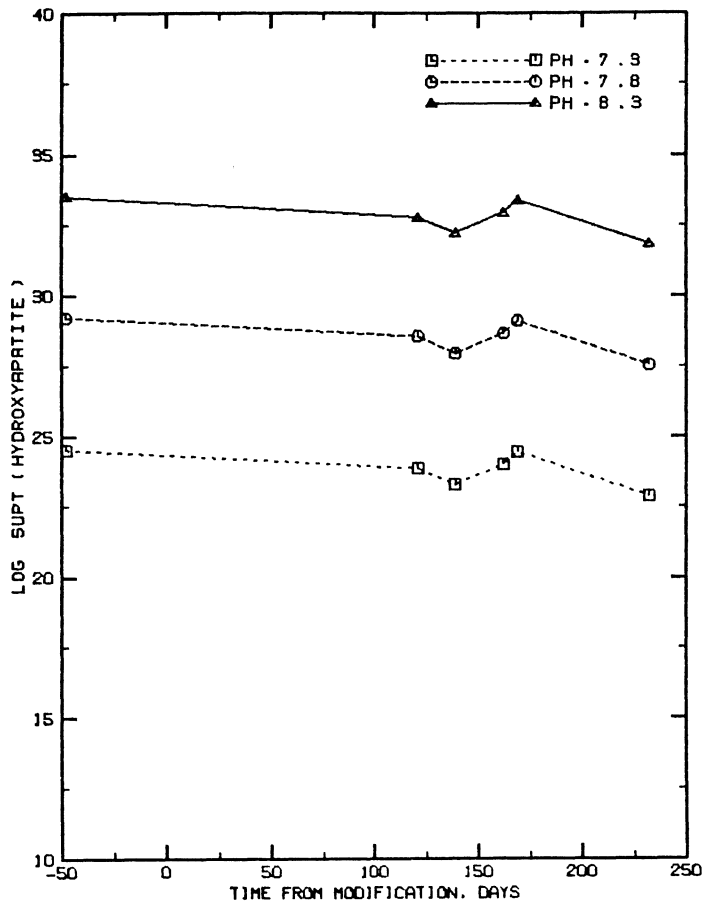

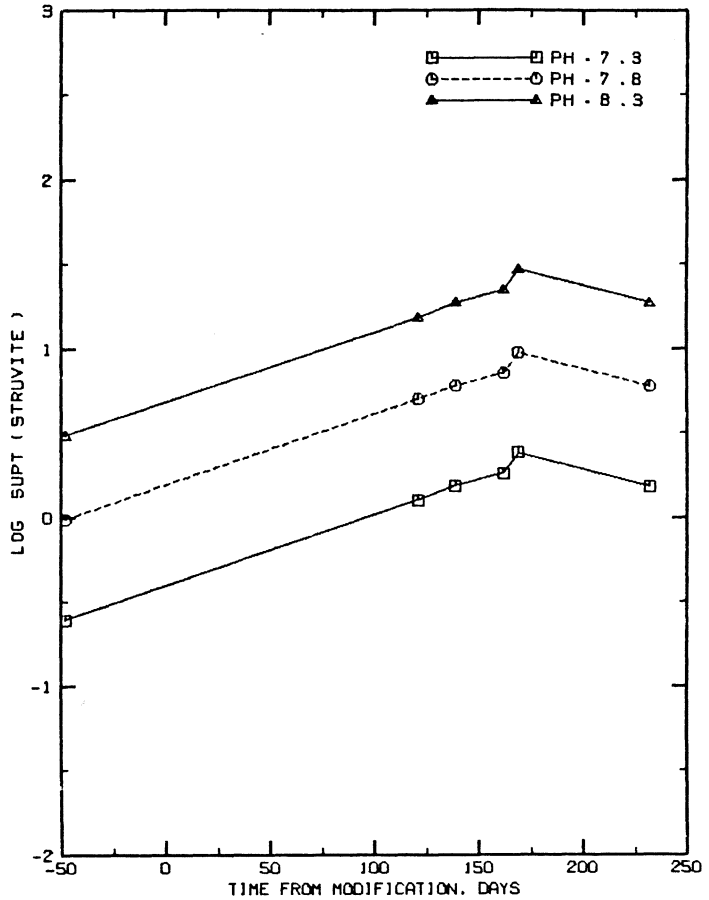

Log SUPT = Log (Q/Ksp)
Struvite = $MgNH_4PO_4.6H_2O$
Hydroxyapatite = $Ca_5(PO_4)_3OH$

Figure 31. Effect of pH on the level of saturation of struvite in the primary digester.

rapid releases from the biomass (50 % in 24 hours, Table 19), most of the struvite precipitates out in the primary digester. If other precipitates like vivianite do not reduce the post-precipitation levels of soluble phosphorus close to the premodification levels, the amount of soluble magnesium available for precipitation beyond the primary digester may be very limited. In an environment nucleated with struvite micro-crystals, the precipitation in the primary digester may occur in the immediate environment of the biomass as a result of the release of magnesium and phosphorus, and not as a result of the effect of temperature and pH on the saturation levels of the ions in solution. If there exists an epitaxial attachment between the flocs of biomass and struvite, most of it may be formed as microcrystals on the flocs. While 85 to 120 mg/L of magnesium precipitated in the primary digester at York River, the amount of magnesium available for precipitation in and after the secondary digester is only 10 mg/L. This is about the same as was available before the modification. In comparison, the amount of magnesium precipitated in the primary digester was negligible before the modification.

The key to having only 10 mg/L of soluble magnesium in the digester effluent is the extent of precipitation of phosphorus by calcium and iron precipitates. At York River, the effluent from the digester contained over 300 mg/L of soluble phosphorus. At another plant having higher levels of calcium and iron to precipitate out the phosphorus, the soluble magnesium flowing into the secondary digester may be higher, resulting in a greater potential for the precipitation of struvite in the secondary digester and beyond.

'Equilibrium' concentrations in the primary digester and simulation samples

Neither the primary digester nor the simulation samples could be presumed to have reached a 'complete' equilibrium with respect to all the species within six months of the BPR modification. However, the residence time for solids within the digester imparts a conditional equilibrium on the extent to which each of the species would be able to precipitate and crystallize in 120 days. The levels of soluble calcium and magnesium in the primary digester and set 6-12 are compared in

Figure 31. It shows that the calcium levels in the digester were much higher than those in laboratory simulations. In a continuous flow system, the level of calcium would be determined by the rate of precipitation, inflow and solubilization of calcium from the biomass. While the rate of precipitation is function of the level of supersaturation with respect to the thermodynamic equilibrium, the extent of solubilization will depend on the solids retention and the concentration of calcium in solution at steady state. A slow rate of precipitation would therefore result in higher levels of calcium. The reasons could be one of many discussed in Chapter II, a few amongst which are the substitution of ions in the crystal lattice, amorphousness and insufficient time to crystallize.

The magnesium levels in the simulations were marginally higher. This was because the rapid rate of precipitation of magnesium helped bring the steady state level close to the level necessary for thermodynamic equilibrium. As a result, the effective value of the solubility product for the digester was $10^{-12.42 \pm 0.11}$, as compared to $10^{-12.29}$ observed for the kinetics study. The lower average may have been caused by larger crystal sizes and longer residence times in the digester. The small drop in soluble magnesium before the modification may be in part due to the substitution of magnesium in some calcium precipitates (Fig 13).

Quantifying Phosphorus Release and Struvite Formation

Fraction of phosphorus released

The saturation levels for siderite and vivianite in the digester (Figure 27) show that while the former could be one of the ferrous precipitates throughout the study, more of vivianite may have precipitated after the BPR modification. The amount of vivianite formed was limited by the kinetics of precipitation of magnesium as struvite, which apparently is faster. Infact, all the magnesium solubilized by the degradation of poly-P was precipitated, removing a certain amount of the phosphorus which could have otherwise precipitated out as vivianite. The extent and kinetics of solubilization of poly-phosphates and the rate of transformation of iron affect the fraction of iron present as vivianite and siderite.

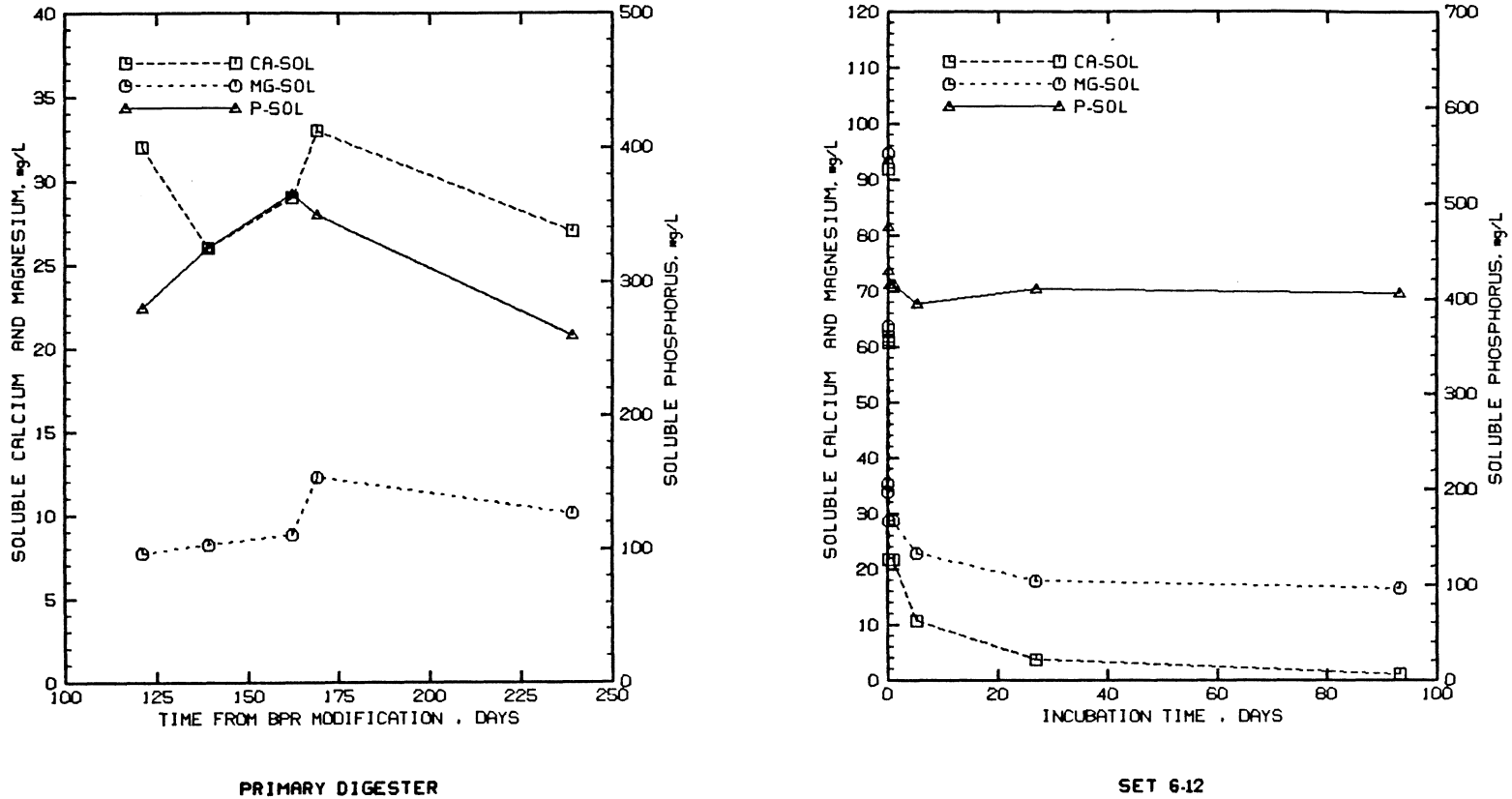

Figure 32. Comparison of the 'equilibrium' levels attained with respect to calcium and magnesium in the primary digester and set 6-12.

The return activated sludge released 62 % of its phosphorus after 12.4 days of anaerobic incubation at room temperature (22°C)[Table 18] Since the sludge in the primary digester is acted upon by methanogenic organisms at 35°C for approximately 120 days, the release fractions phosphorus and associated cations for the digester should be higher than those observed in the experiment with the return activated sludge.

If x, y and z are the mg/L of calcium precipitated as hydroxyapatite, magnesium precipitated as struvite and ferric iron transforming from ferric phosphate to ferrous phosphate, then

x mg/L calcium	= (x/40)*(1/1.67)*31.1	= 0.47 x mg/L P,
y mg/L magnesium	= (x/24)*31.1	= 1.30 y mg/L P and
z mg/L ferric to ferrous	= (z/56.6)*1.5*31.1	= 0.82 z mg/L P.

The total amount of phosphorus precipitated = (0.47x + 1.30y + 0.82z) mg/L.

If x = 80 mg/L, y = 115 mg/L and z = 100mg/L,

the amount of phosphorus precipitated, p = 270 mg/L.

For a post-precipitation soluble phosphorus level of 300 mg/L in the primary digester, the 'actual' (pre-precipitation) level of phosphorus would be

300 + 270 = 570mg/L.

The level of phosphorus in the primary digester before the BPR modification averaged 50 mg/L. The amount of soluble phosphorus released as a result of the modification to the plant therefore was

570 - 50 = 520 mg/L.

The overall increase in total phosphorus in the digester — the difference between the total and soluble phosphorus levels before and after the modification, was

1100 - 340 = 760 mg/L.

On a percentage basis, the release would work out as

(520/760) * 100 = 74 %.

The value of y was the same as that used in the kinetics study with 600 mg/L phosphorus. (The pre-precipitation level of soluble phosphorus arrived at in this sample calculation was 570 mg/L, as against 600 mg/L used in the kinetics study, Table 4.)

It can also be calculated that for 80 % of the iron existing in ferrous forms, the solubilization of all the poly-phosphates would result in an additional 70 % of the ferrous iron precipitating as vivianite, while the solubilization of 75 % of the poly-phosphates would result in additional 30 % of vivianite.

If 100 % of the phosphorus in the poly-phosphate is solubilized, the total amount of phosphorus available as soluble phosphorus

= 760 mg/L

The increase in the level of soluble phosphorus since the modification

= 300 - 50 = 250 mg/L

Amount of phosphorus precipitated by 115 mg/L of magnesium (as struvite) and 80 mg/L of calcium (as hydroxyapatite)

= 149 + 37 = 185 mg/L (rounded off)

Amount of phosphorus available for precipitation as vivianite

= 760 - (250 + 185) = 325 mg/L

Amount of ferrous iron required to precipitate the phosphorus

= 325/0.82 = 400 mg/L

Average level of iron in the digester = 690 mg/L

Assuming 80 % of the iron in ferrous form, additional amount of ferrous iron present as vivianite (as a result of the BPR modification)

= 400/(0.8*690) = 72 %.

If the calculation is repeated for the solubilization of 75 % of the poly-phosphates, the amount of phosphorus solubilized

= 0.75*760 = 570 mg/L

The additional amount of ferrous iron present as vivianite then is 30 %.

Mass of struvite formed

For a magnesium to phosphorus release ratio of 0.26 ± 0.016 , (Table 10)
a 60 to 75 percent release of the phosphorus in the poly-P granules (the increase in total phosphorus, 760 mg/L, equals the phosphorus in the poly-P granules) would release

(760) (0.6)/31.1 * (0.26 - 0.016) * 24 = **85. mg/L**

to

(760) (0.75)/31.1 * (0.26 + 0.016) * 24 = **120. mg/L of magnesium.**

Since the soluble magnesium levels in the digester remained fairly constant, it may be assumed that all the magnesium was precipitated as struvite. As seen from the kinetics study, under conditions conducive to the precipitation of struvite, no other magnesium precipitate was precipitated.

The amount of struvite ($MgNH_4PO_46H_2O$, Molecular weight of 245.1) formed will therefore range between

(85) (245.1/24.) = **870 mg/L** and

(120) (245.1/24.) = **1225 mg/L** .

For a total solids content of 27000 mg/L, struvite can comprise 3.2 to 4.5 % of the solids in the primary digester. This is a significant increase in the potential for struvite formation.

Hard Water and Combined Recycle Stream

An increase in the calcium hardness will serve to increase the amount of soluble calcium available for precipitation. This may react to bring down the level of soluble phosphorus in the effluent from the digester.

Precipitation of phosphorus as a Ca-P compound may take place after the non-potable-water (chlorinated secondary clarifier/plant effluent) mixes with the secondary digester underflow in the belt filter press. This reaction may continue in the grit chambers and primary clarifiers. The increase in soluble phosphorus level in the effluent from the primary clarifier will then be limited by the level to which the belt filtrate soluble phosphorus can increase before it starts forming precipitates with calcium.

Phenomenon of (bio)chemical precipitation

Subjecting the biomass to extended periods of anaerobic stress may release of sufficient amounts of phosphorus (and calcium on occasions) to form calcium-phosphorus precipitates, provided that the pH of the system is not too low. The potential for the formation of such precipitates has been discussed by Brannan (1985). The situation considered here is hypothetical and may not arise in biological phosphorus removal systems.

If it does occur, biochemical precipitation will limit the level of soluble phosphorus in the anaerobic zone of a BPR unit. The amount of phosphorus stored in the *Acinetobacter species* will then decrease by the amount of phosphorus removed by the precipitation (if the precipitate does not dissolve at the lower phosphorus in the aerobic zone). This reduction should not affect the ability of *Acinetobacter species* to store phosphorus because as long as the appropriate enzyme systems exist, *Acinetobacter species* have the propensity to utilize PHB or external substrate and store phosphorus under aerobic conditions (Lotter *et al.*, 1986 and Wentzel *et al.*, 1986). There is evidence of this in the experiment conducted with the return activated sludge. Aeration led to the uptake of substrate (acetates, propionates) and storage of phosphorus. These results were in accordance with the findings of Manning and Irvine (Chapter II) who mentioned that *Acinetobacter species* stored phosphorus even if the entire BPR system was operated aerobically for short periods of time. They suggested that this could be used as a strategy for controlling filamentous organisms in batch reactors.

The Nature of Struvite Crystals

The crystals of struvite had a clear tendency to adhere to the sides of glass bottles, but were not perceptibly adhesive to cotton. Inorder to compare its adhesiveness to that of the calcium precipitates, some samples from the kinetics study were swirled to suspend the precipitate and analyze them for the 'non-adhesive' fractions, based on the concentrations of ions in the mixtures. The increase in magnesium was compared to calcium to make a relative estimate of the adhesiveness of struvite against the calcium precipitates (Table 21).

From the poorer recovery of magnesium tied up in struvite crystals, it is evident that struvite is more adhesive than the calcium precipitate(s). A few general observations made from the kinetics study were:

1) the presence of cotton did not cause any perceptible difference in the amount of calcium and magnesium precipitated in the same amount of time;

2) cotton decreased the amount of struvite adhering to glass;

3) struvite crystals adhered with greater strength to an stiff surface like glass than to a more flexible surface like cotton;

4) the presence of cotton and/or higher levels of magnesium (115 mg/L magnesium as compared to 55 mg/L) decreased the size of crystals formed over the same period of time.

This implies that struvite can deposit on both the biomass (as observed) and on the surfaces and walls of the digester. That depositing on the sides may adhere strongly and prove difficult to remove.

Table 21. Comparison of adhesiveness based on the percent in suspension against the percent adhering to surfaces

Sample	surface	precipitate	Initial (t = 0)		Sample[1]		Suspension[2]		% Recovery[3]	
			Ca	Mg	Ca	Mg	Ca	Mg	Ca	Mg
			mg/l							
6-9-D	glass	struvite	0	115	0	21.3	0.	21.5		0.2
6-9-E	glass + cotton	struvite	0	115	0	22.0	0.	22.6		0.6
6-11-D	glass	struvite + fw	106	54.8	22.6	29.6	71.0	33.0	58.	13.5
6-11-E	glass + cotton	struvite + fw	106	54.8	18.7	28.1	93.5	45.1	85.7	63.7

[1]sample incubated for durations specified in Tables E9 and E11, Appendix E

[2]mixture of precipitate and solution after swirling the samples

[3]Recovery = (Amount of ion in suspension) / (Amount precipitated)

Amount of ion (x) in suspension = $x_{suspension} - x_{sample}$
Amount of ion (x) precipitated = $x_{initial} - x_{sample}$

Conclusions

1) When subjected to conditions of anaerobic stress in the absence of fresh substrate, bacterial species containing excess phosphorus in volutin (poly-phosphate) granules can release atleast 60% of their phosphorus.

2) Potassium, magnesium and calcium accompany the release of phosphorus. Calcium releases can be significant under conditions of extreme anaerobic stress. The level of iron transported across the membrane is negligible for suspended growth systems containing very little soluble iron.

3) In the presence of high background levels of ammonium in anaerobic digesters, the prolific releases of soluble magnesium and phosphorus from the poly-phosphate containing bacterial species result in the formation of a crystalline precipitate — struvite ($MgNH_4PO_4.6H_2O$).

4) The high levels of soluble phosphorus in anaerobic digesters precipitate out some of the soluble calcium. The stoichiometric ratio of calcium to phosphorus in this precipitate averaged 1.6:1 in kinetic studies conducted in a batch environment.

5) High ionic strengths, the possibility of substitution by foriegn ions, amorphous nature and micro-crystalline forms result in elevated amounts of species remaining in solution in anaerobic digesters.

6) If the decrease in phosphorus as a result of its precipitation by the available cationic pool of ions in the anaerobic digester is not high enough, there will be a significant increase in the soluble phosphorus level in the effluent from the digester. If the soluble calcium content of the influent wastewater/secondary effluent is high enough, there will be an interaction between the calcium in this stream and the phosphorus in the dewatered underflow of the secondary digester recycled to the headworks. Therefore the influent wastewater calcium level may indirectly impose as an upper limit on the level of phosphorus feeding back into the biological phosphorus removal system.

7) Because of high levels of soluble magnesium in the thickened waste sludge and the rapid kinetics of precipitation of struvite, it is impossible to prevent the formation of struvite in primary digester unless low pH and high temperatures make the environment thermodynamically undersaturated. If the temperature and pH in the primary digester are such that they prevent supersaturation with respect to struvite, chances are that significant amounts will precipite in the secondary digester when the mixed liquor cools down to normal temperatures, and the pH goes up on exposing the secondary digester effluent to the normal atmosphere.

8) The crystals of struvite are more adhesive than the calcium-phosphorus compounds precipitated from the same sample. The crystals may therefore precipitate on the walls of the primary and secondary digesters, which are also colder, the primary digester effluent line in which the mixed liquor cools, immediately after the secondary digester where its effluent is exposed to the normal atmosphere and on the flocs of biomass in the mixed liquor.

9) The ferrous iron in the digester is precipitated as vivianite if the levels of phosphorus are high enough, and the levels of carbonate alkalinity and sulfides are low enough to give vivanite a competitive edge over siderite and pyrite. The precipitation of vivianite may not influence the formation of struvite whose kinetics of formation are comparatively faster, enabling it to succesfully compete with other precipitates for the soluble phosphorus.

Bibliography

Brannan, K.P., "Substrate Stabilization in the Anaerobic Stage of a Biological Phosphorus Removal System." Ph.D Dissertation, VPI&SU, Blacksburg, Virginia (1986).

Buchan, L., "Possible Biological Mechanisms of Phosphorus Removal." *Water Sci. Technol.* **15**, 87-103 (1983).

Buchan, L. "The Location and Nature of Accumulated Phosphorus in Seven Sludges from Activated Sludge Plants which Exhibited Enhanced Phosphorus Removal." *Water SA* **7(1)** 1-7 (1981).

CH_2M Hill, Virginia Initiative Pilot Plant Report, Lambert's Point, Norfolk, Virginia, 1985.

Comeau, Y., Hall K. J., Hancock, R. E. W. and Oldham, W. K., "Biochemical Model for Enhanced Biological Phosphorus Removal." *Proceedings, Direction and Research in Waste Treatment and Residuals Management*, University of British Columbia, Vancouver, British Columbia, Canada, June 23-28, 324-346 (1985).

CRC Handbook of Chemistry and Physics, 65th ed., CRC Press Inc. (1984-85).

Elliot, J. C. "The Problems of the Composition and Structures of the Mineral Components of Hard Tissues." *Clin Orthop* **93** , 313-333 (1973).

Griffith, D. P. and Musher, D. M. "Pathogenesis of infection stones." In: "Colloquium on renal tissues." Eds. Finlayson, B., Thomas, W. C., Univ Press Florida, 54-65 (1976).

Gulbrandsen, R. A., Roberson, C. E. and Neil, S. T. "Time and the Crystallization of Apatite in Seawater." *Geochemica et Cosmochimica Acta* **48** , 213-218 (1984).

Henriksen, S. D., " *Moraxella, Neisseria, Branhamella* and *Acinetobacter* ." Annual Review, *Microbiology* **30** , 63-83 (1976).

Jenkins D., Ferguson J. F. and Menar A. B., Review Paper "Chemical Processes for Phosphate Removal." *Water Research* **5** , 369-389 (1971).

Juni, E., "Genetics and Physiology of *Acinetobacter* ." Annual Review, *Microbiology* **32** , 349-371 (1978).

LeGeros, R. Z. and LeGeros J. P., "Phosphate Minerals in Human Tissues." In "Phosphate Minerals", Ed. Nriagu, J. O. and Moore P. B., Springer-Verlag Berlin Heidelberg, Chapter 12, 351-385 (1984).

Lindsay, W. L. and Vlek, P. L. G., "Phosphate Minerals." In "Minerals in Soil Environments." Ed. R. C. Dinauer, Soil Science Society of America, Madison, Wisconsin, USA (1977).

Lotter, L. H., Wentzel, M. C., Loewenthal, R. E., Ekama, G. A. and Marais, G. v. R., "A Study of Selected Characteristics of *Acinetobacter spp.* isolated from Activated Sludge in Anaerobic/Anoxic/Aerobic and Aerobic Systems." *Water SA* **12** (4), 209-224 (1986).

Lotter, L. H., "The Role of Bacterial Phosphate Metabolism in Enhanced Phosphorus Removal Systems in Activated Sludge Process." *Water Science Tech.* **17** , 127-138 (1985).

Manning, J. F. and Irvine R. C. "The Biological Removal of Phosphorus in a Sequencing Batch Reactor." *J. Water Pollut. Control Fed.* , **57** (1), 87-94 (1985).

McCarty, P. L., "Phosphorus and Nitrogen Removal by Biological Systems." *Proceedings, Wastewater Reclamation and Reuse Workshop, Lake Tahoe, California.* (1970).

McDowell, H., Gregory, T. M. and Brown, W. E., "Solubility of $Ca_5(PO_4)_3OH$ in the system- $Ca(OH)_2 - H_3PO_4 - H_2O$ at 5, 15, 25 and 37°C ." *Journal of Research of the National Bureau of Standards - A. Physics and Chemistry* **81A** (2 and 3), March-June (1977).

Nash, J., Personal communication, Virginia Polytechnic Institute and State University, 1987.

Nriagu, J. O. and Moore, P. B., Ed., "Phosphate Minerals." Springer-Verlag Berlin Heidelberg (1984).

Nriagu, J., "Stability of vivianite and ion-pair formation in the system iron (II) orthophosphate-phosphoric acid-water." *Geochem. Cosmochim Acta* (36), 459-470 (1972).

Padan, E., Zilberstein, D. and Rottenberg, H., "The Proton Electrochemical Gradient in *Escherichia coli* ." *European Jour. of Biochemistry* **63** , 533-541 (1976).

Posner, A. S., Blumenthal, N. C. and Betts, F., "Chemistry and Structure of Precipitated Hydroxyapatites." In "Phosphate Minerals", Ed. Nriagu, J. O. and Moore P. B., Springer-Verlag Berlin Heidelberg, Chapter 11, 330-331 (1984).

Schuldiner, S. and Padan, E., "How does *Escherichia coli* Regulate Internal pH?" Chapter 97, *Membranes and Transport* Ed. A. N. Martonosis, New York, Plenum Press, Vol. 2, 67-73 (1982).

Singer, P. C. "Anaerobic Control of Phosphate Ferrous Iron." *Jour. Water Pollut. Control Fed.* **44** (4), April (1972).

Sorensen, E. N. and Rosen, B. P., "Cation/Proton Antiport Systems in *Escherichia coli* ." Chapter 97, *Membranes and Transport* Ed. A. N. Martonosis, New York, Plenum Press, Vol 2, 61-64 (1982).

Snoeyink V. L. and Jenkins, D. "Water Chemistry." John Wiley and Sons, Inc. (1980)

Standard Methods for the Examination of Water and Wastewater, 16th Ed., American Public Health Association, Washington D. C. (1980).

Stumm, W. and Morgan, J. J., "Aquatic Chemistry — An Introduction Emphasizing Chemical Equilibria in Natural Waters." 2nd ed. John, Wiley and Sons, Inc. (1981).

Tomson, M. B. and Vignona, L., "Precipitation of Phosphate Minerals in Wastewater Treatment Systems." In "Phosphate Minerals", Ed. Nriagu, J. O. and Moore P. B., Springer-Verlag Berlin Heidelberg, Chapter 13, 390-392 (1984).

Van Groenestijn, J. W. and Deinema, M. H., "Effects of Cultural Conditions on Phosphate Accumulation and Release *Acinetobacter* strain 210A." *Proceedings of the International Conference on Management Strategies for Phosphorus in the Environment.* Selper Ltd., London (1985).

Appendix A. Data from samples collected across the plant

ATE = Aeration Tank Effluent

BF = Belt Filtrate

BFAN = Belt filtrate after mixing with non potable water

CN2 = Cell Number 2

CN4 = Cell Number 4

CN6 = Cell Number 6

FC = filter cake after dyring (103°C, 2 hours)

FTS = Float Thickener Subnatant

GTS = Gravity Thickener Supernatant

NPW = Non Potable Water

PCE = Primary Clarifier Effluent

PD = Primary Digester Mixed Liquor

RI = Raw Influent

SDS = Secondary Digester Supernatant

SDU = Secondary Digester Underflow

SE = Secondary Effluent

SEACl = Secondary Effluent after chlorination

TPS = Gravity Thickened Primary Sludge

TWS = Float Thickened Waste Sludge

Table A1. Results of the analyses of samples collected on June 17, 1986

Sample	FCOD	TCOD	TKN	Org-N	NH_4-N	Alk[1]	Cl	NO_2-N	NO_3-N	P-sol	P-tot	SO_4-S	ORP	
	mg/L												mv*	
RI	150.	345.	30.	6.	24.	200		0.	0.0	7.2	12.0	26.1		
PCE	77.	148.				235		0.	0.1	7.3	11.5	61.0		
SE	20.	53.				85		0.	18.5	6.2		76.		
GTS						305		0.	4.94	13.2	18.0	16.3		
FTS						185		0.8	5.7	13.6	19.0	59.		
TPS	3500.	84100.	1800.	1420	380	1210		0.	0.3	77.	560.	9.5		
TWS	2380.	74850.	3575.	2825	750	305		0.	0.1	82.	2300.	3.5		
PD	330	15850.	1085.	445	640	2675		0.	0.0	53.5	340.	56.		
SDS	470	4375.	1100.	120	980	2550		0.	1.9	43.5	195.	25.3		
SDU	300.	17600.	1575.	725	825	3000		0.	0.3	74.	560.	13.6		
BF	200.	3070.				800		0.	0.0	39.0	240.	87.		

[1]alkalinity expressed as mg/L as $CaCO_3$

* millivolts

Table A2. Results of the analyses of samples collected on June 17, 1986

Sample	Ca-f	Ca-t	Mg-f	Mg-t	Na-f	Na-t	K-f	K-t	Fe-f	Fe-t	Al-f	Al-t		
						mg/L								
RI	41.0	45.1	4.62	4.82	63.0	72.2	9.8	10.0	0.2	3.26				
PCE	45.0		5.83		89.		10.4		0.2					
SE	44.6	42.6	5.83	5.6	88.	105.	10.6	10.3	0.0	0.14				
GTS	53.7	52.5	7.0	6.6	95.	115.	12.2	11.4	0.15	3.2				
FTS	49.2	43.7	6.49	5.94	95.	130.	13.4	13.6	0.1	0.9				
TPS	150.	1650.	18.0	82.	102.	1280.	24.2	125.	0.2	1025.				
TWS	87.	1360.	20.4	70.4	110.	2900.	88.	204.	0.2	800.				
PD	98.	335.	7.6	34.	110.	127.	49.	54.	0.14	230.				
SDS	51.	215.	2.97	19.6	115.	122.	56.0	51.6	0.36	133.				
SDU	90.	4475.	5.40	41.3	110.	210.	54.0	77.	0.23	435.				
BF	65.		11.7		104.		28.0		0.11					

-f stands for 0.45μm filtered sample concentration

-t stands for total concentration

Table A3. Results of the analyses of samples collected on July 8, 1986

Sample	FCOD	TCOD	TKN	Org-N	NH_4-N	Alk[1]	Cl	NO_2-N	NO_3-N	P-sol	P-tot	SO_4-S	ORP	
	mg/L												mv*	
RI	155.	430.	31.	7.	24.	185		0.0	0.0	5.1	10.4	3.4		
PCE	190.	91.4			20.	270		0.0	0.0	5.16	9.9	18.3		
SE	27.	52.	1.1	0.82	0.28	85		0.0	18.5	6.2		76.		
GTS	460.	78.				165		5.0	0.1	6.2	11.5	43.3		
FTS	61.	98.				150		1.01	7.4	8.1	9.0	53.		
TPS	4100.	143600.	19200.	3100	16100	1170		0.0	0.0	18.5	660.	30.1		
TWS	830.	42500.	3000.	2125	925	1525		0.0	0.0	1.7	705.	85.0		
PD	450	1540.	1400.	810	590	2800		0.0	0.0	45.	320.	3.2		
SDS	1250	750.	730.	140	590	2575		0.0	0.0	58.	88.	8.4		
SDU	360.	25900.	1960.	1345	615	2725		0.0	0.0	71.	610.	3.2		
BF BFAN	750. 95.	5225. 2370.	840	335	505	1700 155		0.0 0.0	0.0 0.0	15.0 15.	92. 92.	17. 3.2		
NPW	40.					97.5		0.0	10.2	5.5	8.0	31.5		
CBR	75.	250.				300		1.2	0.7	5.9		63.4		

[1]alkalinity expressed as mg/L as $CaCO_3$

[×] millivolts

Table A4. Results of the analyses of samples collected on July 8, 1986

Sample	Ca-f	Ca-t	Mg-f	Mg-t	Na-f	Na-t	K-f	K-t	Fe-f	Fe-t	Al-f	Al-t		
						mg/L								
RI	38.7	45.5	5.66	6.02	73.0	98.8	9.3	9.74	0.09	2.68				
PCE	38.7		5.48		110.		9.94		0.09					
SE	42.5	41.6	5.74	5.4	108.	106.	10.8	10.2	< 0.03	0.10				
GTS	42.8	51.5	5.42	5.9	105.	114.	9.96	11.3	0.09	2.7				
FTS	43.4	470.	5.60	5.70	103.	112.	11.2	12.2	0.08	0.65				
TPS		2700.		112.3		625.	64.5	104.		1545.				
TWS		840.		91.8	265.	665.	75.5	168.	9.7	566.				
PD		770.		59.0	130.	360.	56.4	72.0		575.				
SDS		1115.			130.		56.0			102.				
SDU		1110.			120.	300.	52.6	84.0		895.				
NPW	42.9	43.3	5.75	5.59	108.	109.	10.9	10.2	0.03	0.19				

-f stands for 0.45μm filtered sample concentration

-t stands for total concentration

Table A5. Results of the analyses of samples collected on July 31, 1986

Sample	FCOD	TCOD	TKN	Org-N	NH_4-N	Alk[1]	Cl	NO_2-N	NO_3-N	P-sol	P-tot	SO_4-S	ORP	
	mg/L												mv*	
RI	150.	455.	29.	7.	22.	220		0.0	0.0	8.8	10.1	1.6		
PCE	85.	185.	31.	3.	28.	285		0.0	0.1	6.9	9.2	25.8		
ATE	57.	895.				170		0.0	16.8	6.6	26.0	61.		
SE	24.	27.	1.2	0.7	0.5	53		2.3	22.0		8.4	60.		
SE	25.	34.				82		0.	20.8	6.6	8.4	56.		
RAS	20.	1520.				113		0.	12.8	7.9	36.0	64.		
PCU	95.	650.				418		0.	0.	5.74	22.0	24.		
GTS	91.	380.				145		0.1	9.9	7.8	12.1	50.		
FTS	32.	92.				168		1.9	1.9	10.7	14.3	57.		
TPS	1475.	86000.	1750.	180	1570	1365		0.0	0.0	48.0	530.	32.1		
TWS	875.	42100.	3750.	2975	775	1525		0.0	5.9	75.	870.	79.0		
PD	400.	20500.	1950.	700	1250	3050		0.0	0.2	48.	370.	4.6		
SDS	400	1400.	850.			3200		0.0	0.0	72.	90.	5.3		
SDU	415.	12840.	1470.	620	850	3100		0.0	0.0	57.	260.	14.1		
BF BFAN	285. 47.	1030. 280.	490	45	445	2010 1850		0.0 0.0	5.7 8.6	5.4 20.	52. 28.	60. 50.5		
NPW	24.	46.				55.		0.0	12.9	5.8	15.2	64.1		
CBR	74.	210.	128.	116.	112.	480		1.4	7.9	5.7	18.5	50.5		

[1] alkalinity expressed as mg/L as $CaCO_3$

[×] millivolts

Table A6. Results of the analyses of samples collected on July 31, 1986

Sample	Ca-f	Ca-t	Mg-f	Mg-t	Na-f	Na-t	K-f	K-t	Fe-f	Fe-t	Al-f	Al-t		
						mg/L								
RI	36.0	40.5	6.32	6.53	86.	88.	10.5	10.3	0.16	2.6				
PCE	33.6	36.8	5.37	5.52	105.	110.	10.4	10.1	0.14	1.0				
ATE	36.5	63.3	5.9	8.8	97.5	118.	11.7	16.3	0.15	28.0				
SE	35.0	35.4	5.51	5.54	90.	89.	10.9	10.5	0.07	0.20				
SEACl	34.1	38.7	5.36	5.46	85.	89.	10.3	10.6	0.07	0.88				
ATE	36.5	63.3	5.9	8.8	97.5	118.	11.7	16.3	< 0.15	28.0				
RAS	42.0	80.	7.2	11.0	110.	160.	14.0	21.0	< 0.03	19.5				
GTS	53.7	52.5	7.0	6.6	95.	115.	12.2	11.4	0.15	3.2				
RAS	36.0	45.5	5.79	6.3	92.	98.	11.0	11.6	0.09	3.80				
FTS	36.0	40.0	5.81	6.0	87.	92.	12.2	13.4	0.15	1.25				
TPS	177.	1575.	23.0	93.6	161.	351.	34.3	57.2		870.				
TWS		840.		105.	168.	1175.	56.1	190.		535.				
PD		763.		65.7	124.	167.	56.6	65.3		555.				
SDS		215.		22.0	119.	195.	55.2	64.0		18.5				
SDU		560.		47.0	114.	240.	53.6	66.0		380.				
BF		130.		20.0	109.	220.	89.	100.*		29.				
BFAN		85.		14.	101.	135.	82.5	86.5	0.15	2.0				
NPW	35.9	36.8	5.5	5.44	87.	90.	9.96	9.8	0.05	0.6				
CBR	38.5	54.0	7.3	7.5	92.	105.	25.6	25.6	0.03	2.7				

× error in analysis

-f stands for 0.45µm filtered sample concentration

-t stands for total concentration

Table A7. Results of the analysis of samples collected on Sept. 4-5, 1986

Sample	FCOD	TCOD	TKN	Org-N	NH_4-N	Alk[1]	Cl	NO_2-N	NO_3-N	P-sol	P-tot	SO_4-S	ORP	
	mg/L												mv*	
RI	119.	345	31.	2.5	28.	225	65	0.	0.0	7.1	9.4	2.8		
PCE	101.	186	32.	3.8	28.	275	61	0.	0.0	9.8		23.2		
CN2	44.7	2215				270	63	0.	0.0	50.	125.	59.		
CN4	42.3	1712				295	95	0.	0.0	41.	88.	63.		
CN6	39.8	930				255	61	0.	0.06	20.7	54.5	61.		
ATE	36.6	1020				240	66	1.4	0.20	12.9	57.	70.		
SE	36.2	37.5	14.3	8.4	5.9	205	61	3.4	0.59	3.2	3.9	79.		
RAS	48.7	4750				255	61	0.0	0.0	62.	300.	82.		
GTS	92.	272				235	66	0.0	0.0	7.1	8.8	50.		
FTS	30.5	91				237	95	0.0	0.0	24.7	27.0	73.		
TPS	1800.	121000	1260	882	380	530	100.	0.0	0.0	53.	575.	23.		
TWS	285.	53500	2570	1960	610	555	90.	0.0	0.0	68.	2575	230		
PD	365.	7150	1150	310	840	2835	123.	0.0	0.0	53.	205	1.9		
SDS	184.	2940	875	116	756	2725	87.	0.0	0.0	47.	89	2.6		
SDU	245.	23401	1943	1135	810	2785	112.	0.0	0.0	51.	490	2.1		
BFAN	145.	294				1865	58.	0.0	0.94	33.	350	49.		
NPW	24.5	31				196	59.	1.35	0.59	2.56	3.5	84.3		
CBR	51.	225	42	3	39	265	60.	2.66	0.38	7.8	105	78.		
FC[2]											31.6[4]			

[1] alkalinity expressed as mg/L as $CaCO_3$

[×] millivolts

[3] filter cake

[4] mg/g

Table A8. Results of the analysis of samples collected on Sept. 4-5, 1986

Sample	Ca-f	Ca-t	Mg-f	Mg-t	Na-f	Na-t	K-f	K-t	Fe-f	Fe-t	Al-f	Al-t		
						mg/L								
RI	39.6	44.3	6.96	7.59	79.8	91.8	9.34	10.1	0.09	3.22				
PCE	40.2	43.4	6.53	6.56	95.0	116.	10.5	10.1	0.12	1.2				
CN2	42.4	84.0	14.5	28.7	99.8	128.	20.6	35.4	0.30	27.3				
CN4	41.0	78.3	13.5	22.6	102.	152.	19.4	28.2	0.15	2 1.2				
CN6	39.0	63.1	9.04	15.6	91.2	118.	12.9	20.4	0.16	12.6				
ATE	40.7	61.7	8.55	16.0	103.	134.	13.1	21.2	0.20	12.8				
SE	41.8	41.8	5.46	5.61	107.	111.	8.34	8.98	0.05	0.19				
RAS	46.3	134.	16.6	63.2	106.	134.	25.8	75.0	0.60	67.4				
GTS	45.8	52.0	6.81	7.3	105.	127.	9.76	9.7	0.05	2.05				
FTS	44.7	45.6	9.23	9.75	101.	122.	15.8	15.6	0.13	1.45				
TPS	222.	2225.	20.0	103.	98.	525.	21.4	52.5	0.68	1490.				
TWS	24.6	900.	6.85	505.	100.	510.	180.	605.	0.69	605.				
PD	51.8	270.	1.76	50.	110.	215.	98.	92.	0.72	150.				
SDS	79.6	200.	4.47	24.4	87.	200.	46.0	55.2	0.14	40.0	< 0.1	6.0		
SDU	58.7	705.	3.00	80.4	110.	320.	70.0	92.	0.23	565.	< 0.1	72.		
BFAN	54.8	75.4	9.79	19.6	105.	200.	67.8	72.8	0.06	24.0				
NPW	40.9	40.8	5.29	5.4	104.	120.	9.4	9.2	0.05	0.14				
CBR	44.7	53.0	6.73	7.7	99.	135.	12.4	13.2	0.08	2.9				
FC(mg/g)		6.3		0.46		0.6		0.19		5.5				

-f stands for 0.45μm filtered sample concentration

-t stands for total concentration

Appendix B. X-Ray diffraction patterns

Table B1. Powder X-ray diffraction characteristics for Struvite Crystals

d A°	2θ degrees	I/I_1	hkl
5.905	15.0	60	020
5.378	16.5	25	011
4.257	20.9	100	111
3.289	27.1	25	130
2.958	30.2	25	012
2.919	30.6	55	211
2.690	33.3	50	022
2.660	33.7	45	221

d = spacing between crystal planes

θ = angle for constructive intereference

I_1 = maximum intensity (I) of diffraction

hkl = the crystal plane

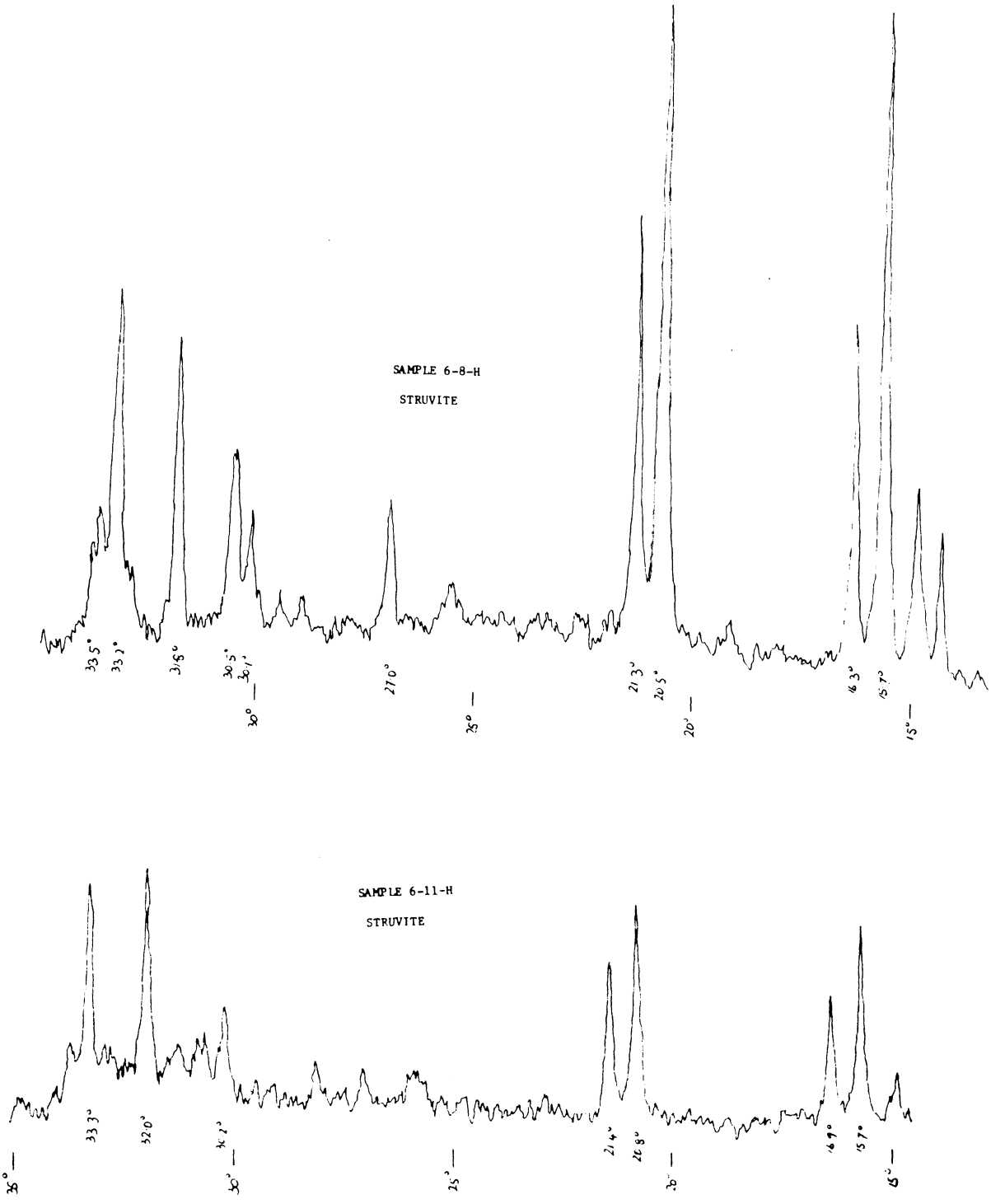

Figure B1. Diffraction patterns for precipitates of samples from the Kinetics study.

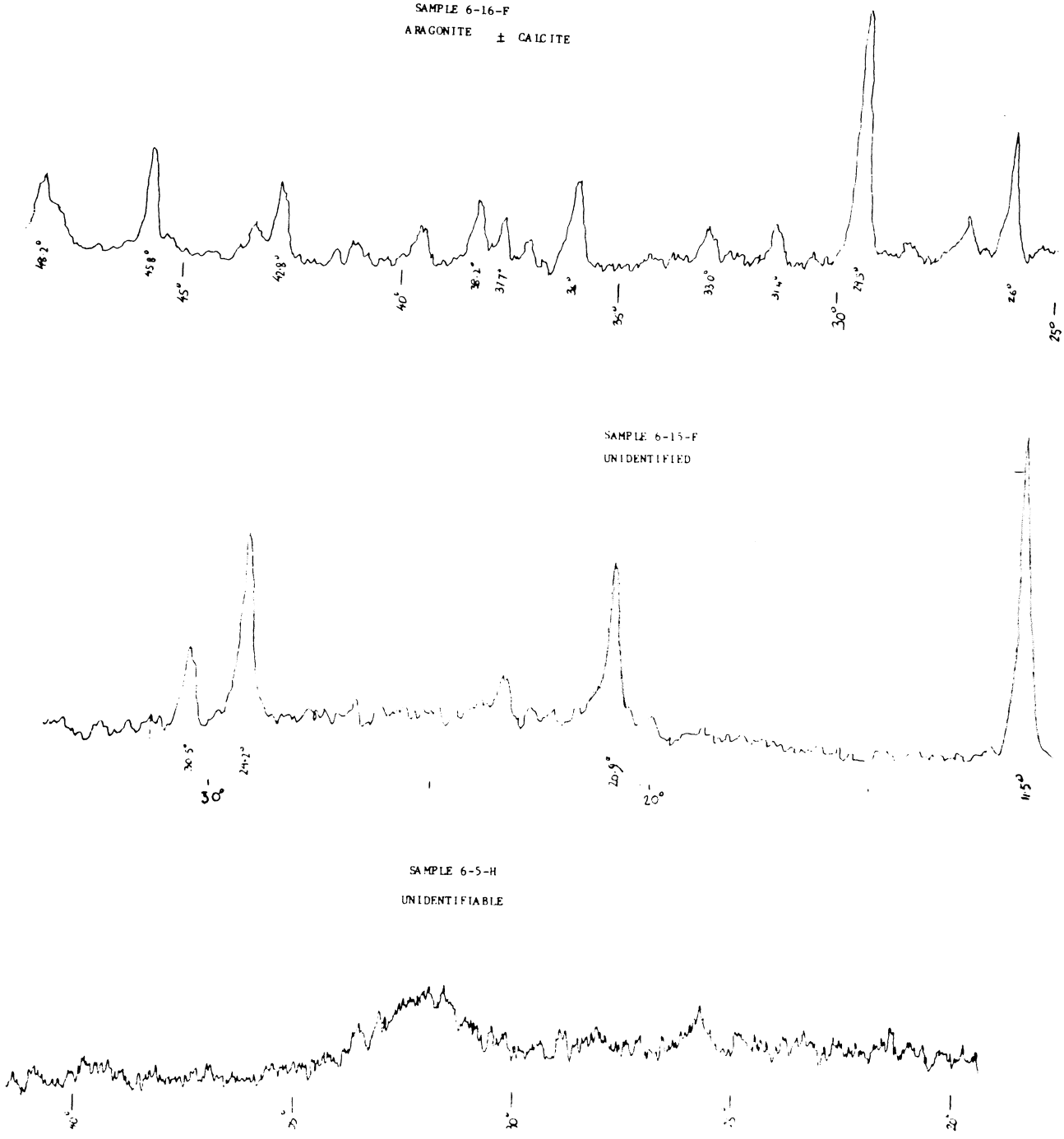

Figure B1 (continued). Diffraction pattern for precipitates of samples from the Kinetics study.

Appendix C. Trend in waste streams around the primary digester

Table C1. Trend in the thickened primary sludge (TPS)

Date	pH	TS	% Vol	P-s	P-t	Ca-s	Ca-t	Mg-s	Mg-t	Na-s	Na-t	K-s	K-t	Fe-s	Fe-t
		mg/l		mg/l											
6/17/86		82950	75	77.	560	150	1660	18.0	82.	102	1280*	24.2	125	0.22	1025
7/ 8/86		149000	89	18.5	660	220	2700	19.8	112.	250	625	64.5	105	8.32*	1550
7/31/86		58200	76	48.0	530	175	1575	23.0	94.	160	350	34.3	57.2	2.08*	870
9/04/86				52.6	580	220	2225	20.0	105.	98.	525	21.4	52.5	0.68	1490
1/13/87**	6.43	52300		83.	1050	315	2790	48.6	170.	117	650	41.0	170	0.25	1100
1/20/87**	6.19	113350		63.	1040	280	3240	40.5	240.	82	420	39.0	155	0.66	3020
3/24/87	6.55	47240		59.1	565	117	1160	14.8	96.	82	550	23.0	130	0.30	880

* stands for error in analysis or non-representative value
** sample was refrigerated for 1-2 weeks before analysis
-s stands for soluble species concentration
-t stands for total species concentration
TS = Total Solids
% Vol = percent of total solids which is volatile
P = Phosphorus
Ca = Calcium
Mg = Magnesium
Na = Sodium
K = Potassium
Fe = Iron

Table C2. Trend in the thickened waste sludge (TWS)

Date	pH	TS	% Vol	P-s	P-t	Ca-s	Ca-t	Mg-s	Mg-t	Na-s	Na-t	K-s	K-t	Fe-s	Fe-t
		mg/l		mg/l											
6/17/86				82.	2300*	87.	1360	20.4	70.	110	2900	88.	205	0.21	1025
7/ 8/86		33300	91	75.	705		840	26.5	92.		660	76.	170	9.7*	570
7/31/86		37200	78	76.	865		840	22.0	105.	170	1180	56.	190	12.7*	530
9/ 4/86				67.	2575	25.*	900	6.85*	505.	100	510	179.	606	0.69	610
1/13/87**	6.96	36000		580.	2150	140.	1230	150.	455.	110	405	355.	600	6.6	700
1/20/87**	5.98	40200		630.	2180	175.	1070	150.	480.	65.	475	360.	625	8.0	650
3/24/87	6.56	44750	76	445.	1880	96.	1120	72.	310.	71.	525	175.	470	2.33	1020

* stands for error in analysis or non-representative value
** sample was refrigerated for 1-2 weeks before analysis
-s stands for soluble species concentration
-t stands for total species concentration
TS = Total Solids
% Vol = percent of total solids which is volatile
P = Phosphorus
Ca = Calcium
Mg = Magnesium
Na = Sodium
K = Potassium
Fe = Iron

Table C3. Trend in the primary digester (PD)

Date	pH[1]	pH[2]	TS	% Vo	Alk	P-s	P-t	Ca-s	Ca-t	Mg-s	Mg-t	Na-s	Na-t	K-s	K-t	Fe-s	Fe-t
			mg/l		mg/l												
6/17/86						53.	335	98.	335	7.6	34.	110	125	49.	54	0.14	235
7/ 8/86			25100			45.	320	115.	770		59.		360	56.	72		580
7/31/86			22000	64.1		48.	370	100.	765		66.	125	165	57.	65		560
9/ 4/86[3]						53.	205.	52.	270	1.76	50.	110	215	98.	92	0.72	150
12/ 3/86			24030	63.2		280.	1140.	32.	840	7.70	160.		355	210	265	0.51	610
12/21/86			27190	64.0		325.	1175.	26.	990	8.25	160.	93	375	225	350	0.63	790
1/13/87**	7.42	8.21	30140	60.7		365.	1040	29.	1000	8.83	115.	115	340	240.	330	0.48	740
1/20/87**	7.18	8.27	30720	56.8		350.	1010	33.	990	12.3	135.	120.	350	250.	310	0.36	720
3/24/87	7.37	8.17	28260	60.7	2300	260.	1115	27.	995	10.1	120.	85.	350	215.	280	0.93	825

* stands for error in analysis or non representative value
** sample was refrigerated for 1-2 weeks before analysis
-s stands for soluble species concentration
-t stands for total species concentration

pH^1 is the pH of the 1.2μm filtrate

pH^2 is the pH of the 0.45μm filtrate

[3]the primary digester was yet to reach an "equilibrium" - 120 days

Alk = Alkalinity in mg/l of $CaCO_3$
TS = Total Solids Average = 26800 mg/L
% Vol = percent of total solids which is volatile
P = Phosphorus Ca = Calcium Mg = Magnesium
Na = Sodium K = Potassium Fe = Iron

Table C4. Trend in the Secondary Digester Underflow (SDU)

Date	pH[1]	pH[2]	TS	% Vol	Alk	P-s	P-t	Ca-s	Ca-t	Mg-s	Mg-t	Na-s	Na-t	K-s	K-t	Fe-s	Fe-t
			mg/l		mg/l												
6/17/86						74.	562	90.	4475*	5.4	41.3	110	210	54.	77	0.23	435
7/ 8/86						71.	610		1110		79.	120	300	53.	84	2.2*	900
7/31/86			14450	69.9		57.	260		560		47.	115	240	54.	66	1.3*	380
9/ 4/86						51.	490.	59.	705	3.00	80.4	110	320	70.	92	0.23	565
12/ 3/86		8.18				250.	1050.	34.	1100	9.90	245.		140	200	255	0.48	880
12/21/86		8.29				295.	1055.	31.	1130	9.35	225.	100	160	205	290	0.43	840
1/13/87**	7.28		19370	64.3		365.	1120*	29.	790	10.4	110.	105	320	200.	270	0.32	535

* stands for error in analysis or non representative sample
** sample was in refrigerated for 1-2 weeks before analysis
-s stands for soluble species concentration
-t stands for total species concentration

pH^1 is the pH of the 1.2μm filtrate

pH^2 is the pH of the 0.45μm filtrate

Alk = alkalinity
TS = Total Solids
% Vol = percent of total solids which is volatile
P = Phosphorus
Ca = Calcium
Mg = Magnesium
Na = Sodium
K = Potassium
Fe = Iron

Appendix D. Data from the kinetics study

Table D4. Kinetics study with Ca, 100 mg/L P but no Mg (Set 6-4)

Sample		Time	pH	Ca	Mg	NH_4N	PO_4P	ΔCa	ΔMg	ΔP	$\Delta Ca/\Delta P$
		days, hr, min		mg/L				milli-moles			
6- 4-A		00, 00, 00	7.29	104.	< 0.15	700	99	0.00		0.00	
6- 4-B		00, 01, 01	7.29	105.	"		99	0.00		0.00	
6- 4-C		00, 06, 03	7.22	105.	"	730	100	0.00		0.00	
6- 4-D		01, 00, 08	7.22	107.	"		98	0.00		0.00	
6- 4-E	Cotton	01, 00, 12	7.26	105.	"		96	0.00		0.00	
6- 4-F		05, 04, 35	7.27	87.6	"	790	89	0.435		0.323	1.35
6- 4-G	Cotton	05, 04, 41	7.16	25.7	"	790	57	1.98		1.35	1.47
6- 4-H		31, 03, 55	7.14	10.8	"		41	2.33		1.87	1.25
6- 4-J	Cotton	31, 08, 00	7.10	13.3	"		50	2.27		1.58	1.44
6- 4-K		96, 09, 21	7.17	4.30	"		47	2.49		1.68	1.48
$MEAN_{i=5}$											1.40**
STANDARD DEV											0.10

* denotes error in analysing the sample - as apparent from trend in data
** Higher levels of precipitation required for reliable stoichiometry
Na = 1250 mg/L N = 750 mg/L
K = 69 mg/L
Cl = 2250 mg/L
Total CO_3 alkalinity = 2250 mg/L

Table D5. Kinetics study with Ca, 300 mg/L P but no Mg (Set 6-5)

Sample		Time	pH	Ca	Mg	NH_4N	PO_4P	ΔCa	ΔMg	ΔP	ΔCa/ΔP
		days, hr, min		mg/L				milli-moles			
6- 5-A		00, 00, 00	7.31	111	< 0.15	725	280	0.00		0.00	
6- 5-B		00, 00, 59	7.32	101.5	"			2.54			
6- 5-C		00, 06, 14	7.13	16.1	"		222	2.74		1.87	1.46
6- 5-D		01, 00, 03	7.13	13.2	"		250*	2.75		1.13	2.43*
6- 5-E	Cotton	01, 00, 09	7.15	12.0	"		230	2.75		1.77	1.55
6- 5-F		05, 04, 41	7.14	2.30	"	800	231	2.72		1.74	1.56
6- 5-G	Cotton	05, 05, 07	7.14	1.75	"	735	227	2.73		1.86	1.48
6- 5-H		30, 04, 47	7.54	2.0	"		220	2.73		2.09	1.31
6- 5-J	Cotton	30, 07, 52	7.19	2.91	"		235	2.70		1.61	1.68
6- 5-K		96, 08, 09	7.08	0.97	"		240	2.75		1.45	1.85
$MEAN_{i=6}$											1.57
STANDARD DEV											0.18

* denotes error in analysing the sample - as apparent from trend in data
Na = 1425 mg/L N = 750 mg/L
K = 125 mg/L
Cl = 2200. mg/L
Total CO_3 alkalinity = 2100 mg/L

Table D6. Kinetics study with Ca, 600 mg/L P but no Mg (Set 6-6)

Sample		Time	pH	Ca	Mg	NH_4N	PO_4P	ΔCa	ΔMg	ΔP	ΔCa/ΔP
		days, hr, min		mg/L				milli-moles			
6- 6-A		00, 00, 00	7.30	112.	0.14	845	570	0.00		0.00	
6- 6-B		00, 00, 59	7.24	17.7	< 0.15		525	2.36		1.45	1.63
6- 6-C		00, 06, 03	7.17	8.58	"		495*	2.59		2.41*	1.07*
6- 6-D		00, 23, 56	7.19	7.40	"	720	525	2.62		1.45	1.81
6- 6-E	Cotton	01, 00, 06	7.20	7.04	"	735	510	2.62		1.93	1.36
6- 6-F		05, 04, 40	7.15	1.31	"	710	485*	2.77		2.73*	1.01*
6- 6-G	Cotton	05, 04, 49	7.16	0.96	"	770	530	2.78		1.29	2.16*
6- 6-H		31, 03, 30	7.20	2.17	"		510	2.75		1.93	1.42
6- 6-J	Cotton	31, 07, 40	7.22	2.15	"		505	2.75		2.09	1.32
6- 6-K		127, 04, 26	7.48	0.37	"		510	2.79		1.93	1.45
$MEAN_{i=6}$											1.50
STANDARD DEV											0.19

* denotes error in analysing the sample - as apparent from trend in data
Na = 1750 mg/L N = 750 mg/L
K = 210 mg/L
Cl = 2300 mg/L
Total CO_3 alkalinity = 2500 mg/L

Table D7. Kinetics study with magnesium and 100 mg/L P but no calcium (Set 6-7)

Sample		Time	pH	Ca	Mg	NH_4N	PO_4P	ΔCa	ΔMg	ΔP	ΔMg/ΔP
		days, hr, min		mg/L				milli-moles			
6- 7-A		00, 00, 00	7.28	< 0.07	14.5	800	98.		0.00	0.00	
6- 7-B		00, 00, 59	7.29	"	14.4		99		0.00	0.00	
6- 7-C		00, 06, 00	7.22	"	14.3		99		0.00	0.00	
6- 7-D		00, 23, 59	7.24	"	14.5		99		0.00	0.00	
6- 7-E	Cotton	01, 00, 06	7.25	"	14.2		97		0.00	0.00	
6- 7-F		05, 04, 45	7.42	"	14.4	730	96		0.00	0.06	
6- 7-G	Cotton	05, 04, 53	7.26	"	14.3	740	99		0.00	0.00	
6- 7-H		30, 18, 32	7.34	"	14.1		95		0.03	0.10	
6- 7-J	Cotton	30, 23, 15	7.27	"	13.9		95		0.03	0.10	
6- 7-K		95, 00, 05	7.92	"	14.3		96		0.00	0.01	
MEAN						735					No ppt.
STANDARD DEV											

* denotes error in analysing the sample - as apparent from trend in data
No ppt. = No precipitation
Na = 1250 mg/L N = 760 mg/L
K = 69 mg/L
Cl = 2100 mg/L
Total CO_3 alkalinity = 2350 mg/L

Table D8. Kinetics study with magnesium and 300 mg/L P but no calcium (Set 6-8)

Sample		Time	pH	Ca	Mg	NH_4N	PO_4P	ΔCa	ΔMg	ΔP	ΔMg/ΔP
		days, hr, min		mg/L				milli-moles			
6- 8-A		00, 00, 00	7.30	< 0.07	61.2	750	305		0.00	0.00	
6- 8-B		00, 01, 00	7.31	"	51.8		280		0.39	0.81	0.48**
6- 8-C		00, 06, 00	7.23	"	41.9		285		0.804	0.64	1.26
6- 8-D		00, 23, 57	7.18	"	27.4		264		1.41	1.32	1.07
6- 8-E	Cotton	01, 00, 01	7.16	"	22.8		242		1.60	1.45	1.10
8-D(uf)		00, 23, 57		"	28.5	765	270				
8-E(uf)	Cotton	01, 00, 01		"	26.4	750	285				
6- 8-F		05, 04, 42	7.17	"	23.6	720	245		1.57	1.93	1.81
6- 8-G	Cotton	05, 04, 47	7.16	"	23.3		265		1.58	1.29	1.22
6- 8-H		28, 18, 40	7.13	"	19.2		250		1.75	1.77	0.99
6- 8-J	Cotton	29, 23, 36	7.14	"	21.0		250		1.68	1.77	0.95
6- 8-K		95, 00, 24	7.17	"	17.4		245		1.83	1.93	0.95
$MEAN_{i=9}$											1.07
STANDARD DEV											0.16

* denotes error in analysing the sample - as apparent from trend in data
** higher levels of precipitation required for accurate analysisi of stoichiometric ratio
(uf) = swirled and unfiltered sample
Na = 1450 mg/L N = 750 mg/L
K = 125 mg/L
Cl = 2200. mg/L
Total CO_3 alkalinity = 2150 mg/L

Table D9. Kinetics study with magnesium and 600 mg/L P but no calcium (Set 6-9)

Sample		Time	pH	Ca	Mg	NH_4N	PO_4P	ΔCa	ΔMg	ΔP	ΔMg/ΔP
		days, hr, min		mg/L				milli-moles			
6- 9-A		00, 00, 00	7.29	< 0.07	115.	765	660		0.00	0.00	
6- 9-B		00, 01, 00	6.98	"	20.8		545		3.93	0.65	1.08
6- 9-C		00, 06, 01	7.06	"	20.8		570		3.93	2.97	1.32
6- 9-D		00, 23, 58	7.05	"	21.3		560		3.90	3.26	1.20
6- 9-E	Cotton	01, 00, 14	7.05	"	22.0		550		3.89	3.58	1.09
9-D(uf)		00, 23, 58		"	21.5	740	550				
9-E(uf)	Cotton	01, 00, 14		"	22.6	800	625				
6- 9-F		05, 04, 19	7.05	"	21.2	725	565		3.91	3.06	1.28
6- 9-G	Cotton	05, 04, 22	7.10	"	19.1	780	571		4.00	2.87	1.39
6- 9-H		29, 18, 38	7.20	"	14.4		510		4.19	4.83	0.87
6- 9-J	Cotton	29, 22, 48	7.20	"	11.6		520		4.31	4.51	0.96
6- 9-K		94, 23, 57	7.60	"	5.37		485		4.56	5.65	0.81
$MEAN_{i=9}$											1.11
STANDARD DEV											0.20

* denotes error in analysing the sample - as apparent from trend in data
** higher levels of precipitation required for accurate analysisi of stoichiometric ratio
(uf) = swirled and unfiltered sample
Na = 1825 mg/L N = 760 mg/L
K = 210 mg/L
Cl = 2450 mg/L
Total CO_3 alkalinity = 2000 mg/L

Table D10. Kinetics study with calcium, magnesium and 100 mg/L P (Set 6-10)

Sample		Time	pH	Ca	Mg	NH_4N	PO_4P	ΔCa	ΔMg	ΔP	$\Delta Ca/(\Delta P - \Delta Mg)$
		days, hr, min		mg/L				milli-moles			
6-10-A1		00, 00, 00	7.30	106.	15.1		96	0.00	0.00	0.00	
6-10-A2		00, 00, 04	7.30	107.	15.1		94	0.00	0.00		
6-10-B1		00, 59, 00	7.29	106.	15.1	765	92	0.00	0.00	0.00	
6-10-C		00, 06, 00	7.24	107.	15.5	810	88	0.00	0.00	0.00	
6-10-D		01, 00, 23	7.26	106.	15.5	730	93	0.00	0.00	0.00	
6-10-E	Cotton	01, 00, 29	7.27	105.	15.5	740	89	0.00	0.00	0.00	
6-10-F		05, 04, 48	7.11	39.3	14.2	765	59	1.67	0.04	1.19	1.63
6-10-G	Cotton	05, 05, 04	7.14	35.3	14.0	800	57	1.77	0.04	1.26	1.62
6-10-H		27, 23, 50	7.42	14.7	12.3			2.28	0.12		
6-10-J	Cotton	28, 04, 02	7.18	17.8	11.7		58	2.21	0.14	1.23	2.03
6-10-K		93, 04, 41	7.31	7.27	12.1		49	2.47	1.51		1.78
$MEAN_{i=4}$											1.77**
STANDARD DEV											0.19

* denotes error in analysing the sample as apparent from trend in data
** higher levels of precipitation required for accurate analyses of stoichiometric ratio
Na = 1250 mg/L N = 770 mg/L
K = 69 mg/L
Cl = 2300 mg/L
Total CO_3 alkalinity = 2250 mg/L

Table D11. Kinetics study with calcium, magnesium and 300 mg/L P (Set 6-11)

Sample		Time	pH	Ca	Mg	NH_4N	PO_4P	ΔCa	ΔMg	ΔP	$\Delta Ca/(\Delta P - \Delta Mg)$
		days, hr, min		mg/L				milli-moles			
6-11-A1		00, 00, 00	7.30	106	54.8	785	285	0.00	0.00	0.00	
6-11-A2		00, 00, 04		99.7	53.3	820	275	0.16	0.063	0.32	0.62**
6-11-B1		00, 00, 31	7.28	88.1	47.8	765	265	0.45	0.29	0.64	1.27
6-11-B2		00, 01, 04	7.25	81.7	44.7		260	0.61	0.42	0.80	1.60
6-11-C		00, 05, 59	7.19	65.9	36.6	775	250	1.00	0.76	1.13	2.70*
6-11-D		01, 00, 02	7.12	22.6	29.6	730	210	2.09	1.05	2.41	1.58
6-11-E	Cotton	01, 00, 08	7.09	18.7	28.1		210	2.18	1.11	2.41	1.68
11-D(uf)		01, 00, 02		71.0	33.0	720	250				
11-E(uf)	Cotton	01, 00, 08		93.5	45.1	765	250				
6-11-F		05, 04, 45	7.10	13.8	27.6	730	200	2.31	1.13	2.73	1.44
6-11-G	Cotton	05, 05, 00	7.09	13.6	28.7	800	205	2.31	1.09	2.57	1.56
6-11-H		26, 22, 37	7.10	7.9	23.9		195	2.45	1.29	2.89	1.53
6-11-J	Cotton	28, 03, 35	7.10	7.5	25.9		205	2.46	1.20	2.57	1.80
6-11-K		93, 04, 15	7.30	1.68	17.6		190	2.61	1.55	3.05	1.74
$MEAN_{i=8}$											1.62
STANDARD DEV											0.12

* denotes error in analysing the sample as apparent from trend in data
** higher levels of precipitation required for accurate analyses of stoichiometric ratio
Na = 1450 mg/L N = 770 mg/L
K = 125. mg/L
Cl = 2500. mg/L
Total CO_3 alkalinity = 2250 mg/L

Table D12. Kinetics study with calcium, magnesium and 600 mg/L P (Set 6-12)

Sample		Time	pH	Ca	Mg	NH_4N	PO_4P	ΔCa	ΔMg	ΔP	$\Delta Ca/(\Delta P - \Delta Mg)$
		days, hr, min		mg/L				milli-moles			
6-12-A1		00, 00, 00	7.29	91.9	94.7	835	545	0.00	0.00	0.00	
6-12-A2		00, 00, 04		61.9	63.6	810	475	0.75	1.30	2.25	0.79[1]
6-12-B1		00, 00, 30	7.13	60.6	35.3		430	0.78	2.48	3.70	0.64[1]
6-12-B2		00, 01, 00	7.12	61.1	33.8		430	0.77	2.54	3.70	0.66
6-12-C		00, 06, 00	7.04	21.6	28.7	730	415	1.76	2.75	4.18	1.23
6-12-D		01, 00, 12	7.00	14.9	25.0	740	415	1.93	2.90	4.02	1.51
6-12-E	Cotton	01, 00, 37	7.00	13.3	23.0		400	1.97	2.99	4.66	1.18
6-12-F		05, 04, 15	7.04	10.7	22.9	730	395	2.03	2.99	4.82	1.11
6-12-G	Cotton	05, 04, 30	7.03	10.6	23.5	720	410	2.03	2.97	4.34	1.48
6-12-H		26, 22, 36	7.04	3.74	17.9		410	2.20	3.20	4.34	1.93
6-12-J	Cotton	27, 02, 57	7.04	2.74	20.0		405	2.23	3.11	4.50	1.60
6-12-K		93, 03, 29	7.10	1.00	16.5		405	2.27	3.25	4.50	1.81
$MEAN_{i=4}^{3}$											1.71
STANDARD DEV											0.20

* denotes error in analysing the sample as apparent from trend in data
** higher levels of precipitation required for accurate analyses of stoichiometric ratio

[1]presence of transient precipitates discussed in Chapters IV and V of text

[3]Mean of last four samples

Na = 1760 mg/L N = 760 mg/L
K = 210 mg/L
Cl = 2550 mg/L
Total CO_3 alkalinity = 2150 mg/L

Table D13. Kinetics study with magnesium , 300 mg/L P, no calcium and ammonium (Set 6-13)

Sample		Time	pH	Ca	Mg	NH_4N	PO_4P	ΔCa	ΔMg	ΔP	ΔMg/ΔP
		days, hr, min		mg/L				milli-moles			
6-13-A		00, 00, 00	7.31	0.44	54.4	0.0	300	0.00	0.00	0.00	
6-13-A1		00, 00, 04		"	54.6		295		0.00	0.00	
6-13-B		00, 01, 00	7.29	"	54.3		285		0.	0.	
6-13-C		00, 06, 02	7.31	"	54.2		280		0.	0.	
6-13-D		01, 02, 08	7.32	"	53.6		290		0.	0.	
6-13-E	Cotton	01, 02, 16	7.32	"	53.7		295		0.	0.	
6-13-F		05, 02, 55	7.32	"	53.8		290		0.	0.	
6-13-G	Cotton	05, 03, 17	7.32	"	53.7		280		0.	0.	
6-13-H		26, 23, 02	7.40	"	46.7		285		0.	0.	
6-13-J	Cotton	27, 01, 40	7.30	"	51.7		280		0.	0.	
6-13-K		92, 01, 02	7.38	"	50.4		295		0.	0.	
MEAN											No ppt.
STANDARD DEV											

* denotes error in analysing the sample - as apparent from trend in data
** higher levels of precipitation required for accurate analysisi of stoichiometric ratio
(uf) = swirled and unfiltered sample
No ppt. = No precipitate could be detected
Na = 1150 mg/L N = 0 mg/L
K = 119. mg/L
Cl = 300. mg/L
Total CO_3 alkalinity = 2200 mg/L

Table D14. Kinetics study with magnesium, 600 mg/L P, no calcium and ammonium (Set 6-14)

Sample		Time	pH	Ca	Mg	NH_4N	PO_4P	ΔCa	ΔMg	ΔP	ΔMg/ΔP
		days, hr, min		mg/L				milli-moles			
6-14-A		00, 00, 00	7.35	0.33	113.	0.0	585		0.00	0.00	
6-14-A1		00, 00, 04		"	113.		565		0.00	0.00	
6-14-B		00, 01, 00	7.32	"	113.		575		0.00	0.00	32
6-14-C		00, 06, 02	7.31	"	113.		565		0.00	0.00	
6-14-D		01, 01, 50	7.30	"	114.		560		0.00	0.00	
6-14-E	Cotton	01, 02, 25	7.30	"	114.		570		0.00	0.00	
6-14-F		05, 02, 57	7.32	"	113.		555		0.00	0.00	
6-14-G	Cotton	05, 03, 29	7.32	"	113.		570		0.00	0.00	
6-14-H		18, 15, 28	7.34	"	109.		575		0.00	0.00	
6-14-J	Cotton	27, 00, 12	7.41	"	113.		585		0.00	0.00	
6-14-K		92, 01, 11	7.40	"	106.		585		0.00	0.00	
MEAN											No ppt.
STANDARD DEV											0.20

* denotes error in analysing the sample - as apparent from trend in data
** higher levels of precipitation required for accurate analysisi of stoichiometric ratio
(uf) = swirled and unfiltered sample
No ppt. = No precipitate could be detected, even at 30K filtration for 6-14-H
Na = 1570 mg/L N = 0 mg/L
K = 210 mg/L
Cl = 560 mg/L
Total CO_3 alkalinity = 2350 mg/L

Table D15. Kinetics study with calcium, magnesium, 600 mg/L P and no ammonium (Set 6-15)

Sample		Time	pH	Ca	Mg	NH_4N	PO_4P	Alk	ΔCa	ΔMg	ΔP	Comments
		days, hr, min		mg/L				milli-moles				
6-15-A		00, 00, 00	7.30	114.	114.	0.0	585	2880	0.00	0.00	0.00	
6-15-B		00, 01, 02	7.27	44.5	102.		560		1.74	0.48	0.81	
6-15-C		01, 23, 08	7.21	27.3	95.2		525		2.17	0.78	1.93	
6-15-D		07, 05, 07	7.22	18.3	92.7		475	2590	2.40	0.89	3.54	
6-15-E		64, 03, 23	7.22	4.85	89.6		500		2.73	1.02	2.73	
6-15-F		94, 22, 01	7.28	4.80	92.0		510	2575	2.73	0.92	2.41	
MEAN												Un. ppt.
STANDARD DEV												

* denotes error in analysing the sample - as apparent from trend in data
** higher levels of precipitation required for accurate analysisi of stoichiometric ratio
Un. ppt. = An unidentified crystalline precipitate accompanied the fine white calcium precipitate.
Na = 1690 mg/L N = 0 mg/L
K = 210 mg/L
Cl = 730 mg/L

Table D16. Kinetics study with calcium, magnesium, no phosphorus and ammonium (Set 6-16)

Sample		Time	pH	Ca	Mg	NH_4N	PO_4P	Alk	ΔCa	ΔMg	ΔCO_3	
		days, hr, min		mg/L				milli-moles				
6-16-A		00, 00, 00	7.29	112.	127.	0.0	0.0	2165	0.00	0.00	0.00	
6-16-B		00, 01, 03	7.25	109.	126.		0.0	2140	0.00	0.00	0.00	
6-16-C		01, 22, 53	7.25	111.	128.		0.0		0.00	0.00	0.00	
6-16-D		07, 06, 50	7.33	103.	124.		0.0	2090	0.225	0.125	0.75	
6-16-E		64, 03, 13	7.07	49.9	107.		0.0		1.55	0.83		
6-16-F		95, 00, 13	7.70	7.54	108.0		0.0	1870	2.61	0.79	2.95	
Precipitate											Aragonite[2]	
STANDARD DEV												

* denotes error in analysing the sample - as apparent from trend in data
** higher levels of precipitation required for accurate analysisi of stoichiometric ratio

[2]Aragonite identified by X-Ray diffraction, magnesium ppt. unidentified

Aragonite = $CaCO_3$
Na = 1175 mg/L N = 0 mg/L
K = 210 mg/L
Cl = 860 mg/L

The vita has been removed from the scanned document